China's Food Production under Water and Land Limitations

by

Piyatida Hoisungwan

B.Eng. Civil Engineering
Chulalongkorn University, 2002

Submitted to the Department of Civil and Environmental Engineering in partial fulfillment of the requirements for the degree of

Doctor of Philosophy

at the

MASSACHUSETTS INSTITUTE OF TECHNOLOGY

June 2010

Author.....
Department of Civil and Environmental Engineering
May 13, 2010

Certified by.....
Dennis McLaughlin
H.M. King Bhumibol Professor of Civil and Environmental Engineering
Thesis Supervisor

Accepted by.....
Daniele Veneziano
Chairman, Departmental Committee for Graduate Students

China's Food Production under Water and Land Limitations

by

Piyatida Hoisungwan

Submitted to the Department of Civil and Environmental Engineering on May 13, 2010,
in partial fulfillment of the requirements for the Degree of Doctor of Philosophy
in the field of Civil and Environmental Engineering

ABSTRACT

The future availability of the natural resources (water and land) needed for food production is highly uncertain. Evidence shows diminishing natural resources and growing food demand throughout many parts of the world. China is one of the countries that face the challenge of managing its finite water and land resources to support their population. Difficulties mainly arise from: (1) the geographic mismatch between the location of water resources and available land; (2) a large and growing number of population; and (3) limited natural resources per capita. This thesis presents a systematic approach to evaluate the effects of water and land constraints on food production and applies it to China as a case study.

Based on the basic principle of water and land balance, crop resource requirements, and per capita consumption, the assessment of natural resources limitations on food production can be formulated into an optimization model, with the objective function maximizing the number of people fed subject to resource constraints. This formulation makes it possible to systematically and efficiently evaluate the effects of natural resource constraints for such a complex and large scale study regions such as China. Even though our approach is based on the basic principle, we incorporate several significant features into the model to realistically represent the spatial and temporal heterogeneity in climate, land use, and crop requirements. Our analysis is conducted at a detailed spatial resolution of 0.5° by 0.5°, includes water movement at the same resolution, accommodates the mixture of crops in people's diet, and distinguishes irrigated from rainfed agriculture.

Our optimization model presents an average long term analysis. The model is developed and calibrated to reproduce long-term observed conditions during the nominal period of 1990-2000. We then use the model together with globally and locally available data to make future predictions of China's food production capacity during the future period of 2046-2065. These future predictions include the impacts of the South-to-North Water Diversion project and projected climate change. The future climate scenarios are taken from the general circulation model predictions and represent diverse seasonal and regional patterns.

Regionally, land is a limiting factor in the south, while water is a limiting factor in the north. Our results suggest that irrigation and multiple-cropping are keys in enhancing China's food production capacity to support increasing population. The spatial and seasonal distribution of rainfall changes is critical for agriculture in meeting future food requirements under climate change

Thesis supervisor: Dennis McLaughlin
Title: H.M. King Bhumibol Professor of Civil and Environmental Engineering

Acknowledgements

I would like to express my deepest gratitude to my advisor, Professor Dennis McLaughlin, for his patience, advice, guidance, and encouragement throughout my PhD. It has been a great honor and pleasure to work with him. I would also like to extend my gratitude to my thesis committee members, Professor Elfatih Eltahir, Professor Dara Entekhabi, and Professor Peter Rogers, who have provided guidance and suggestions in carrying out this research.

I wish to gratefully acknowledge the fellowship from the Anandamahidol Foundation under the Royal Patronage of His Majesty the King of Thailand. I am greatly indebted to the Foundation for a great opportunity to study in this program. I also would like to extend my deepest gratitude to Professor Anukalya Israsena Na Ayudhaya for his guidance and support.

I would like to thank previous students and UROPs who contributed to the development of this research project: Amy Watson, Marine Herrmann, Holly Johnson, and April Tam.

I have learned from and enjoyed many fruitful discussions and interactions with past and present members of McLaughlin's and Entekhabi's research groups. I also would like to thank members of Parsons Laboratory who make the lab an enjoyable workplace. Special thanks to Crystal Ng, David González Rodríguez, Marcos, and Lawrence David for making my times here a memorable and precious experience.

I am thankful to the Thai community at MIT for their friendship and support throughout this journey. Special thanks to Virat Chatdarong, Watjana Lilaonikul, Panitarn Wanakamol, Wanida Pongsaksawad, Samerkhae Jongthammanurak, Kittiwit Matan, Ratchatee Techapiesancharoenkij, Warit Wichakool, Kalaya Kovidvisith, Numpon Insin, Nonglak Meethong, Chonlagarn Iamsumang, Virot Chiraphadhanakul, and Nisanart Charoenlap.

Finally, I would like to express my deepest gratitude to my parents, P'Golf, and P'Jeab, to whom I dedicate this thesis to. I am also thankful to Uncle Lek and Auntie Wee for their tremendous help since my first day in the U.S.

Contents

List of Figures

List of Tables

Chapter 1

Introduction

1.1 Context

Increasing global population requires increasing demand for food. This entails increasing demand for the two basic natural resources needed for food production, freshwater and cropland. In 2000, agriculture already accounted for 67% of the world's total freshwater withdrawal (UNESCO 2000).

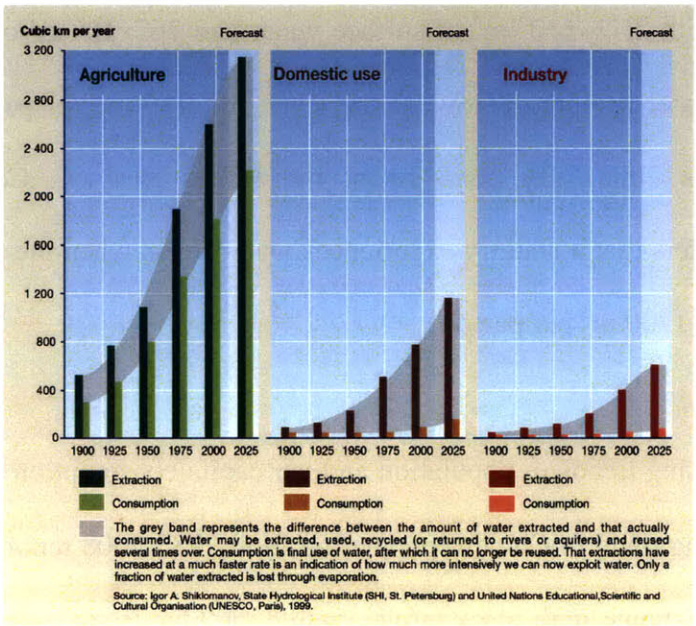

Figure 1-1: Trends in global water use by sector.

The supply of arable land is largely limited by available water, soil conditions, and topography. Irrigation plays a significant role in bridging the gap between naturally available water and crop water demand, making it possible to increase crop production and expand cultivated land. About 10% of the earth's land surface is devoted to cropland, and 16% of this land is supplied with irrigated water (Postel 1993). However, since the late 1970s, the rate of global irrigation development has dropped considerably due to soil salinization, the high cost of irrigation networks, the depletion of irrigation water sources, and other environmental problems. Thus, there is no easy solution for meeting the increasing food demand.

China is one of the countries that face the challenge of managing water and land resources to support their growing population. With a population of 1.32 billion in 2007 (National Bureau of Statistics 2008), China is the world's most heavily populated nation. Limitations on China's water and land resources are evident. China's total water resource in 2007 has been estimated to be $2{,}526 \times 10^9$ m^3, with $2{,}424 \times 10^9$ m^3 of surface water and 762×10^9 m^3 of groundwater, and the annual per capita water resource is low, at the level of 1,916 m^3 per person in 2000 (National Bureau of Statistics 2008). By comparison, the World Business Council for Sustainable Development considers that a country experiences water stress when the annual per capita water resource is less than 1700 m^3 per person.

Furthermore, increasing trends in population and per capita consumption are observed. Figure 1-2 shows an increasing trend in Chinese population from 1985-2008 reported by National Bureau of Statistics (2008) (shown with black circles) while the blue triangles represent predicted mid-

year population from 2009-2050 by the U.S. Census Bureau. The United Nations estimates that China's population will reach its peak at 1.46 billion people by 2030. Changes in per capita consumption in the Chinese diet are also straining resources. Figure 1-3 shows trends in Chinese per capita consumption from 1990-2005 for four major crop categories: wheat, rice, maize, oil crops, and tubers (FAOSTAT 2009). The consumption here refers to a total domestic utilization quantity, which is the sum of the amount of feed, seed, waste, processing, food, and other utility. We see increasing trends in maize, oil crops, and tubers per capita consumption with an exception of slightly decreasing trends in rice and wheat consumption rates. The Food and Agricultural Organization reports per capita consumption (including food and feed) for maize has risen by almost 45% from 1980s to 2003. This increase in a large part due to the increase in meat consumption (feed part). Feeding 160 million more people with increasing per capita consumption is a challenge that some researchers feel cannot be met with available natural resources. For example, Brown (1995) believes that China is already operating beyond a sustainable level of production, a situation that they will have to import from other nation's to make up the difference between domestic production and demand.

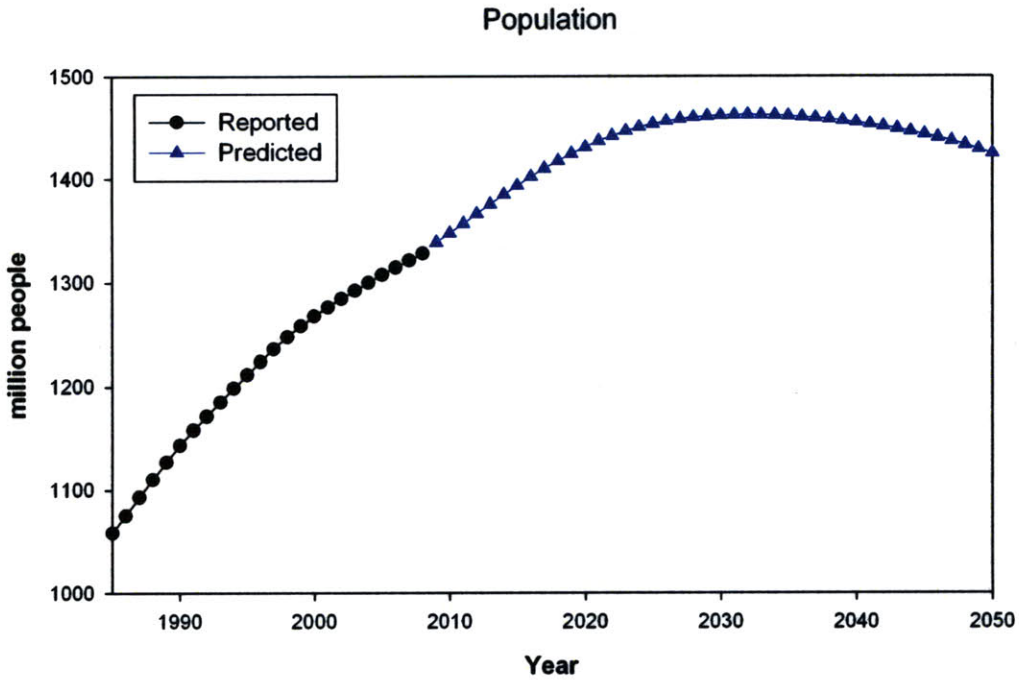

Figure 1-2: Trend in Chinese population. Black circles represent reported population from 1985-2008 by the National Bureau of Statistics of China. Blue triangles represent the predicted mid-year population from 2009-2050 by the U.S. Bureau of Statistics.

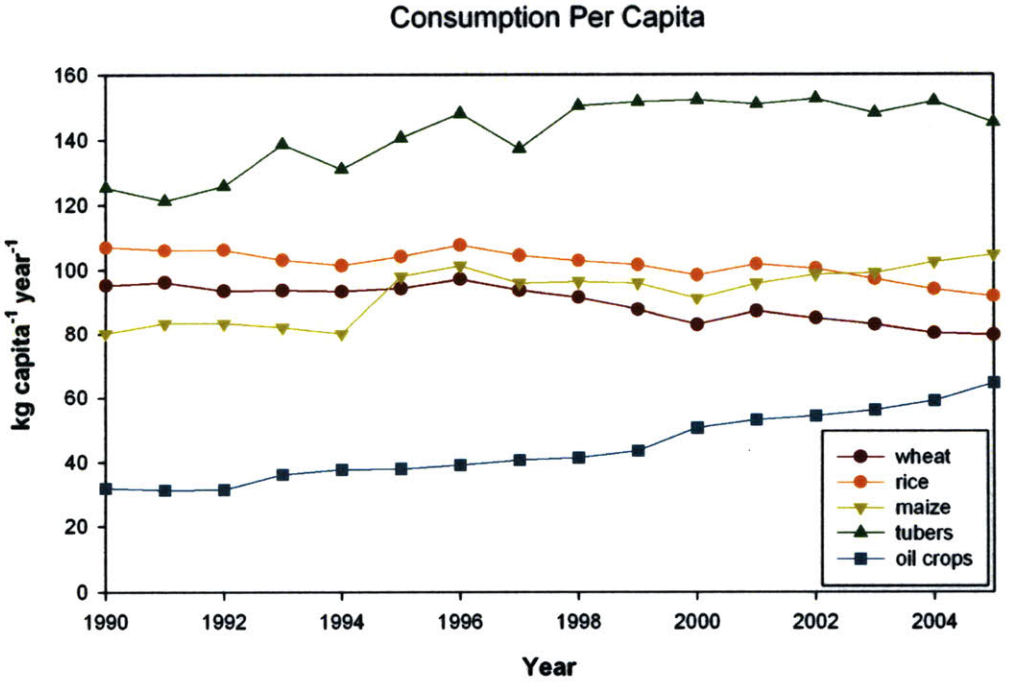

Figure 1-3: Trends in Chinese per capita consumption from 1990-2005 reported by The Food and Agricultural Organization.

China's agriculture is further complicated by an uneven distribution of land and water resources. One of the main challenges of managing natural resources in China is that there is a mismatch between the location of water resources and available land. Water availability can be approximately quantified by the difference between precipitation and potential evapotranspiration, as shown in Figure 1-4 (a)-(c) (Thomas 2007 and 2008). Precipitation is the original source of water supply in both surface and groundwater flows. Potential evapotranspiration is an upper bound of actual evapotranspiration (water demand) by crops. If potential evapotranspiration is high, there is a high demand in atmospheric moisture. As shown in Figure 1-4 (c), most of the country's available water is concentrated in the south, which experiences a strong monsoon climate.

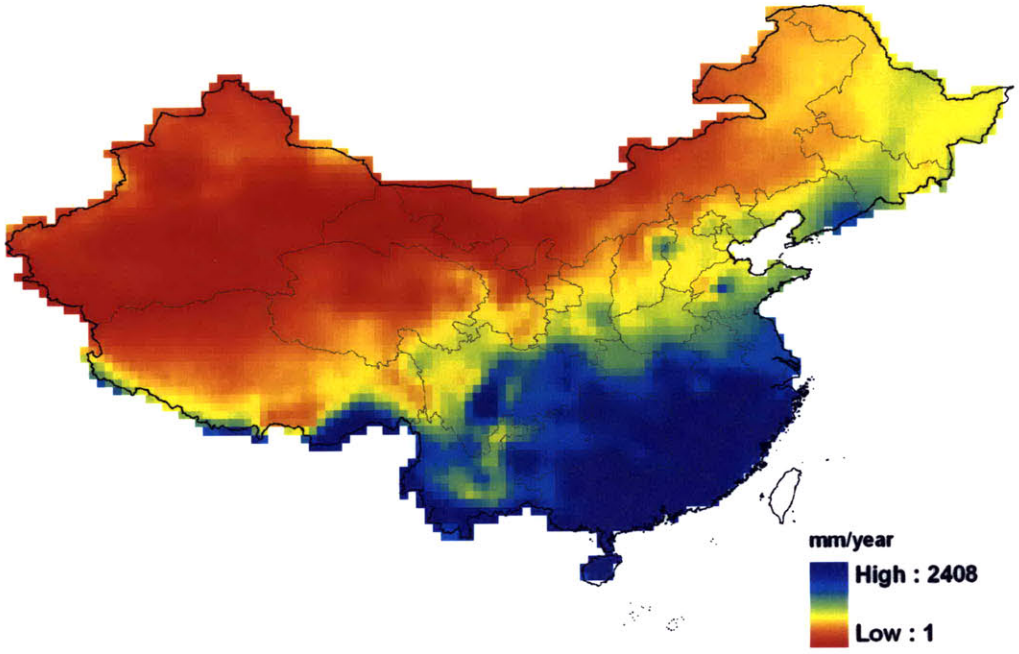

(a) Annual precipitation average over the period 1951-1990.

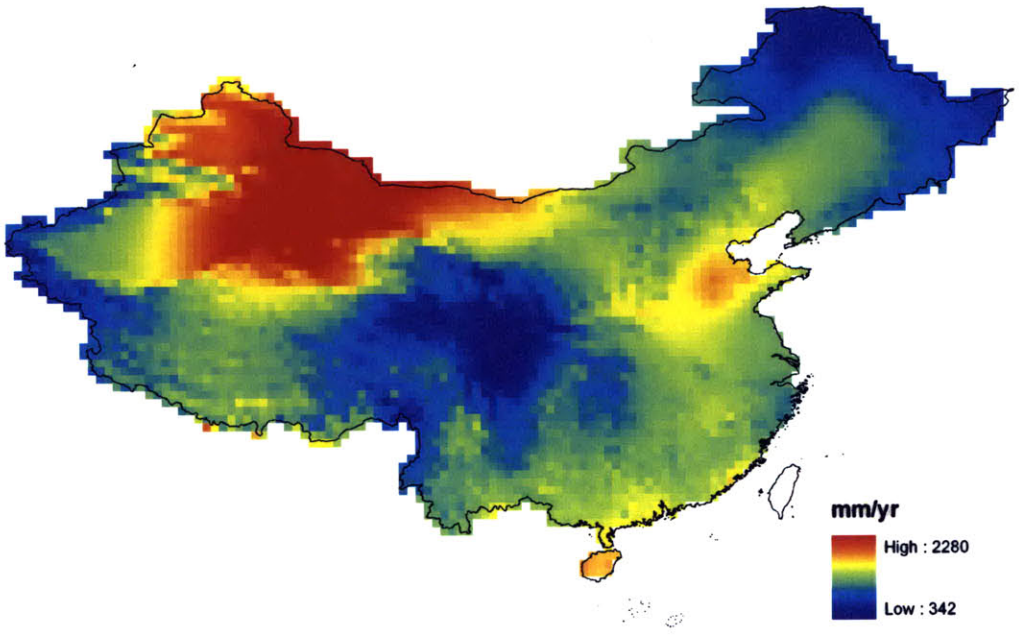

(b) Annual PET average over the period 1951-1990.

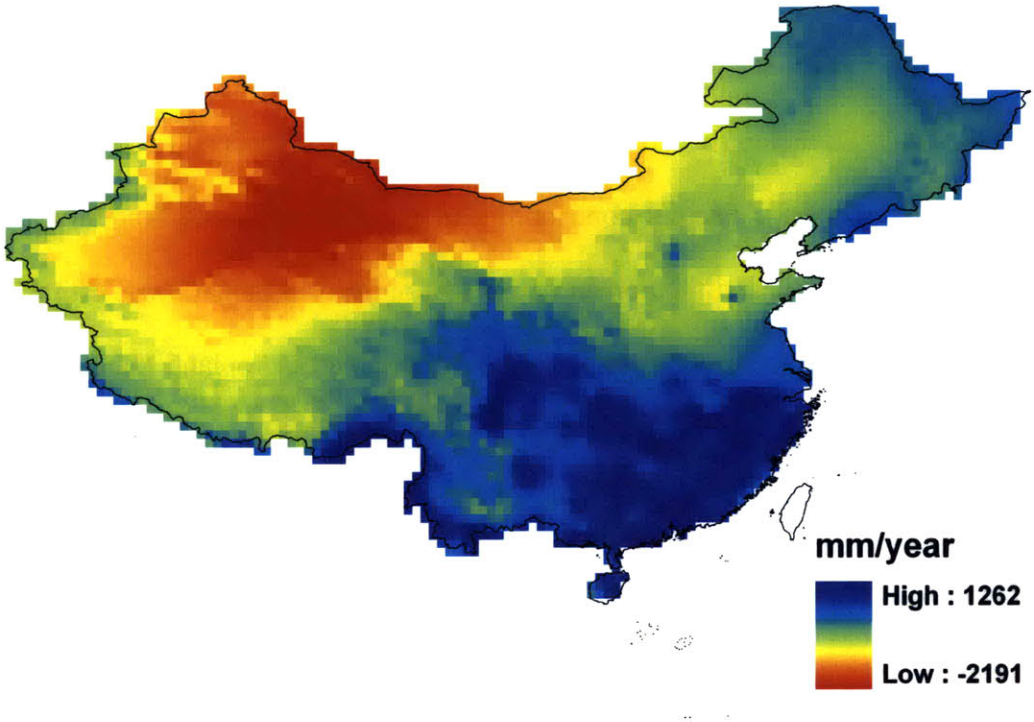

(c) Water availability index (precipitation – potential evapotranspiration). The blue region is where precipitation is greater than potential evapotranspiration; while the red region is where potential evapotranspiration is greater.

Figure 1-4 (a)-(c): Annual average precipitation, potential evapotranspiration, and water availability.

While water resources are most abundant in southern areas, cropland and population are concentrated more in the central and northern regions, where water is more limited. Figure 1-5 shows the extent of cropland distribution around 1995-1996 (Frolking et al. 2002) and Figure 1-6 below shows the population distribution in 2005 (CIESIN 2005). The population distribution more or less coincides with the cropland distribution and both differ noticeably from the water availability distribution in Figure 1-4 (c).

While there is large uncertainty in cropland estimates, many studies suggest that the land devoted to agriculture in China was on the order of 130 Mha in the late 1990's (Smil 1999). Smil (1995) reports that approximately 0.5 Mha of cropland have been lost every year since the early 1980's. As of the end of 2007, the cultivated area was reported to have dropped to 121.7 Mha (National Bureau of Statistics 2008). Factors contributing to the loss of arable land in China include conversion to other uses, desertification and afforestation. World Bank (2001) estimated that 331 Mha of land in China are prone to desertification. The area of cropland that was converted to forest in 2007 was estimated to be on the order of 85,000 ha (National Bureau of Statistics 2008).

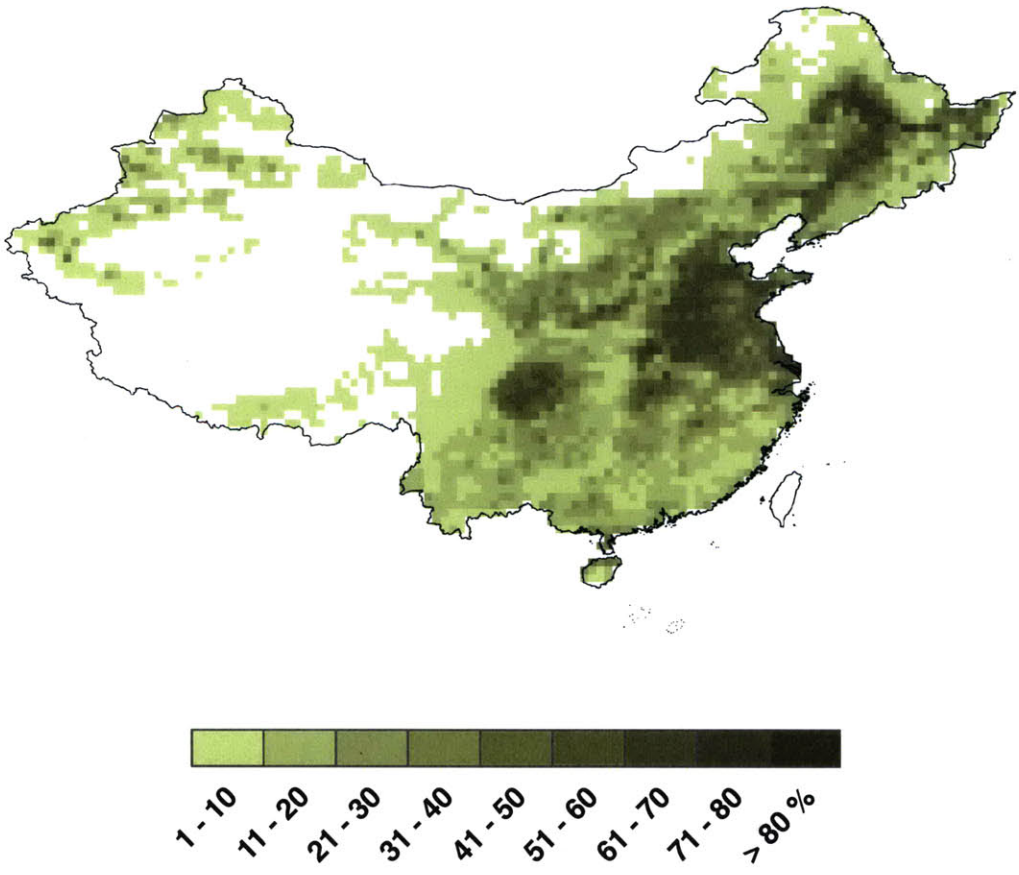

Figure 1-5: Map of cropland distribution in China as a percentage of total area in each 0.5° pixel. It was constructed by combining census data from 1990 with Landsat TM from the years 1995/1996.

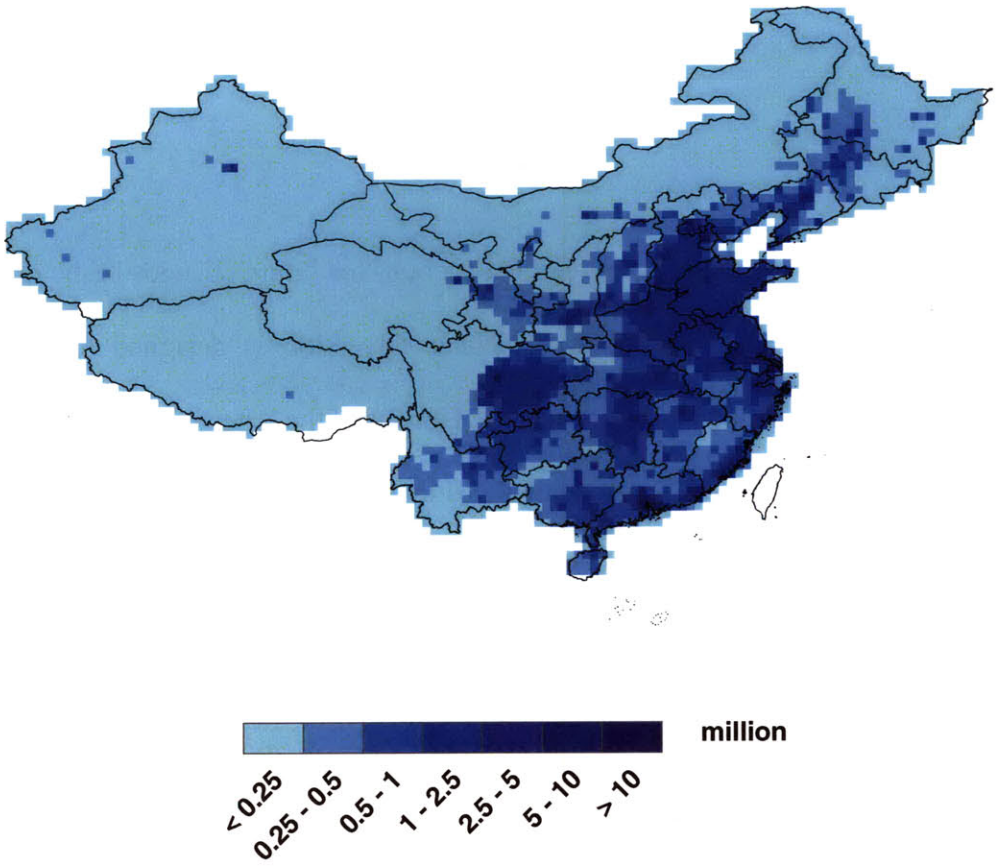

Figure 1-6: Population distribution over China in 2005. The legend shows number of people in each 0.5° pixel.

One of the extreme examples of the inconsistency in resource distributions is the North China Plain (NCP, areas around the lower reaches of the Yellow, Huaihe and Haihe rivers). This region accounts for one third of the national GDP, produces about half of the nation's wheat and one third of its maize, but only receives 7.7% of national water resources (Ministry of Water Resources, PRC 2004). Furthermore, 83% of China's irrigated land occurs in this semi-arid region, and it is estimated that the water tables in the three major river basins of the North China Plain (NCP) have dropped 50 m in some areas (World Bank 2001). A large scale project to divert water from the Yangtze River to alleviate water shortages in the NCP was initiated in 1950s.

This South-to-North Water Diversion project is underway, with the construction of three major routes, and expected to divert 44.8 billion m^3 $year^{-1}$ by 2050, which is equal to the amount of annual runoff of the Yellow River, to over ten provinces in the NCP, arid northwestern and northern regions.

An assessment of China's food production must account for future changes in the distribution of its natural resources. The South-to-North Water Diversion is designed to increase water availability in the northern part of the country. However, the effects of this project could be modified or even overwhelmed by climate changes that are very difficult to predict. Most global climate models (IPCC 2007) predict a warming trend over all China, but changes in precipitation subject to significant uncertainty. A combination of warming temperatures and changes in precipitation may have a significant impact on crop viability in different regions.

1.2 Literature Review

Will China be able to support its population with finite water and land resources? Smil (1995) provided an overview of China's food production capacity by investigating three critical issues. First, there were great uncertainties in the official estimates in the total area of China's cultivated land before the 1990's. The cropland was substantially larger than the official reports and as a consequence the estimated average yields were considerably too high, leaving room for improvement. Second, the use of national averages and generalizations misrepresented the complex realities of the country. Finally, there were opportunities for higher efficiencies in irrigation water and agricultural practice. Smil (1995) concluded that China should be able to continue support itself without drastic adjustments or substantially advance technology.

Another study conducted by IIASA (International Institute for Applied Systems Analysis) addressed this question using a detailed Agro-Ecological Zoning (AEZ) methodology (Heilig et al. 2000). The AEZ methodology uses a land resources inventory to assess feasible agricultural land-use options and to quantify the expected production of relevant cropping activities. They looked closely at changes in arable land, potentials for multi-cropping, urbanization and changes in diet. However, the assessment of China's arable land potential was only based on grain suitability under rainfed condition.

A more recent study investigated the effects of climate change on China's food production. (Thomas 2006) simulated the potential yield for rainfed cropping systems during the period 1951–1990 and the climate scenarios for the year 2030 with gridded (0.25° × 0.25°) climate dataset and digital soil data. The results showed that potential crop yields displayed a tremendous variation both in temporal and spatial respects during the period 1951-1990. Results for future scenarios indicated an enlargement of the subtropical cropping zone.

However, the studies by Heilig et al. (2000) and Thomas (2006) essentially ignored water demand from noncrop areas and non-agricultural water use. They also did not incorporate important information on networks of water movement and river basins in water balance calculation. Further, they did not include validation with observed conditions. They also did not include the South-to-North Water Diversion in their studies.

1.3 Research Questions

The aim of this thesis is to address the following questions:

1) What is the maximum food production possible with specified (existing or future) land and water resources in China?
2) What are the effects of climate change and the South to North Water Diversion project on China's food production?

1.4 Research Approach

This thesis presents a systematic evaluation of how land and water resource limitations will affect agricultural production in China. Our approach is based on the following principles:

1) The focus of our study is to better understand how natural resources of land and water limit crop production. As a result, we do not take into account the various economic factors that affect food production, such as policy, institutions, capital, and labor in our analysis.
2) Our approach is based on basic principles of:
    - Water balance
    - Land balance
    - Crop resource requirements
    - Consumption requirements

    Base on these four basic principles, the assessment of natural resources limitations on food production can be formulated into an optimization model, with the objective function maximizing the number of people fed subject to resource constraints. We begin our evaluation of water and land limitations on food production with a simplified model

and illustrate with it how water and land resources constrain food production differently in different regions in China.

3) We rigorously assess China's food production potential by formulating an optimization problem (a detailed model) that includes a physically-based model that represents heterogeneous conditions and is calibrated with observations. Heterogeneities across meteorological, geographical, and dietary conditions are all considered. Specifically, we formulate the problem at the spatial and temporal resolutions needed to properly describe trends in climate, land use and crop parameters. This allows for fine scale networks of water movement in the model, along with water balance at the river basin scale. Complexity in diet is expressed using mixtures of crops. We assume that food can be freely transferred within the country.
4) The detailed model developed is calibrated to reproduce long-term observed conditions during the nominal or calibration period of 1990-2000 and used to estimate unknown model inputs.
5) We then use the model together with globally and locally available data and estimated inputs to simulate China's food production capacity during the year 2010 (Baseline simulation) and the future period of 2046-2065. Our baseline simulation relies on meteorological data from the period 1951-1990. The future predictions include the impacts of the South-to-North Water Diversion project and projected climate change. The future climate alternatives are selected from the general circulation models' prediction to represent diverse seasonal and regional patterns. A summary of the time periods used within this thesis is provided in Table 1-1.

Table 1-1: Time periods used within this thesis.

	Time period
Nominal/Calibration period	1990-2000
Baseline	2010
Climate change alternatives	2046-2065
Meteorological period	1951-1990

1.5 Thesis Organization

The content of the thesis is described below and outlined in Figure 1-7.

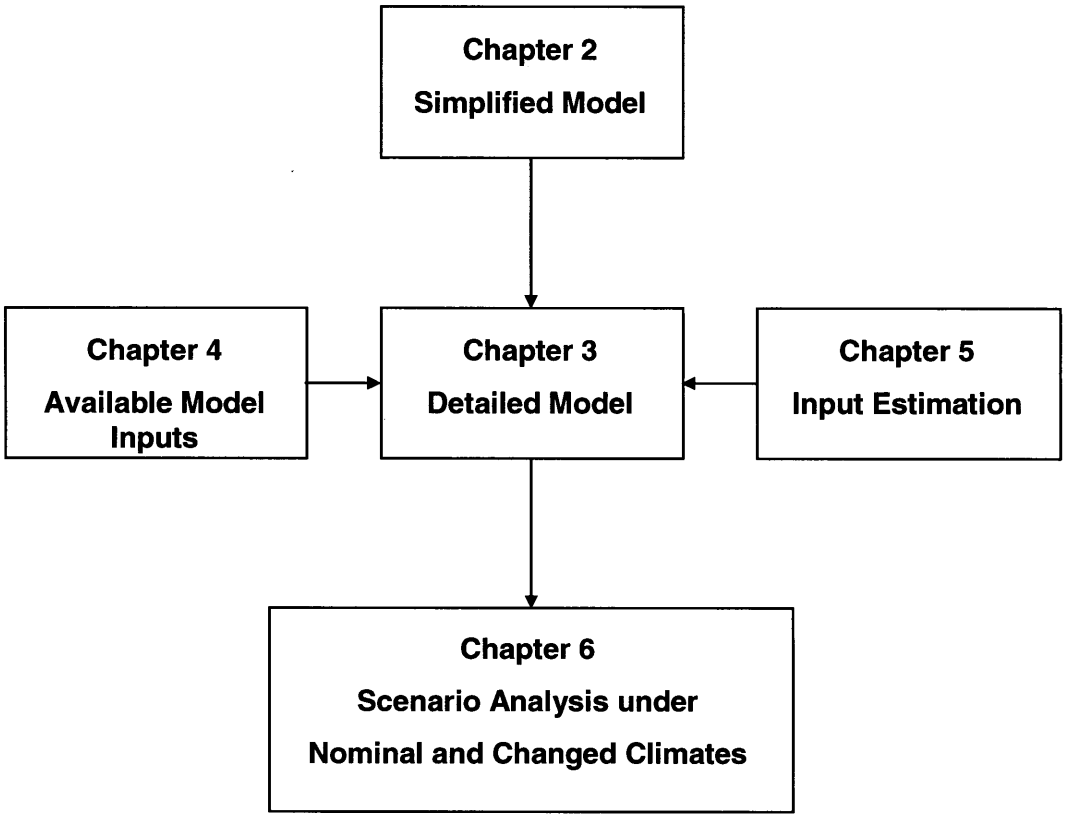

Figure 1-7: Outline of the thesis.

We begin our evaluation of water and land limitations on food production with a simplified analysis in Chapter 2. In Chapter 3, we show how the simplified model can be extended to include heterogeneous representation of China's resources and hydrologic flux balance. The full

formulation of the detailed optimization problem is presented in this Chapter. Chapter 4 is devoted to a comprehensive review of available inputs for the model. Then we discuss how to estimate some inputs that are not readily available and derivable from other data in Chapter 5. In Chapter 6, we present a scenario analysis of China's food production during the future period of 2046-2065 under nominal and changed climate using the model of Chapter 3, and data and inputs discussed in Chapter 4 and 5. Chapter 7 summarizes results from this research and original contributions, and discusses suggestions for future improvements of the model.

Chapter 2

Simplified Model

This main objective of this research is to evaluate the land and water resources limitations on food production. In this chapter, we introduce a simplified analysis based on the basic principle of land balance, water balance, and food consumption and production balance. We present the formulation of the simplified problem and illustrate with it how water and land resources constrain food production differently in different regions in China.

2.1 Simplified Problem Formulation

In China, both water and cropland resources are unevenly distributed across the country. While the southern region receives much more rainfall, arable land is more concentrated in the eastern and northern regions. For the simplified analysis, we assume that:

1) China is divided into two regions, north and south as shown in Figure 2-1.
2) Land is categorized as cropland or noncropland. Noncropland includes both natural and built environment that are not used for agriculture.

3) For crop type, we simply consider the aggregation of major grains that are grown in China, which are maize, rice, and wheat.
4) Cropland is further constrained by the total arable land. Arable land here refers to land with adequate accumulated degree days in a year, suitable soil characteristics, and slope for those three grains.
5) Precipitation is the only source of available water. This implies that water can be stored intra-annually and can be readily transported anywhere in each region.

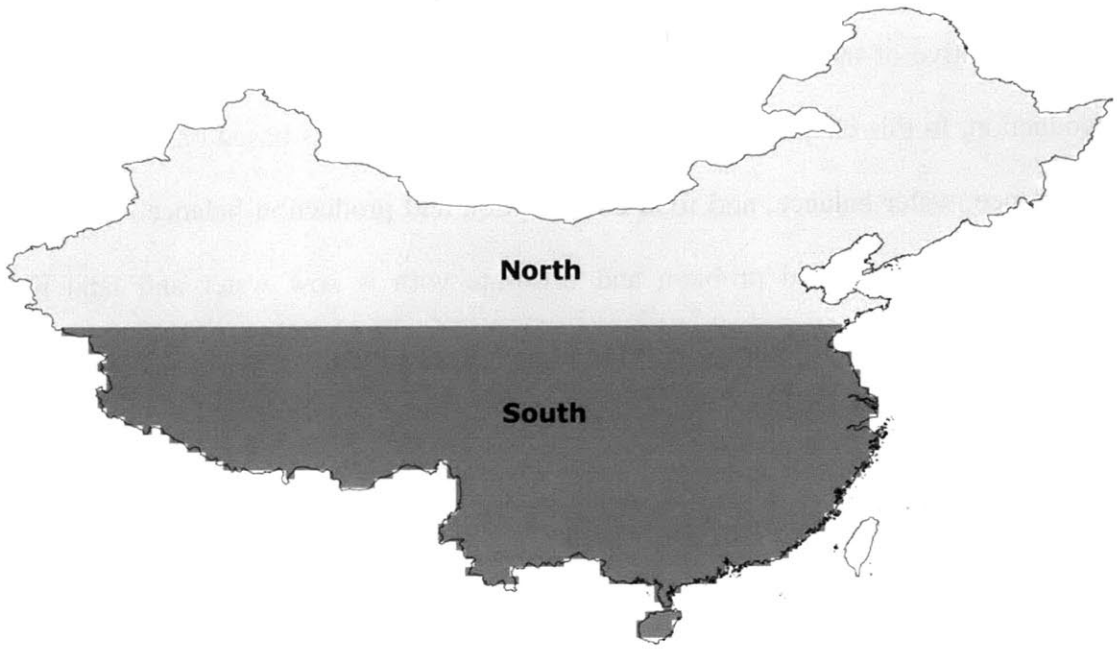

Figure 2-1: The division between north and south regions for the simplified analysis.

To determine how many people can be fed subject to water or land limitation in each region, we formulate a multi-objective optimization to maximize the number of people fed and minimize an adjustable mean-squared deviation of cropland from nominal values subject to land and water

resource constraints. The primary unknown in this simplified problem is the amount of cropland for each region. The inputs and results are annual long-term averages.

The problem can be formulated as shown in Equations (2-1) to (2-5) below. In the objective function, the first term is a maximization of number of people fed and the second term is a minimization of the deviation of cropland from nominal values, as shown in Equation (2-1). α is an adjustable weighting factor indicating priority given to the second term. For α equal to zero, priority is given entirely to maximizing the number of people fed. When α is increased, more weight is placed on the land deviation term. Equations (2-2) to (2-4) represent land and water constraints for each region. Cropland is converted into number of people fed via yield and consumption rates in Equation (2-5).

Objective function:

$$Maximize \quad peoplefed - \alpha \sum_{i=N,S} \left\| cropland_i - nominal\ cropland_i \right\|^2 \qquad (2\text{-}1)$$

Decision variables: *peoplefed, cropland*$_i$

Land constraints (i = N, S):

$$cropland_i + noncropland_i = totalland_i, \qquad (2\text{-}2)$$

$$cropland_i \le arableland_i, \qquad (2\text{-}3)$$

Water constraints (i = N, S):

$$(cropET)(cropland_i) + (noncroplandET_i)(noncropland_i) \le (precip_i)(totalland_i), \qquad (2\text{-}4)$$

Production-Consumption balance:

$$(\ peoplefed\ )(\ consumption\ ) = \sum_{i=N,S} (\ cropland_i\ )(\ cropyield\ ) \qquad (2\text{-}5)$$

2.2 Problem Solving and Solutions

This simplified model is a quadratic programming problem (QPP) since it has a quadratic objective function and only linear constraints. Using a quadratic programming formulation allows for a computationally efficient solution of the problem. Moreover, with all linear constraints, the feasible region of the optimization problem is convex, while its objective function is strictly concave. With these two conditions, a unique solution is guaranteed for the detailed model (Bradley et al. 1977).

We can solve this simplified problem manually for two extreme values of α using graphical method. When α is equal to zero, the objective function becomes a maximization of people fed. The objective function can be rewritten using the relationship in Equation (2-5) between the number of people and the unknown cropland in north and south regions. Figure 2-2 shows a graphical representation of the feasible region with the linear objective function. The inputs for the simplified problem are summarized in Table 2-1. The arable land constraints (green lines) are from Equation (2-3). Equation (2-4) together with Equation (2-2) form water constraints (blue lines). The red dash lines are the objective function with different levels of people fed. The red arrow indicates a direction of increasing number of people fed. The optimal cropland in this case is thus the intersection between the water constraint of the northern region and the arable land constraint of the southern region.

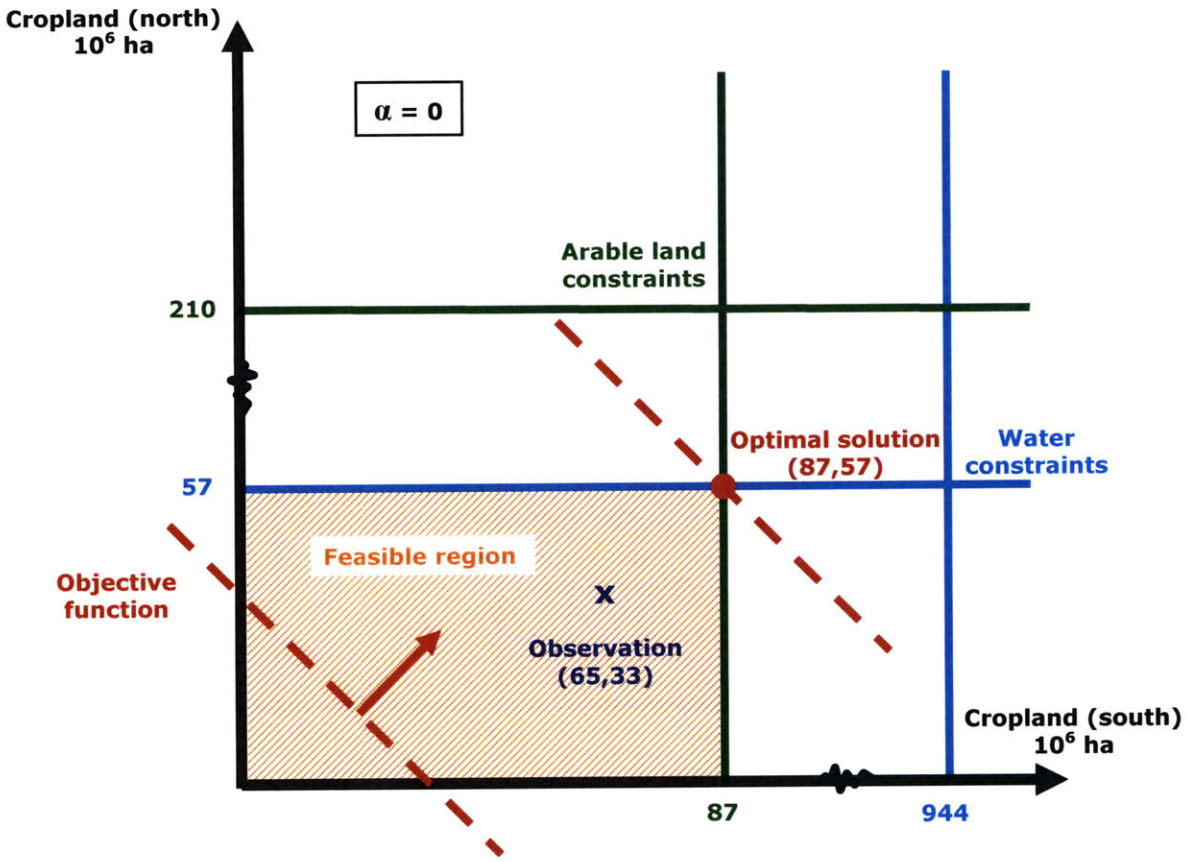

Figure 2-2: Graphical representation of the simplified problem when the objective function is to maximize people fed or α is equal to zero.

For the case of α equal to one, the constraints remain the same but the objective function depends only on the deviation from existing conditions. Here, the objective function is a circle with a center at the existing conditions. Figure 2-3 shows a graphical representation of this case with the red arrow indicating the direction of decreasing value of the deviation term. The optimal cropland allocation in this case is equal to the values of existing conditions.

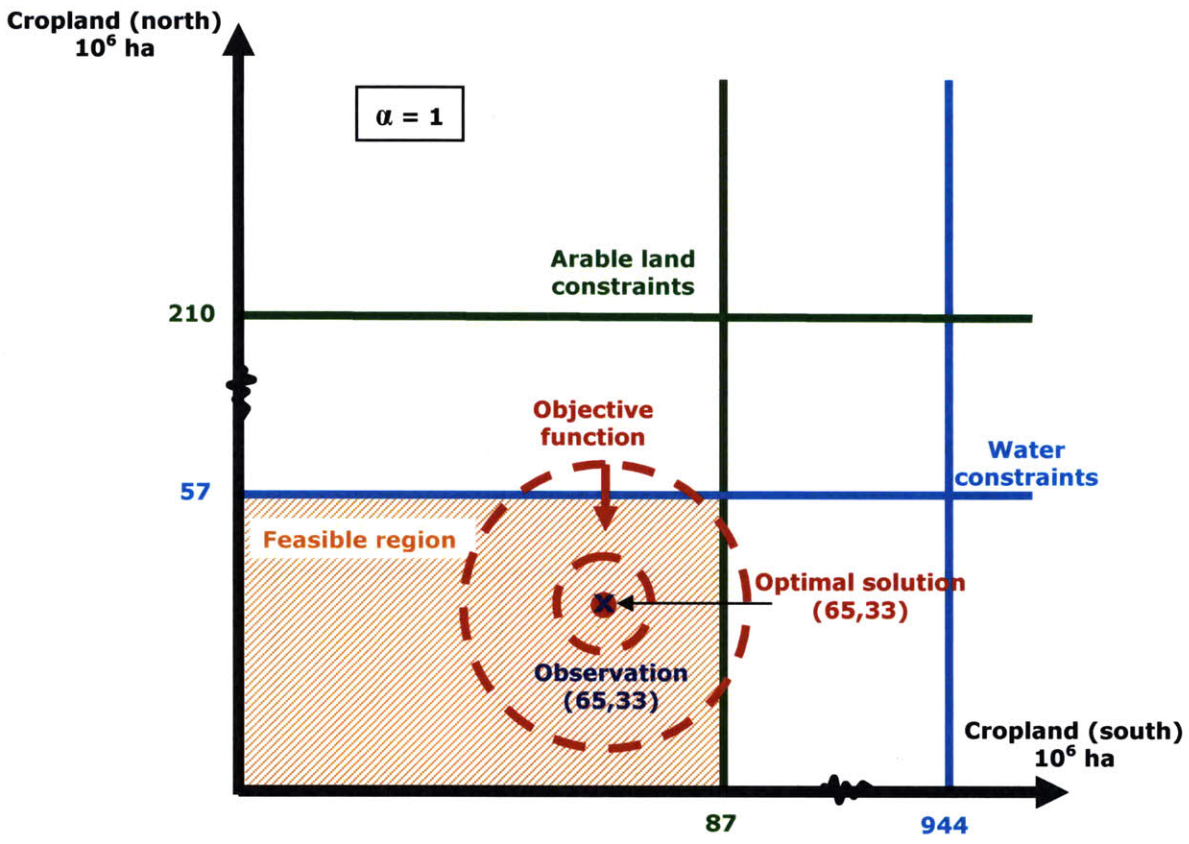

Figure 2-3: Graphical representation of the simplified problem when the objective function is to minimize the deviation from existing conditions or α is equal to one.

When α is between zero and one, there is a tradeoff between the number of people fed and the deviation from nominal conditions. Table 2-1 summarizes inputs and results for the two cases. The uneven resources distribution in China is clear from the precipitation and arable land data. The mean annual precipitation in the south is more than three times higher than in the north while arable land in the north is much more abundant than in the south. Other inputs, except for evapotranspiration from noncropland are assumed to be uniform and the same for both regions.

Table 2-1: Inputs and solutions for two extreme values of α.

	North	South	Units
Inputs			
Total land[1]	459	491	10^6 ha
Grains arable land[2]	210	87	10^6 ha
Observed grains cropland[3]	33	65	10^6 ha
Precipitation[4]	280	940	mm/yr
Grains water demand[5]	700	700	mm/yr
Grains consumption[6]	330	330	kg/(capita-yr)
Grains yield[7]	4880	4880	kg/ha
Non arable land ET[8]	220	440	mm/yr
Results			
Matching observation			
Cropland	33	65	10^6 ha
Flow to ocean	117	2286	km^3
Total people fed	**$1.4\ 10^9$**		
Maximizing peoplefed			
Cropland	57	87	10^6 ha
Flow to ocean	0	2229	km^3
Total people fed	**$2.1\ 10^9$**		

Data sources: 1. (Chuang et al. 1996)); 2. Section 4.4; 3. (Frolking et al. 2002)); 4. (Thomas 2007); 5. Section 4.3.2; 6. (FAOSTAT 2007a); 7. (FAOSTAT 2007b); 8. Chapter 5

As mentioned above, the weighting factor, α, allows us to examine the problem in two different ways. When α is equal to one, priority is entirely given to matching existing conditions. The optimal result for this case matches the observed cropland for both regions exactly, and the number of people fed is 1.4 billion. This calculated number of people fed is close to the current population of 1.3 billion, which provides some confidence in the model. On the other hand, when α is equal to zero, the amount of cropland calculated in the optimization problem deviates notably from existing conditions, and the calculated number of people fed jumps to 2.1 billion. Cropland in the south reaches the extent of the total arable land for this solution. In the north, even though arable land is abundant, only one fourth is allocated as cropland because of limited

water resources. These results show significant potential for increasing food production in China, yet it is in ways that could involve dramatic changes in land use.

In conclusion, our simplified optimization model is able to provide a rough estimate of how many people China can feed, given a specified priority for matching existing land use conditions. Although the model as formulated above is highly simplified, results from it serve to highlight the importance of including a penalty term for deviations from existing conditions. Without this term, the model could predict a scenario that is very optimistic in terms of production capacity, but involve significant and unrealistic land use changes. Therefore, the penalty term implicitly serves as a simplified representation for other constraints not included in the model such as economic, institutional, and political conditions.

The simplified problem presented in this Chapter provides a basis for understanding where land or water resources limit food production in China. The northern region has abundant arable land with limited water resources. In contrast, in the south, arable land is the limiting factor. The simplified problem provides a good basis from which to build a more sophisticated model that can appropriately characterize China's resources distribution, as well as natural and managed conditions. In the following Chapter, the motivations for the improvements needed for the detailed model are outlined and the full formulation of the detailed model is presented.

Chapter 3

Detailed Model

In this Chapter, we begin by considering how the simplified model of Chapter 2 can be extended to include a more realistic heterogeneous representation of China's resources and hydrologic flux balance. Then we present the full formulation of the detailed optimization problem for evaluating food production capacity in China. The detailed version of the model provides a basis for predictions of the population that can be sustainably fed under various scenarios. Finally, we conclude with a summary of required data for the detailed model.

3.1 Motivation for A More Detailed Model

Although the simplified model of Chapter 2 predicts a number of people fed that is close to the current population when matching nominal conditions (α is equal to one), it ignores many realistic features such as spatial and temporal heterogeneity in climate, land use and crop parameters within each region, water balance at the river basin scale, and the mixture of crops in people's diet. This reduces its credibility for predicting the response to changes in climate, arable

land, and diet as well as the impact of large infrastructure project such as the South-to-North Water Diversion. In this section, we highlight the major limitations of the simplified model and outline the improvements needed to provide credible predictions of food production in China.

Spatial Variability

In the simplified problem of Section 2.1, we divided China into only two regions. However, climate and land use over China are greatly heterogeneous. To account for the heterogeneity, China should be divided into much smaller units. Because much of the available data are available at the resolution of 0.5° by 0.5°, this is a convenient size to adopt for our analysis unit, which we will refer to as a pixel. The size of a pixel is about 2,500 km^2. There are about four thousands pixels covering mainland China.

Crop Type

In the simplified model, only a single crop type was considered. However, all the main crop types consumed in China should be included in the extended model in order to represent the typical Chinese diet. Figure 3-1 illustrates the average daily breakdown of the food types included in the Chinese diet, expressed in caloric content (FAOSTAT 2009). The largest food groups are wheat, rice, maize, starchy roots (tubers), oil crops, vegetables, meats, milk, and eggs which comprise at least 90% of the daily caloric demand in China for each year from 1990-2005. The daily caloric consumption per person increased about 300 calories during this period. There is a decreasing trend in cereals consumption and an increasing trend in oil crops, vegetables, meat, and eggs consumption.

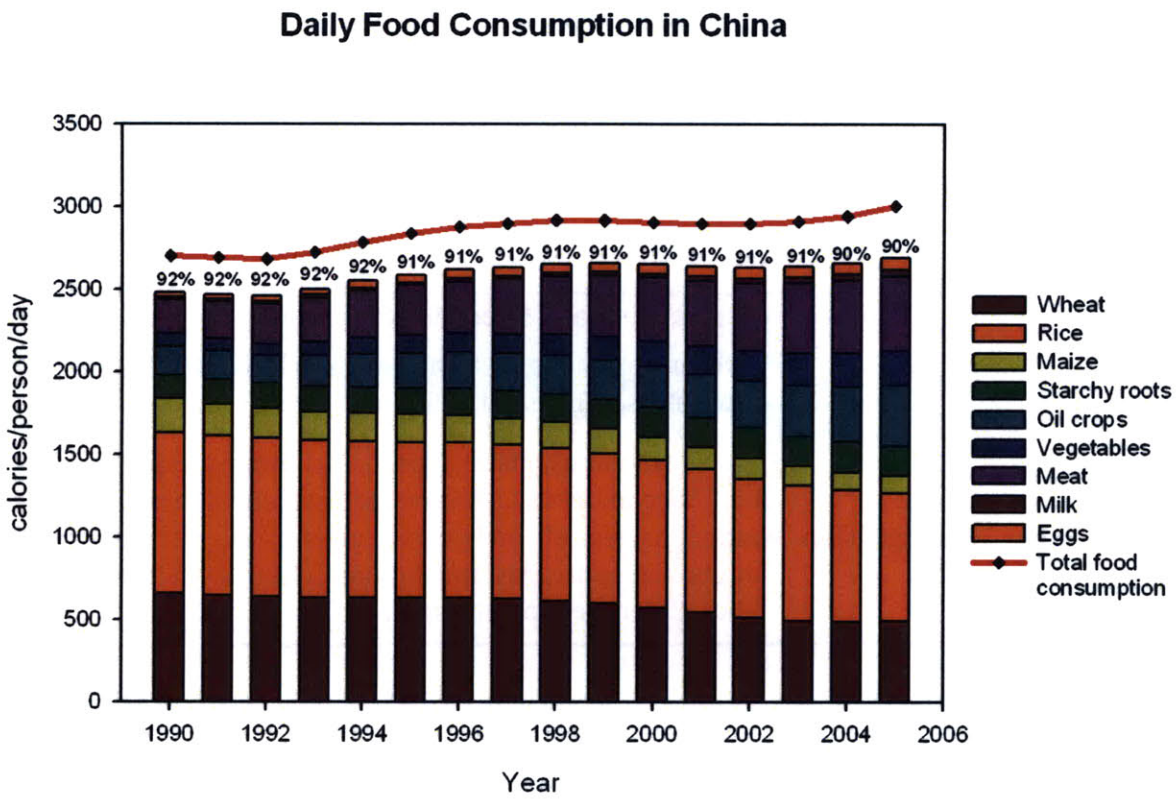

Figure 3-1: Daily caloric consumption in Chinese diet and contribution from the model food categories during 1990-2005.

Domestic utilization provided in (FAOSTAT 2009) includes crop use for direct food consumption, animal feed and seed, and other net uses. The domestic crop utilization thus implicitly includes animal products consumed in the Chinese diet. In total, there are seven crop categories considered in the model. Among them, starchy roots (tubers), oil crops, and vegetables categories include several sub-species. Adding one more crop category from seven crops would result in 185 more possible crop sequences for each pixel (one more single, 15 more double, and 169 more triple sequences) . We represent these crop categories as a multiple-crop group in order to control the complexity of the model. Table 3-1 summarizes the seven model crop categories and their main sub species according to (FAOSTAT 2007b).

Table 3-1: The model crop categories and sub categories.

	category	sub-category
Individual crops	Spring wheat	-
	Winter wheat	
	Rice	-
	Maize	-
Crop group	Tubers	cassava, potatoes, sweet potatoes, yams
	Oil crops	soybeans, groundnuts, sunflower seed, cottonseed, coconuts, sesame seed, palm nuts-kernels, olives, linseed
	Vegetables	tomatoes, onions, garlic, carrots and turnips, cauliflowers and broccoli, leeks, cabbages, lettuce, cucumbers, pumpkins, squash, and gourds, green peas, green beans, artichokes, asparagus, mushrooms, chillies, watermelons, other melons, eggplants, spinach

Imports and Exports

The simplified model considers China's domestic production. According to FAOSTAT, China imported more oil crops than the amount that was domestically produced in 2005. On the other hand, cereal imports were close to exports, which were about 3.5 percents of domestic cereal production (FAOSTAT 2007a). We need to account for the amount of imports and exports in the detailed model in order to insure flexibility for analysis of alternative scenarios.

River Basins and Flow Routing

In the simplified model, the water balance is greatly simplified with precipitation and evapotranspiration evenly distributed over each half of the country. It was also assumed that water can be readily transported anywhere in each region. However, precipitation and evapotranspiration vary greatly throughout the country and water can only be moved naturally via gravity or artificially through infrastructure. A more realistic model needs to incorporate an

accurate water balance that accounts for the movement of water. Since precipitation and evapotranspiration vary at scales much smaller than river basins, it is necessary to perform water balance calculations at both pixel and basin scales. Flow routing information is necessary for these calculations. The model needs to know the pixels tributary to each pixel as well as the identity of all pixels included in each river basin. Figure 3-2 shows an example of a drainage basin and its flow routing. The red arrow represents flow direction of each pixel. In this example, tributary or upstream pixels of pixel no. 6 are pixel no. 1 and 2. Pixel no. 12 is the outlet of the basin.

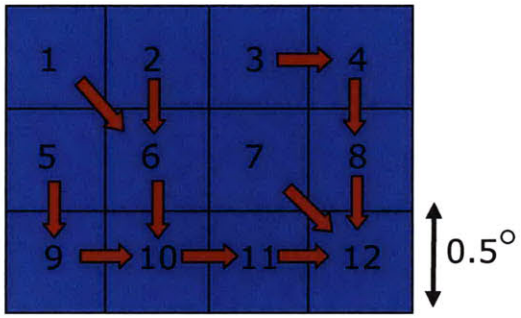

Figure 3-2: Flow routing scheme.

Typically, high resolution topographic data are used to determine flow directions and delineate the boundaries of a river basin. There are about thirty major river basins in China. We assume that these basins are self-contained, and there is no distinction between surface and groundwater flows.

3.2 Decision Variables

Decision variables are the problem unknowns that are adjusted to maximize or minimize the objective function. This section describes the decision variables introduced by the model enhancement summarized in Section 3.1.

3.2.1 Crop Categories

The crops included in the model are winter wheat, spring wheat, rice, maize, tubers, oil crops, and vegetables. Winter wheat and spring wheat are assumed to have the same expected yield and are counted as one crop for consumption purposes. The model is intended to simulate crop production, but the Chinese diet also includes meats, milk, and eggs. These animal products are not included directly but are accounted for by the crops they consume. In this model, meat produced from grazing is neglected both in the diet and in production.

3.2.2 Crop Sequence

In China, roughly half of the cropland is cultivated for more than one season per year (i.e. is multicropped) (Frolking et al. 2002). We allow up to three crop sequences to grow in one calendar year in the model. Winter wheat is unique from the other sequences because it can only be grown over the winter. When there are no constraints 7 crops give 49 double-crop combinations and 343 triple-crop combinations. When the winter wheat constraint is added these figures drop to 42 double-crop and 252 triple-crop combinations. The total possible crop sequences from one-, double-, and triple-crop sequences are 301.

3.2.3 Irrigated vs Rainfed Agriculture

In the simplified model, we assumed that water supply from precipitation can be transported anywhere in each region. However, we need infrastructure to store rainfall that falls on

noncropland and off growing season, and a system to deliver this water supply to crop fields. Irrigation plays a major role in improving and expanding agricultural practices in China. Approximately 47% of China's cropland is irrigated (Doll & Siebert 1999). Therefore in the detailed model, we distinguish between cropland that is irrigated and rainfed. Crops can be grown on an irrigated pixel so long as water demand can be met throughout the growing season from water flowing from tributary (upstream) pixels. Crops that are not grown on a non-irrigated pixel must obtain enough water to sustain their growth from precipitation falling only in that pixel. This is known as rainfed agriculture.

The primary decision variables for this model are $LI_{p,s}$ and $LD_{p,s}$ the amount of irrigated cropland devoted to crop sequence s in pixel p and the amount of rainfed cropland devoted to crop sequence s in pixel p, respectively. Several of the remaining decision variables, such as basin runoffs R_b, evapotranspiration E_p and $E_{p,nc}$, and municipal and industrial water loss to evaporation W_b, appear in the water balance constraints. The production variable $M_{p,c}$, and the number of people fed N, appear in the food balance constraints. The list of the model's decision variables are summarized in Table 3-2 below.

Table 3-2: Summary of the decision variables of the detailed model

Decision variables	Description	Units
$LI_{p,s}$	irrigated cropland devoted to crop sequence s in pixel p	ha
$LD_{p,s}$	rainfed cropland devoted to crop sequence s in pixel p	ha
LN_p	noncrop area in pixel p	ha
R_b	runoff in basin b	10^6 m^3 year^{-1}
E_p	actual evapotranspiration from pixel p	10^6 m^3 year^{-1}
$E_{p,nc}$	noncrop evapotranspiration from pixel p	10^6 m^3 year^{-1}
W_b	water loss associated with municipal and industrial water use in basin b	10^6 m^3 year^{-1}
$M_{p,c}$	total production of crop c in pixel p	10^3 kg year^{-1}
N	number of people supported by agricultural production in China	10^6 people

3.3 Objective Function

The objective of the detailed model maximizes the number of people fed while minimizing the misfit between simulated and nominal conditions. However, now the nominal condition is described by the cropland in each pixel for each crop sequence during the calibration period:

$$\underset{LI_{p,s},LD_{p,s},N}{\text{minimize}} \quad \boldsymbol{F}(N, LI_{p,s}, LD_{p,s}) = N - \alpha\left(\sum_{p,s}\left\|\frac{LI_{p,s} - LI^{o}_{p,s}}{\left\langle LI^{o}_{p}\right\rangle}\right\|^2 + \sum_{p,s}\left\|\frac{LD_{p,s} - LD^{o}_{p,s}}{\left\langle LD^{o}_{p}\right\rangle}\right\|^2\right). \tag{3-1}$$

Here $LI^{o}_{p,s}$ is the nominal or calibration period irrigated cropland [ha], $LD^{o}_{p,s}$ is the nominal or calibration period rainfed cropland [ha], while $\left\langle LI^{o}_{p}\right\rangle$ and $\left\langle LD^{o}_{p}\right\rangle$ are the corresponding average over all sequences. α is a weighting factor determining whether the objective is

prioritized toward maximizing people fed or matching calibration period conditions, as discussed in Chapter 2.

3.4 Constraints

3.4.1 Land Constraints

Total area for pixel *p*:

In each pixel, a total land area is divided into cropland and noncropland. The total cropland is a summation of irrigated and rainfed cropland devoted to each crop sequence. Therefore, the total area is expressed as follow:

$$\sum_{s \in all\ crop\ sequences} \left(LI_{p,s} + LD_{p,s} \right) + LN_p = AT_p, \tag{3-2}$$

where AT_p is the total land in pixel p [km^2].

Arable land constraint for pixel *p*:

There are several factors that determine whether an area is suitable for growing crops. Temperature, crop water demand, slope and soil suitability are key factors. In our model, arable land strictly refers to an area that has suitable slope and soil properties for agriculture. Soil properties considered in the model include physical soil characteristics, soil fertility, and salinity and alkalinity. Section 4.4 explains in detail how we quantify arable land area from soil properties. The arable land constraint is only applied to maize, rice, and wheat. Due to the aggregation of the three food groups of tubers, oil crops, and vegetables, we could not apply the soil suitability approach to them since the soil requirements are different for each species in the

category. However, the amount of cropland for tubers, oil crops and vegetables is implicitly controlled by dietary demand.

There are three upper bound constraints on the total cropland, one for each crop, as shown in Equation (3-3).

$$\begin{aligned} &Maize: && \sum_{s \in seq\ with\ maize} \left(LI_{p,s} + LD_{p,s}\right) \le AR_{p,maize}, \\ &Rice: && \sum_{s \in seq\ with\ rice} \left(LI_{p,s} + LD_{p,s}\right) \le AR_{p,rice}, \\ &Wheat: && \sum_{s \in seq\ with\ wheat} \left(LI_{p,s} + LD_{p,s}\right) \le AR_{p,wheat}, \end{aligned} \tag{3-3}$$

where $AR_{p,crop}$ is the total arable land in pixel p for the specified crop [km^2]. Note that the summation of the cropland is not over all crop sequences. There are 115 crop sequences that include maize and 115 that include rice. The 146 crop sequences for wheat include both spring and winter wheat.

3.4.2 Water Constraints

Annual water balance for river basin b:

Our climatological analysis considers long-term average conditions. This can be equated with steady-state conditions for water balance, because the change in water storage within a unit area is negligible over time-scales greater than one year. Using this steady-state assumption, the basin water balance equation becomes

$$P_b - E_b - W_b = R_b, \tag{3-4}$$

where P_b is the total basin precipitation [10^6 m^3 year^{-1}], E_b is the non-municipal and industrial basin evapotranspiration [10^6 m^3 year^{-1}], W_b is the water loss (evaporation) associated with

municipal and industrial water use in the basin, and R_b is the runoff. Runoff includes both direct surface runoff through rivers and groundwater flow which eventually appears as base flow to streams or as direct recharge to the ocean.

Total basin precipitation is calculated as,

$$P_b = \sum_{p \in pixels\ in\ basin\ b} \left(P_p\right)\left(AT_p\right), \tag{3-5}$$

where P_p is the precipitation rate in pixel p [mm year^{-1}], A_p is the total area of pixel p, and B_b is the total number of pixels within basin b. A similar equation gives the total basin evapotranspiration,

$$E_b = \sum_{p \in pixels\ in\ basin\ b} E_p, \tag{3-6}$$

where E_p is the actual evapotranspiration (AET) from pixel p [10^6 m^3 year^{-1}]. AET is different for different land uses, so E_p is expanded to:

$$E_p = \sum_{s \in all\ crop\ sequences} \left[\left(EI_{p,s}\right)\left(LI_{p,s}\right)+\left(ED_{p,s}\right)\left(LD_{p,s}\right)\right]+\left(E\_N_p\right)\left(LN_p\right), \tag{3-7}$$

where $EI_{p,s}$ and $ED_{p,s}$ are the actual evapotranspiration rates of crop sequence s in pixel p for irrigated and rainfed cropland, respectively. Crop water demand (i.e. crop actual evapotranspiration) can be estimated using the crop coefficient approach, which is described in Section 4.3.2. This approach requires knowledge of monthly temperature and potential evapotranspiration at each pixel and a crop coefficient for each crop type. The final term in (3-7) is the actual evapotranspiration from noncropland which is highly variable and uncertain.

The water loss associated with municipal and industrial (M&I) water use, W_b, is calculated as

$$W_b = \sum_{p \in pixels\ in\ ba\ sin\ b} W_p, \tag{3-8}$$

where W_p is the water loss from M&I in pixel p [10^6 m^3 $year^{-1}$]. W_p is calculated from provincial M&I water diversion (the actual water required for M&I) per capita, WP_v [m^3 $capita^{-1}$ $year^{-1}$] as follows:

$$W_p = (1 - effc) \times WP_v \times F_p \times N \tag{3-9}$$

where N is the total number of people fed and F_p is a fraction of national population in pixel p. $effc$ is a ratio between M&I return flow and M&I diversion. Note that the water loss to evaporation from M&I decreases to zero as the $effc_w$ increases to one. The remaining water diverted for M&I appears as outflow.

Annual water balance in pixel p:

Assuming steady-state conditions, the change in storage in a pixel is negligible and the water balance in pixel p is

$$(P_p)(AT_p) + R_{p,tributary} - E_p - W_p = Q_p. \tag{3-10}$$

Q_p is the outflow from pixel p. This outflow is the inflow to the immediate downstream pixel and include both streamflow and groundwater flow. W_p is the water loss from M&I in pixel p.

The extra term $R_{i,tributary}$, which represents water flow between units, is the sum of all the runoff generated from tributary pixels entering pixel p:

$$R_{p,tributary} = \sum_{n \in pixels\ tributary\ to\ pixel\ p} [(P_n)(AT_n) - E_n - W_n]. \tag{3-11}$$

Since we assume that rainfed cropland is sustained solely by precipitation, flow from tributary pixels is only available for pixels that are specified to include irrigated cropland. Therefore, there is an extra pixel annual water constraint for a pixel with only rainfed cropland. This constrain is to check whether there is enough precipitation for total evapotranspiration, as follows:

$$E_p \leq (P_p)(AT_p) - W_p \tag{3-12}$$

3.4.3 Production-Consumption Constraints

The total supply of crop c in all of China is its total crop production plus net imports S_c [10^9 kg year^{-1}]. The total demand of the crop depends on the Chinese population and their consumption rate of that crop C_c [kg capita^{-1} year^{-1}]. The balance between supply and demand of each crop is:

$$\sum_{p \in all\ pixels\ in\ China} \left(M_{p,c}\right) + S_c = (N)(C_c), \tag{3-13}$$

where $M_{p,c}$ is the production of crop c in pixel p. $M_{p,c}$ is further expanded into:

$$M_{p,c} = \sum_{s \in all\ crop\ sequences} \left[\left(LI_{p,s} + LD_{p,s}\right)\left(Y_{c,s}\right)\right] \tag{3-14}$$

where $Y_{c,s}$ is the expected yield of crop c from sequence s [10^3 kg ha^{-1}]. Equation (3-13) is then re-written as follow

$$\sum_{p \in all\ pixels\ in\ China} \left(\sum_{s \in all\ crop\ sequences} \left[\left(LI_{p,s} + LD_{p,s}\right)\left(Y_{c,s}\right)\right] \right) + S_c \geq (N)(C_c). \tag{3-15}$$

Equation (3-15) yields the total number of people fed from optimal allocation of cropland for each crop sequence.

3.5 Summary of Required Inputs

One of the most crucial tasks in this work is acquisition of all required model inputs. It is possible to estimate many of these inputs from ground-based sources and from remote sensing data sets. However, not all necessary data are available, especially at the pixel scale. Table 3-3 summarizes required inputs that are either available or derivable from data in literature and Table 3-4 summarizes not available inputs.

Table 3-3: Summary of available and derivable inputs for the detailed model.

	Inputs	Symbol	Units	Reference
1	Total pixel area	AT_p	km^2	(Chuang et al. 1996)
2	Delineation of major river basins and pixels tributary to pixel *p*		-	(ATLAS 1999) and (Oki & Sud 1998)
3	Arable land for grains	AR_p	km^2	Chapter 4
4	Meteorological data			
	Precipitation	P_p	mm $year^{-1}$	
	Potential evapotranspiration		mm $month^{-1}$	(Thomas 2008)
	Temperature		°C	
5	Actual evapotranspiration from irrigated cropland	$EI_{p,s}$	mm $year^{-1}$	Chapter 4
6	Actual evapotranspiration from rainfed cropland	$ED_{p,s}$	mm $year^{-1}$	Chapter 4
7	Municipal and industrial water diversion	WP_v	m^3 $capita^{-1}$	(National Bureau of Statistics 2008)
8	Population fraction	F_p	-	(CIESIN 2005)
9	Crop consumption	C_c	kg $capita^{-1}$ $year^{-1}$	(FAOSTAT 2009)
10	Average annual yield	$Y_{c,s}$	10^3 kg ha^{-1}	(FAOSTAT 2009)
11	Net crop import	S_c	10^9 kg $year^{-1}$	(FAOSTAT 2009)

Table 3-4: Summary of unavailable inputs.

	Description	Symbol	Units
1	Nominal irrigated cropland for each crop sequence	$LI^{o}_{p,s}$	ha
2	Nominal rainfed cropland for each crop sequence	$LD^{o}_{p,s}$	ha
3	Actual evapotranspiration from natural land	E_N_{p}	mm year^{-1}

In Chapter 4 we will review and discuss the available inputs in detail. Some of the inputs are readily available, such as pixel-scale precipitation and temperature. However, some need to be derived from other variables, such as pixel-scale arable land and the actual evapotranspiration from cropland. In Chapter 5, we will focus on the estimation of the inputs that are not available and not readily derived from other available data. These inputs are existing cropland for each crop sequence and AET from noncropland.

Chapter 4

Review of Available Model Inputs

In this chapter, we present a comprehensive review of the required inputs for the detailed model. Inputs described in this Chapter are either readily available from the literature or can be derived from other available variables. The model inputs are categorized into three groups: (1) Land-related inputs, (2) Water-related inputs, and (3) Production/consumption-related inputs. Variables discussed here correspond to the indicated entries in Table 3-1.

4.1 Land-Related Inputs

4.1.1 Study Area and Model Grid

In this research, we use ArcGIS software to analyze, manipulate, and compare spatially distributed data. Our study area is defined by the pixels in China for which all the required model data available. The different data types, or "layers", considered are China's boundary (Chuang et al. 1996), climatological data (Thomas 2007), flow routing data (Oki & Sud 1998), and cropland data (Frolking et al. 2002). In Figure 4-1, the dark gray area is the intersection between these

four layers; this area defines our study domain and will be referred to as the China mask. Note that our study domain only includes mainland China because the cropland data set does not cover Taiwan, Hong Kong, Macau, and the small islands beyond Hainan. Our analysis units are square grid cells (pixels) specified in geographical coordinates because most of the data sets used in this research were provided in this coordinate system. The geographic coordinate system enables us to specify location on Earth in latitude and longitude using a spherical coordinate system. The size of each pixel is 0.5° by 0.5°. For area-related inputs, we use the Lambert azimuthal equal-area projection to project data to geographic coordinate. A map projection is a method to represent the surface of a sphere or other shape on a plane and the Lambert azimuthal equal-area projection accurately represents area in all regions of the sphere. The actual area in each pixel ranges from 1900 km^2 to almost 3000 km^2 as we move from north to south.

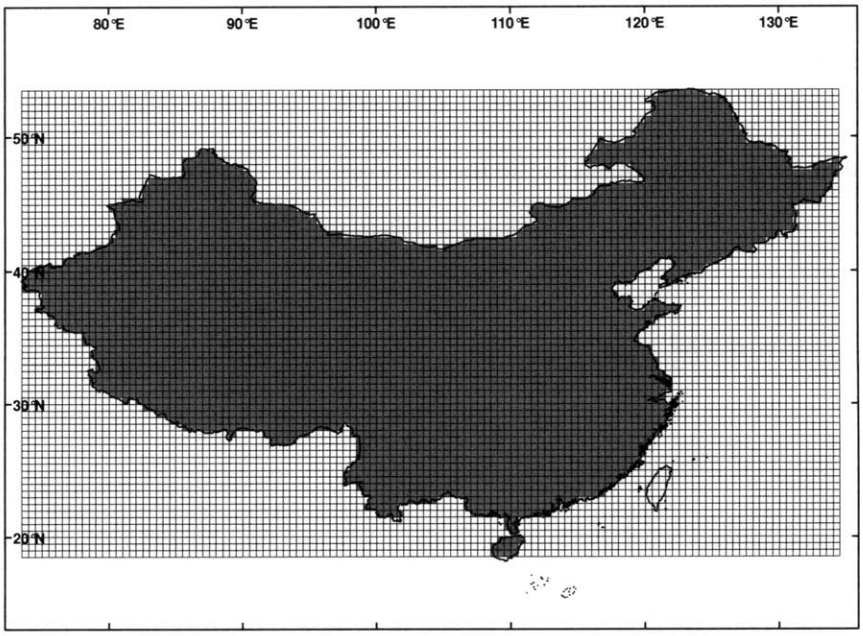

Figure 4-1: China mask and model grid in geographical coordinates.

4.1.2 Delineation of Basin Boundary and Definition of Tributary Areas

Typically, fine-resolution topographic data are used to determine the flow direction and the boundaries of river basin. An example is HYDRO1k, which is a global geographic database of topographically derived information about drainage basins, streams, flow directions, and flow accumulation. The HYDRO1k database is derived from USGS' 30 arc-second digital elevation model of the world (GTOPO30), which is a global raster Digital Elevation Model (DEM) with a horizontal grid spacing of approximately 1 kilometer. However, for our model we need to obtain the flow direction and the drainage basins at the same resolution of our analysis, which has much lower resolution than DEM. The DEM cannot be directly aggregated to the 0.5° by 0.5° resolution to obtain coarse resolution or upscale river basins as this approach would not take into account the fine-scale movement of the stream network. There are several methods developed to derive coarse-scale flow routing and river basin boundaries from fine-scale topographical data.

The river channel network used in our model is based on the Total Runoff Integrated Pathways (TRIP) network developed by Oki & Sud (1998). TRIP provides information of lateral water movement at 0.5° by 0.5° resolutions. Basin boundaries and flow directions in TRIP were derived from a global DEM called ETOPO5. They employed the lowest neighbor algorithm to determine flow directions and verified the river network obtained with two atlases by Teikoku-Shoin (1985) and Rand McNally (1995). The information from TRIP flow directions is used to provide the tributary pixels of each pixel and each basin in the water balance constraints of our model. We also compare TRIP delineated basin boundaries with a map from the National Physical Atlas of China (shown in Figure 4-2). The red outline represents basin boundaries from TRIP and the map is the drainage basins from the Atlas. We then aggregate small basins in TRIP

that belong to the same basin in the Atlas. The map of basin boundaries used in our model is shown in Figure 4-3.

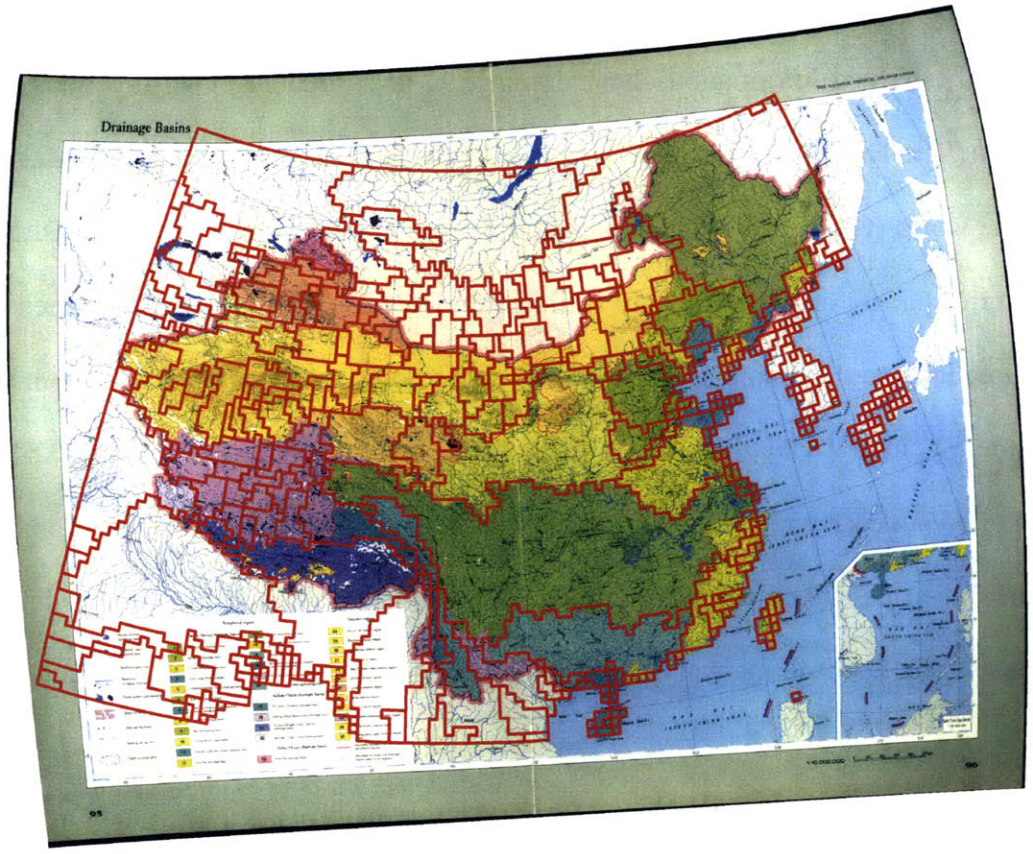

Figure 4-2: TRIP basin boundaries (red outline) overlaid on drainage basins map. They are shown with the original projection of the drainage basins map which is the azimuthal equal-area projection.

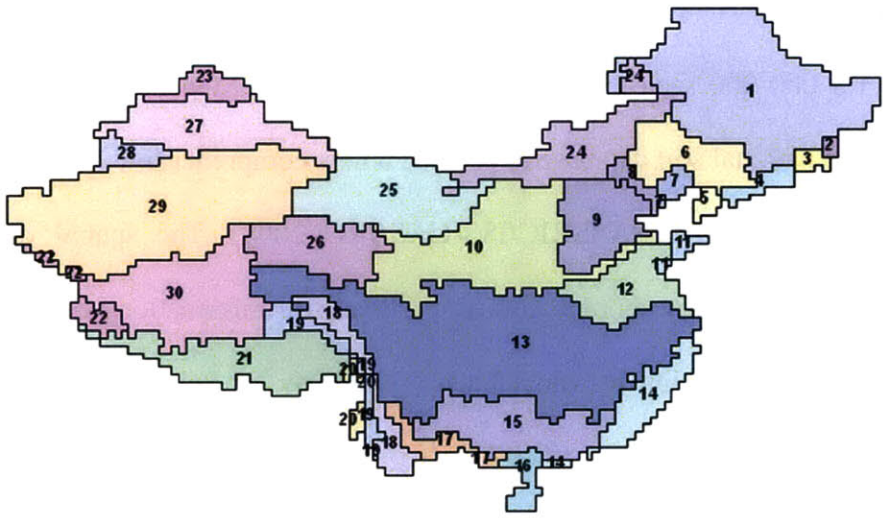

1 Heilong Jiang
2 Suifen He
3 Tumen Jiang
4 Yalu Jiang
5 Liaodong Bandao
6 Liao He
7 West Liaoning & Hebei coastal rivers
8 Luan He
9 Hai he
10 Huang He
11 Shandong Bandao
12 Huai He
13 Chang Jiang (Yangtze)
14 South-east China coastal rivers
15 Zhu Jiang (Pearl)
16 Guangdong & Guangxi coastal rivers
17 Yuan Jiang (Hong Ha)
18 Lancang Jiang (Mekong)
19 Nu Jiang (Thanlwin)
20 Dulong Jiang
21 Yarlung Zangbo Jiang - Ganga
22 Sengge Zangbo (Indus)
23 Ertix He
24 Wuyur He
25 Baicheng
26 Nei Mengol
27 Junggar
28 Ili He
29 Tarim
30 Qiangtang Gaoyuan

Figure 4-3: River basins of the optimization model in geographical coordinates.

4.1.3 Arable Land

Arable land is land that has suitable slope, soil properties, water availability, and climate for a particular crop. In this section, we consider the first two factors: slope and soil properties which are land-related. Water availability and climate factors will be accounted for in Section 4.2 of Water-related inputs. The amount of arable land provides an upper bound constraint on cropland. This becomes especially important for the scenario analysis under climate change, because cropland could expand within arable land area where climatic conditions permit.

4.1.3.1 Soil Properties

Recently the 1:5 000 000 scale FAO-UNESCO Digital Soil Map of the World was combined with regional and national soil database to provide a new comprehensive Harmonized World Soil Database (HWSD) (FAO/IIASA/ISRIC/ISS-CAS/JRC 2008). The spatial resolution of this database is 30 arc-second (or about 1 km). For China, soil information is based on the 1:1 000 000 scale Soil Map of China by the Chinese Academy of Sciences. The HWSD database provides soil parameters for the surface layer (0-30 cm) and the subsoil layer (30-100 cm). Available soil physical and chemical properties are shown in Table 4-1 below.

Table 4-1: Physical and chemical properties provided in HWSD.

Soil Properties	UNITS
Gravel Content	%vol.
Sand Fraction	%wt.
Silt Fraction	%wt.
Clay Fraction	%wt.
USDA Texture Classification	name
Reference Bulk Density	kg/dm^3
Organic Carbon	%weight
pH (H2O)	-log(H+)
CEC (clay)	cmol/kg
CEC (soil)	cmol/kg
Base Saturation	%
TEB	cmol/kg
Calcium Carbonate	%weight
Gypsum	%weight
Sodicity (ESP)	%
Salinity (Elco)	dS/m

However the HWSD database does not provide slope information, which is also an important factor in determining arable land.

4.1.3.2 Slope

We use slope data set provided in HYDRO1k. The resolution of this database is also 30 arc-second (about 1 km). The slope data describes the maximum change in the elevations between each grid cell and its eight neighboring cells. The slope is expressed in integer degrees of slope between 0 and 90. The map below illustrates slope information over China. The dark green color represents plain areas where slope is suitable for most crops (0-1 degree).

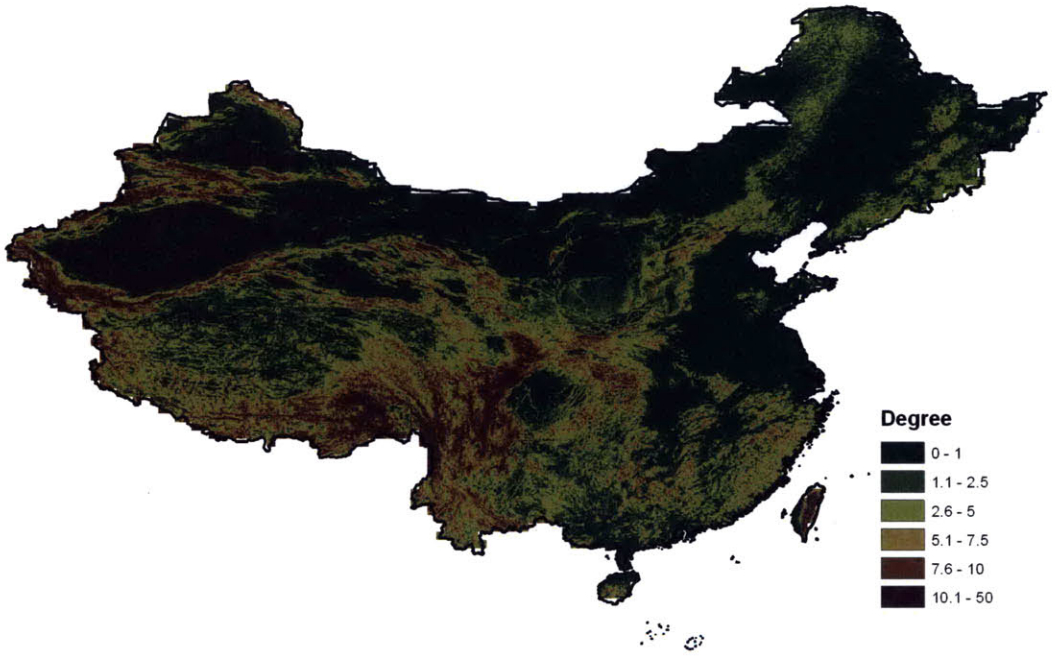

Figure 4-4: Slope information over China from HYDRO1k.

4.1.3.3 Crop Requirements

To determine arable land, we use a matching method between slope and soil properties with requirements for a particular crop. The publication series of Land Evaluation by Sys et al. (1991 and 1993) provide principles and guidelines for land-use planning emphasizing agricultural land-use. Slope and soil properties influence the suitability of land. Sys et al. (1991) define the different levels of land suitability in the degree of limitation, where limitations are deviations from the optimal conditions, as follows:

- **no limitations (level 0):** the characteristic (quality) is optimal for plant growth;
- **slight limitations (level 1):** the characteristic is nearly optimal for the land utilization type and affects productivity for not more than 20% with regard to optimal yield;
- **moderate limitations (level 2):** the characteristic has moderate influence on yield decreases; however, benefit can still be made and use of the land remains profitable;
- **severe limitations (level 3):** the characteristic has such an influence on productivity for the land that the use becomes marginal for the considered land utilization type; and
- **very severe limitations (level 4):** such limitations will not only decrease the yields below the profitable level but even may totally inhibit the use of the soil for the considered land utilization type.

Part III of the series provides a comprehensive list of crop requirements with regard to slope and soil conditions for a wide range of crops commonly cultivated in the tropical and subtropical regions. The crop requirements were provided for five suitability classes: S1, S2, S3, N1 and N2. The limitation levels explained earlier could be expressed as land classes as follows Sys et al. (1993):

Limitation levels	Class levels
0, no	S1
1, slight	
2, moderate	S2
3, severe	S3
4, very severe	N1 and N2

An example of soil requirements for maize for class S1, S2, and S3 is shown in Table 4-2 below.

Table 4-2: Soil requirements for maize from Sys et al. (1993).

Land characteristics	Class			
	S1		S2	S3
	0	1	2	3
Topography				
Slope (%)				
(1)	0-1	1-2	2-4	4-6
(2)	0-2	2-4	4-8	8-16
(3)	0-4	4-8	8-16	16-30
Wetness				
Flooding	Fo	-	-	F1
Drainage				
(4)	good	moderate	imperfect	poor and
(5)	imperfect	moderate	good	aerobic
Physical characteristics				
Texture/structure	C<60s,Co,SiC,SiCL,Si,SiL,CL	C<60v, SC, C>60s,L,SCL	C>60v,SL,LfS,LS	fS,S,LcS
Coarse fragment (vol %)	0-3	3-15	15-35	35-55
Soil depth (cm)	> 100	100-75	75-50	50-20
CaCO3 (%)	0-6	6-15	15-25	25-35
Gypsum (%)	0-2	2-4	4-10	10-20
Fertility characteristics				
Apparent CEC (cmol(+)/kg clay)	> 24	24-16	< 16(-)	< 16(+)

Base saturation (%)	> 80	80-50	50-35	35-20
Sum of basic cations (cmol(+)/kg soil)	>8	8-5	5-3.5	3.5-2
pH	6.6-6.2	6.2-5.8	5.8-5.5	5.5-5.2
	6.6-7.0	7.0-7.8	7.8-8.2	8.2-8.5
Organic carbon (%)				
(6)	> 2.0	2.0-1.2	1.2-0.8	< 0.8
(7)	> 1.2	1.2-0.8	0.8-0.5	< 0.5
(8)	> 0.8	0.8-0.4	< 0.4	-
Salinity and Alkalinity				
Ece (dS/m)	0-2	2-4	4-6	6-8
ESP (%)	0-8	8-15	15-20	20-25

(1) Irrigated agriculture, basin furrow irrigation
(2) High level of management with full mechanization
(3) Low level of management animal traction or handwork
(4) Medium and fine textured soils.
(5) Coarse textured soils (sandy families).
(6) Kaolinitic materials.
(7) Non kaolinitic, non-calcareous materials.
(8) Calcareous materials.

We take into account all soil requirements (slope and 12 soil properties) presented in the table except the soil depth due to lack of data from the HWSD. To determine areas with suitable slope and soil properties, we first plot maps of slope and each soil property with ranges according to crop requirements for a particular class. Figure 4-5 below illustrate areas (in grey) where slope and soil properties are very suitable (Class S1) for maize. We can see that the limiting factors here are pH and organic carbon. We then overlay all these layers to obtain the areas where slope and all soil properties match the requirements.

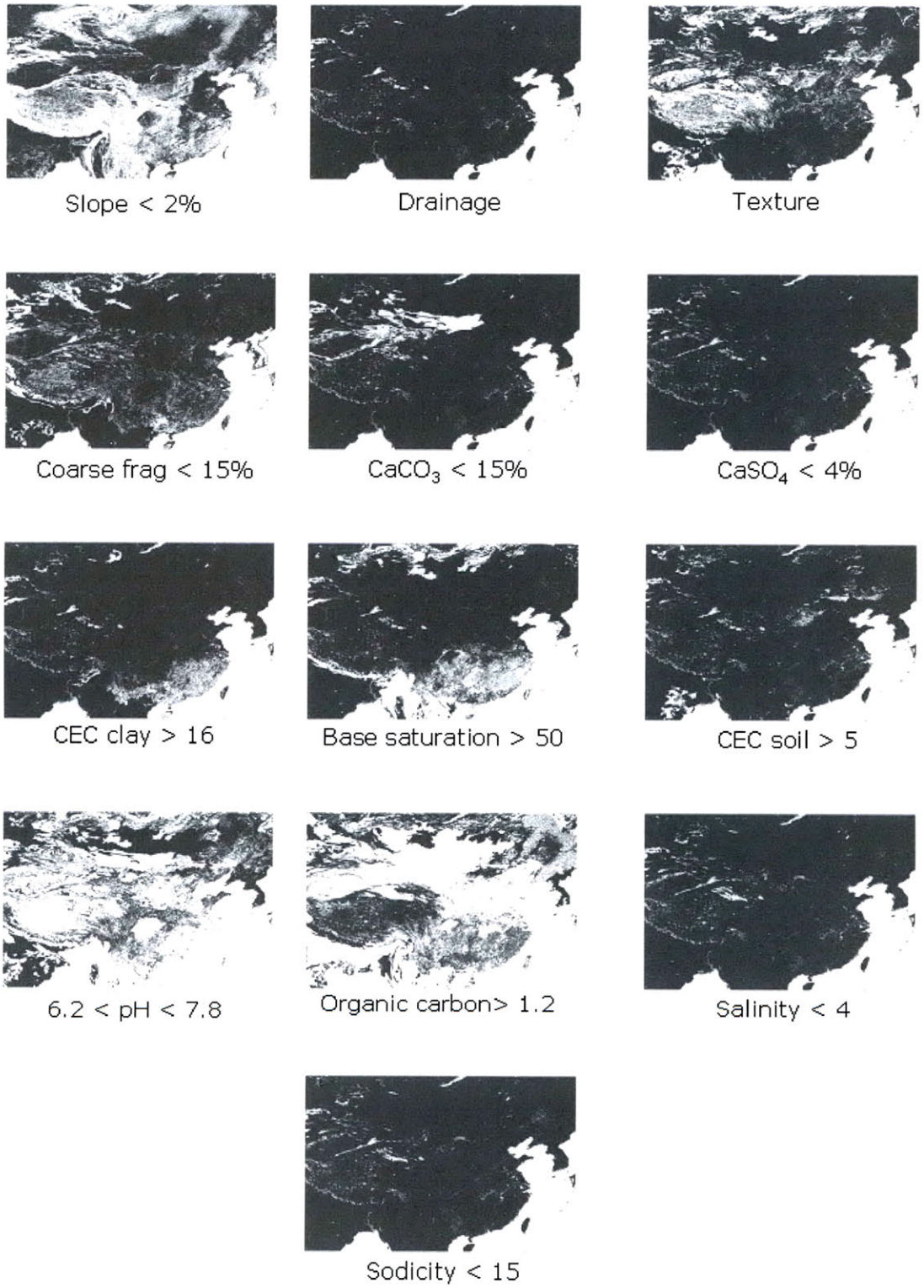

Figure 4-5: Maps of area where slope and soil characteristics are very suitable for maize (Class S1 requirements).

Figure 4-6 below shows the comparison between maize cultivated land (Frolking et al. 2002), and maize arable land of class S1, S2, and S3, respectively at 0.5° resolution.

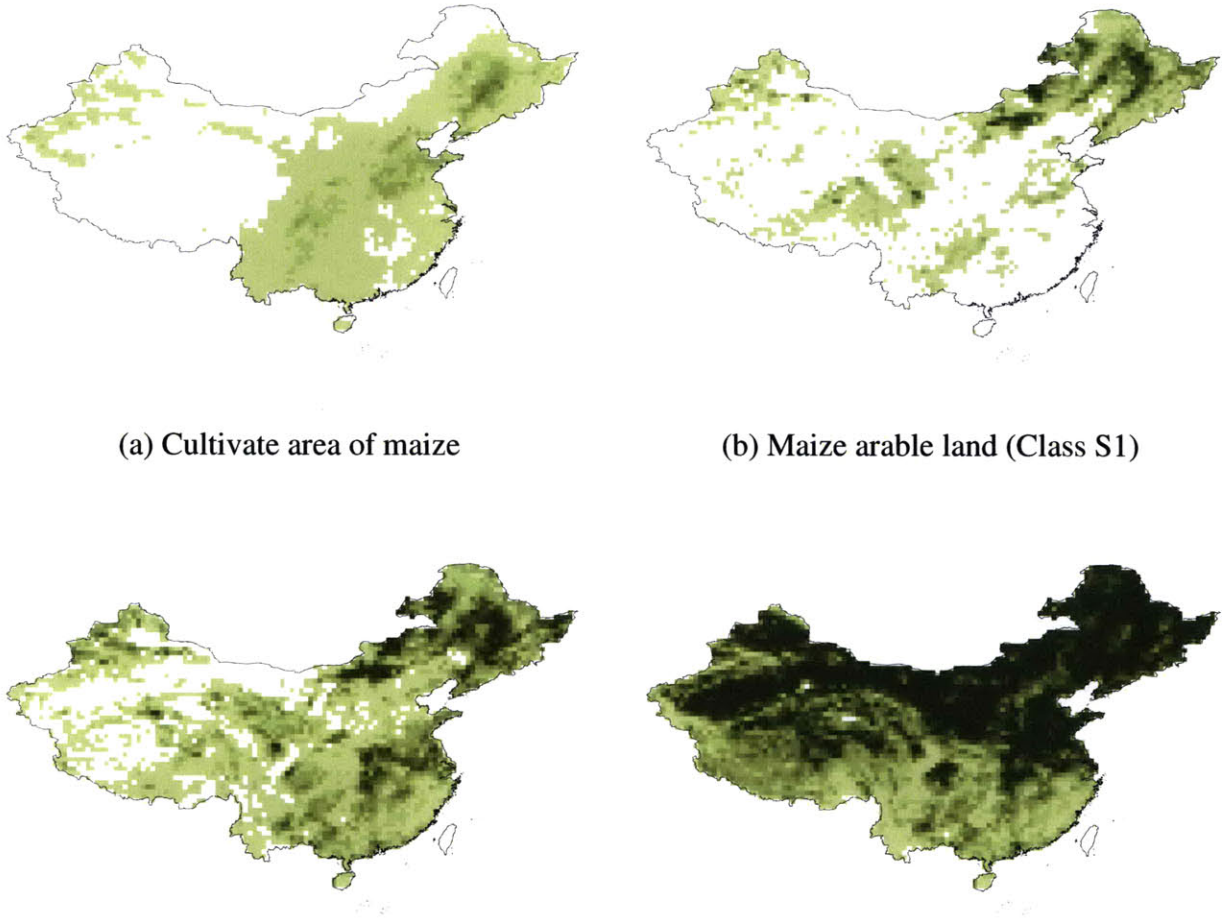

(a) Cultivate area of maize

(b) Maize arable land (Class S1)

(c) Maize arable land (Class S2)

(d) Maize arable land (Class S3)

Figure 4-6: The comparison between maize cultivated land, and estimated arable land. (a) maize cultivated land (Frolking et al. 2002); (b) maize arable land based on soil requirements for class S1; (c) maize arable land based on class S2, and (d) maize arable land based on class S3. The legend is percentage of arable land over total pixel area.

The maize cultivated land from Frolking et al. (2002) is a product of the combination between county-scale agricultural census statistics in 1990 and a fine-resolution land-cover map derived from 1995-1996 Landsat data. The map provides a basis to determine which suitability class appropriately represents arable land. From the comparison, we see that class S1 and S3 produce two extreme limits on the arable land. Therefore the suitability class S2 is selected as a criterion to determine the arable land extent for our study. There might be some areas that are not suitable for growing maize based on class S2 requirements but were reported as a maize cultivated land because these areas were fertilized or adjusted to have suitable soil conditions. As a result, the arable land will include all observed cultivated land provided by Frolking et al. (2002).

As mentioned in Section 3.1.2, we only calculate the arable land for maize, wheat, and rice due to data limitations and aggregation of multiple-crop categories of tubers, oil crops, and vegetables. Based on the method described in this Section, we obtain maps of arable land in the class S2 for major grains as shown in Figure 4-7.

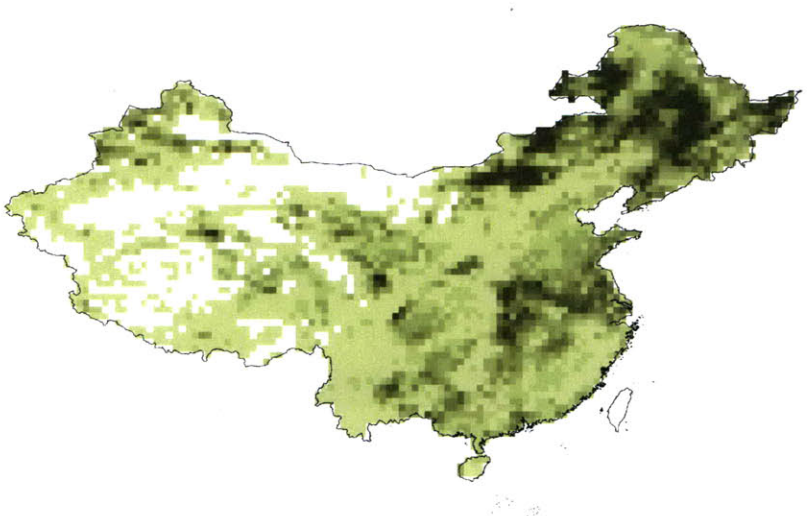

(a) Maize arable land

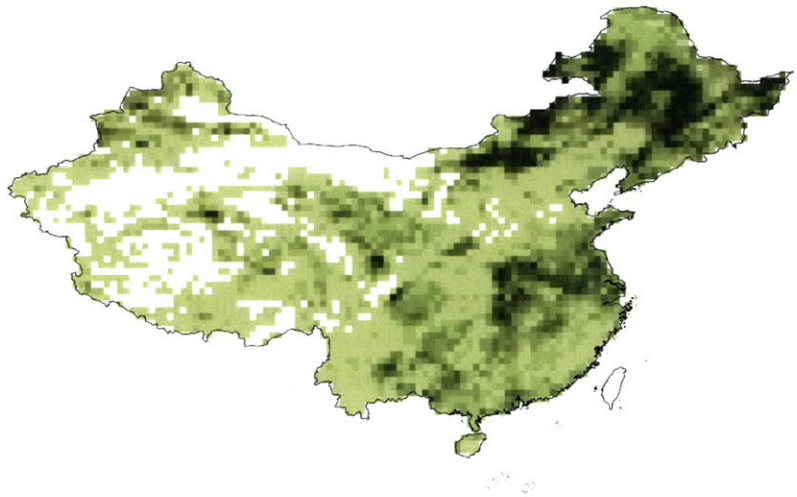

(b) Rice arable land

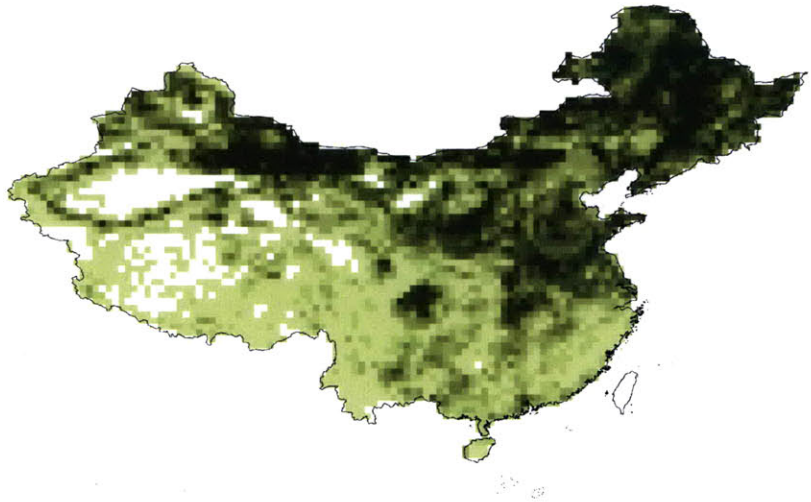

(c) Wheat arable land

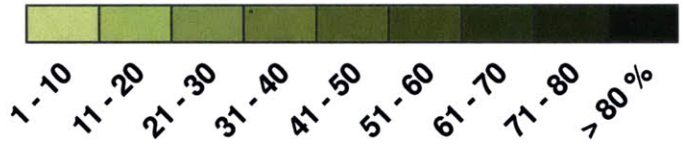

Figure 4-7: Arable land for (a) maize, (b) rice, and (c) wheat based on soil properties as a percentage of the total pixel area.

4.2 Water-Related Inputs

4.2.1 Meteorological Inputs

As described in Chapter 3, our model requires precipitation as the source of water supply, and temperature and potential evapotranspiration to calculate crop water demand. There are several monthly data sets of meteorological inputs over China such as Willmott and Matsuura's monthly and annual climatology, Global Climate Dataset from the Climate Research Unit (CRU), TRMM product 3B43, and monthly climatology from (Thomas 2007 and 2008). We use Thomas' data set in our model mainly because its potential evapotranspiration data set was constructed using the FAO Penman-Monteith method which is consistent with the crop coefficient approach. Thomas' meteorological data sets are monthly time series for the period 1951-1990 (hereafter, meteorological period). Even though the meteorological period is older than the baseline and calibration periods, according to a study by Qian & Zhu (2001) temperature anomaly in the recent years is consistent with the anomaly in the past, and year to year fluctuation in precipitation roughly accounts for 10% of the long term mean but there is no obvious trends during 1951-2000. Therefore, the climate data from the meteorological period are accurate indication for the baseline and calibration periods.

The spatial resolution of Thomas' data sets is 0.25° by 0.25°, which is finer than our model's pixel. We upscale them by taking the average of four neighboring pixels to arrive at 0.5° resolution data set. Figure 4-8 below illustrates the average annual precipitation (1951-1990) over China and the average annual temperature is shown in Figure 4-9 (Thomas 2007).

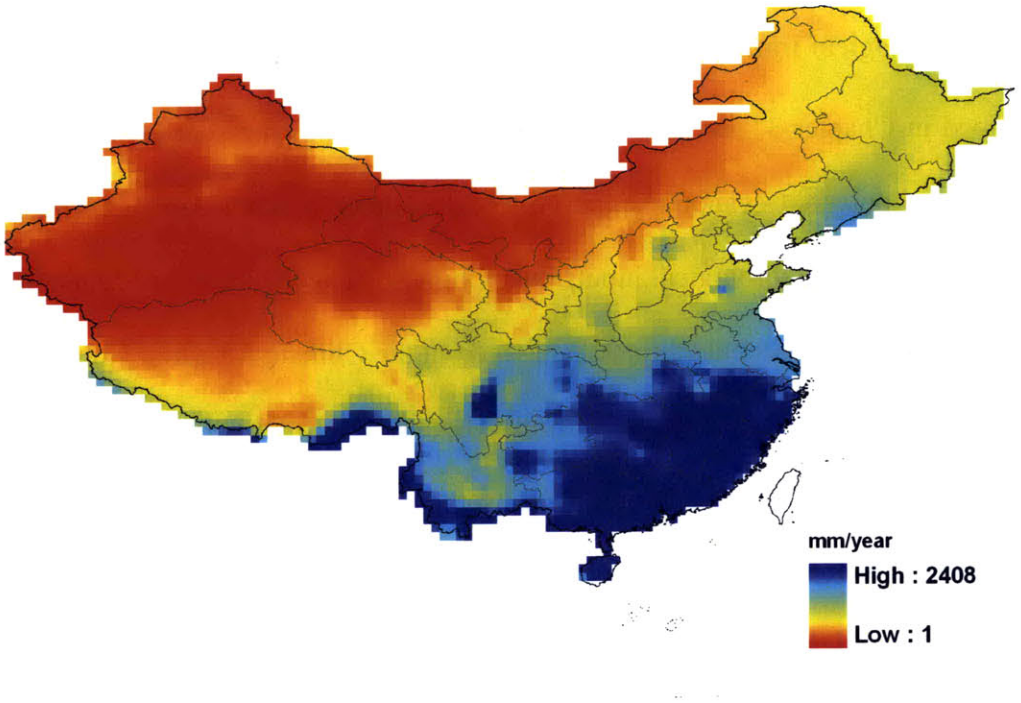

Figure 4-8: The average annual precipitation from 1951-1990.

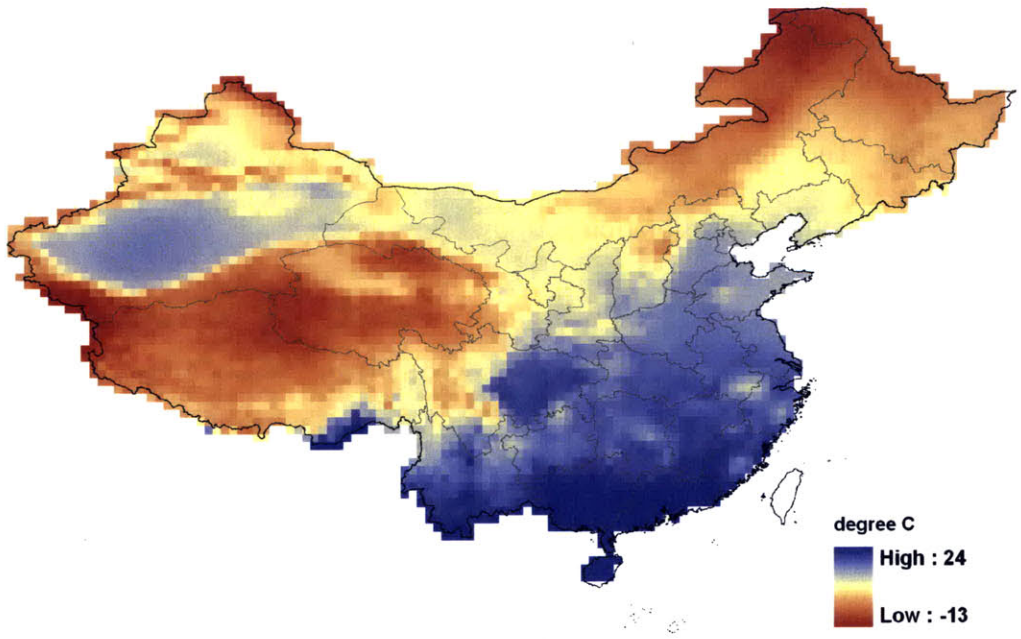

Figure 4-9: The average annual temperature from 1951-1990.

Potential evapotranspiration (PET) is a measure of the ability of the atmosphere to remove water from the surface through the process of evaporation and transpiration assuming there was sufficient water available. PET is usually calculated from other climatic factors and depends on type of surface. PET calculated from observed climatic variables on a reference surface is called reference evapotranspiration. Crop evapotranspiration can be estimated from the reference evapotranspiration by multiplying with the crop coefficient. The recommended method to calculate the reference evapotranspiration is the Penman-Monteith combination method, which is a procedure representing a climatological standard that depends on atmospheric conditions with land surface parameters assigned values for specified reference crop. The original form of the Penman-Monteith equation is:

$$ET_o = \frac{\frac{\Delta}{\lambda}(R_n - G) + \frac{\rho_a c_p}{\lambda}\frac{(e_s - e_a)}{r_a}}{\Delta + \gamma(1 + \frac{r_s}{r_a})} \qquad (4\text{-}1)$$

where R_n is the net radiation, λ is the latent heat of vaporization, G is the soil heat flux, $(e_s - e_a)$ represents the vapour pressure deficit of the air, ρ_a is the mean air density at constant pressure, c_p is the specific heat of the air, Δ represents the slope of the saturation vapour pressure temperature relationship, and γ is the psychrometric constant. There are two parameters that depend on reference surface: r_s and r_a, the (bulk) surface and aerodynamic resistances.

The FAO Penman-Monteith method was developed by defining the reference crop as a hypothetical crop with an assumed height of 0.12 m, with a surface resistance of 70 s m^{-1}, and albedo of 0.23, closely resembling the evaporation from an extensive surface of green grass of uniform height, actively growing and adequately watered (Allen et al. 1998). The FAO Penman-Monteith method uses standard climatic data (solar radiation, temperature, relative humidity,

wind speed) that can either be measured or derived from commonly measured data. The FAO Penman-Monteith equation can then be derived as:

$$ET_o = \frac{0.408\Delta(R_n - G) + \gamma \frac{900}{T+273} u_2 (e_s - e_a)}{\Delta + \gamma(1 + 0.34u_2)} \quad (4\text{-}2)$$

where u_2 is wind speed at 2 m height and T is air temperature at 2 m height. Albedo is used in the calculation of R_n which is the difference between incoming and outgoing radiation of both short and long wavelengths. Soil heat flux, G beneath the grass reference surface is relatively small and the monthly soil heat flux can be estimated from monthly temperature (Allen et al. 1998) :

$$G_i = 0.07(T_{i+1} - T_i) \quad (4\text{-}3)$$

where T_{i-1} is mean air temperature of previous month [°C] and T_{i+1} is mean air temperature of next month [°C].

Thomas (2008) constructed a 0.25° resolution gridded data set of monthly FAO Penman-Monteith reference evapotranspiration estimates over the territory of China and adjacent areas for the period 1951-1990. To construct the gridded data, Thomas (2008) interpolated an ET_o database by Gao et al. (2006) that includes estimates at observation stations across China. The interpolation was carried out using the REGEOTOP procedure (Thomas and Herzfeld 2004), which accounts explicitly for the influence of topographic relief on climate. This is very important for mountainous regions in China. Figure 4-10 shows the 0.5° average annual reference evapotranspiration for the meteorological period (Thomas 2008).

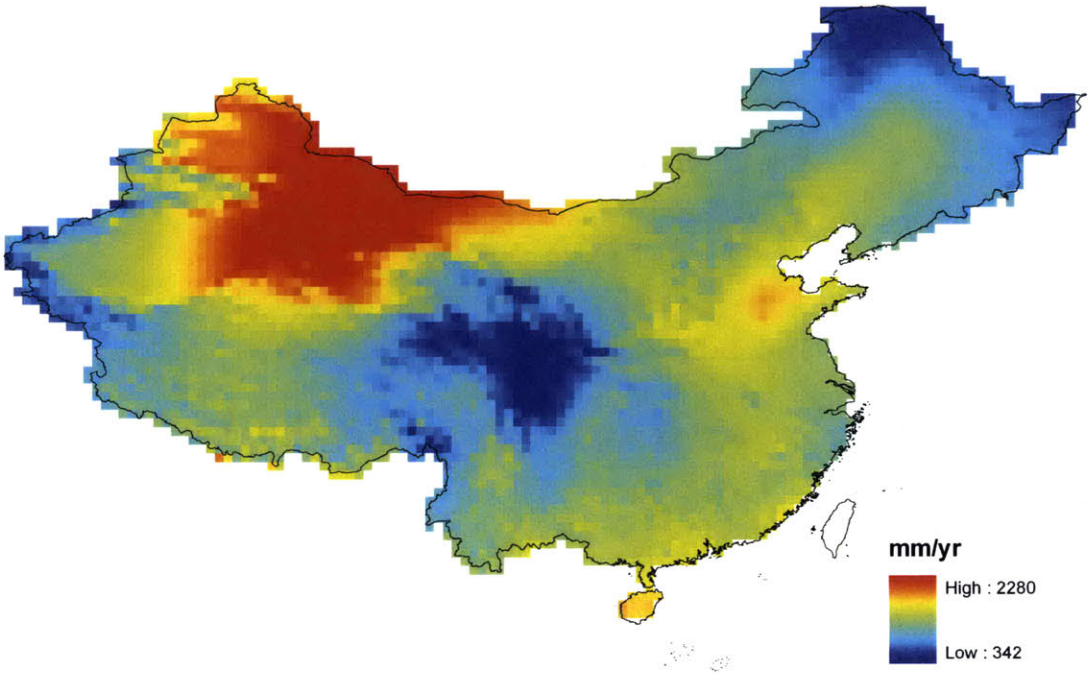

Figure 4-10: The average annual reference evapotranspiration.

4.2.2 Crop Sequence and Viability

In this study, we focus on finding the optimal allocation of cultivated land for each crop sequence. By crop sequence, we mean a combination of up to three crops from seven crop categories (maize, rice, spring wheat, winter wheat, tubers, oil crops, and vegetables) and fallow allocated to three growing seasons during the calendar year. An example of a typical pixel is illustrated in Figure 4-11. The notion of crop sequence entails two important steps:

1) Determination of the viability of a particular crop in a particular season at a particular pixel.
2) Calculation of the crop evapotranspiration rates for each viable three season crop sequence.

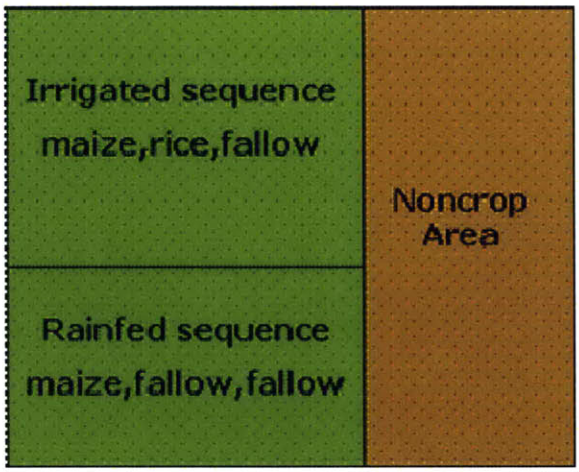

Figure 4-11: A typical pixel showing a combination rainfed cropland, irrigated cropland, and noncrop area.

Crop viability depends on slope, soil properties, and climatic conditions. In particular, crops need warm temperature for a sufficiently long time, an adequate water supply, and favorable soil characteristics in suitable terrain for all stages of the growing period. In Section 4.1.3, we already account for slope and soil requirements in arable land. In this section, we consider climate and water availability factors in determining a viable crop sequence. We also need to know when a crop can be planted, how long it takes until harvesting, and how much water it requires (evapotranspiration).

We use the agronomic concept of Growing Degree Days (GDD) to determine when a crop can be planted and when it should be harvested. Plants require a certain amount of energy input during each developmental stage and grow until they have accumulated enough "heat units" to reach maturity. The GDD concept allows for spatially-varying growing period lengths that reflect regional climatic differences. Daily GDD value is the temperature difference between average daily temperature and base temperature (Miller et al. 2001) as follow:

$$GDD_{t,c} = \frac{T_{max,t} + T_{min,t}}{2} - T_{base,c} \quad where \begin{cases} GDD_{t,c} = 0 \; if \; T_{avg,t} < T_{base,c} \\ T_{avg,t} = 30^{\circ}C \; if \; T_{avg,t} > 30^{\circ}C \end{cases} \tag{4-4}$$

$T_{base,c}$ is the temperature below which development stops. If the daily average temperature drops below the base temperature, the daily GDD is set to zero. And the daily average temperature is capped at 30 °C because above this temperature, most plants reach maximum growth rate. The base temperature varies among different crops as shown in Table 4-3 for our seven crop categories.

Table 4-3: Crop base temperature above which growth is possible.

Crop	T_{base} [°C]	Reference
Maize	8	(Kucharik & Twine 2007))
Rice	10	(Angima 2003)
Spring Wheat	4.1	(Angima 2003)
Winter Wheat	0	(Miller et al. 2001)
Tubers	7.2	(Angima 2003)
Oil crops	10	(Angima 2003)
Vegetables	10	(Angima 2003)

The planting time t_p is when the daily average temperature is above the base temperature. The daily GDD are calculated and summed over time and the harvest time t_n is obtained by solving (4-5) for t_n.

$$\sum_{t=t_p}^{t_n} GDD_{t,c} = GDD_{req,c}, \tag{4-5}$$

where $GDD_{req,c}$ is the total required GDD (heat units) for crop c from planting until harvesting. Additional constraint is placed on the growth period for winter wheat so that it cannot begin to grow until September. This date is consistent with winter wheat phenology information provided by Cui et al. (1984). Due to lack of available observed daily maximum and minimum temperature data at pixel scale for China, we use a linear interpolation of the monthly temperature time series from Thomas (2007) to estimate daily long-term average temperature for the GDD calculation by assuming that the monthly temperature represents temperature at mid month.

We calculate the required GDD for spring wheat, winter wheat, maize, and rice using the Atlas of Phenology by Cui et al. (1984). The Atlas provides maps of planting and harvesting dates of these crops. We use the specified planting and harvesting dates, base temperature in Table 4-3, and temperature data (Thomas 2007) to obtain the required GDD shown in Table 4-4. Since planting and harvesting dates vary slightly across China, we calculate GDD requirement of each area and take the average value.

Table 4-4: Crop Growing Degree Days requirement.

Crop	GDD_{req} [°C]
Maize	1129
Rice	1039
Spring Wheat	1223
Winter Wheat	1752

For multiple-crop categories of tubers, oil crops, and vegetables, the GDD requirement of each individual crop varies greatly. We have to employ an average growing period for these categories instead of using $GDD_{req,c}$. The average growing periods for tubers, oil crops, and

vegetables are 135, 120, and 60 days, respectively. These estimates are based on information from United States Department of Agriculture's Agricultural Handbooks no. 507 (USDA 1977a) and 628 (USDA 1997b).

4.2.3 Crop Evapotranspiration

The crop evapotranspiration rates used in the model are actual evapotranspiration from irrigated cropland of crop sequence s in pixel p ($EI_{p,s}$) and actual evapotranspiration from rainfed cropland of crop sequence s in pixel p ($ED_{p,s}$). These are annual average values. However, water demand is a function of a crop's growth stage, and the function is different for each crop. We first calculate daily water demand for each part of the crop sequence and then sum the daily demands to obtain the total annual water demand for the entire growing season. The annual crop evapotranspiration rates ($EI_{p,s}$ and $ED_{p,s}$) used in the model are the sums of the daily crop evapotranspiration rates for the entire growing period over all viable sequences in a pixel, including evapotranspiration rates from fallow. Figure 4-12 illustrates an example of the water demand curve (specifically, crop coefficient curve) of the double cropping sequence fmr (fallow, maize, rice).

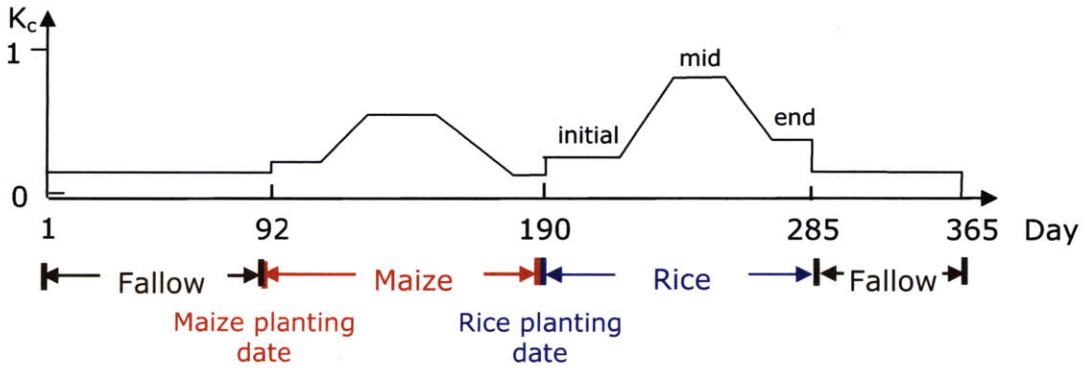

Figure 4-12: Time-dependent crop coefficient curve for the double cropping sequence fmr (fallow, maize, rice).

To calculate crop water requirements (crop evapotranspiration rate), we follow a guideline provided in the FAO Irrigation and Drainage Paper 56 (Allen et al. 1998). The approach described there is termed the 'K_cET_o' or crop coefficient approach, whereby the effect of the climate on crop water requirements is represented by the reference evapotranspiration ET_o and the effect of the crop by the crop coefficient K_c. Crop evapotranspiration or crop water demand, ET_c, can then be calculated as follows:

$$ET_c = (K_c)(ET_o). \tag{4-6}$$

The crop coefficient, K_c represents the physical and physiological differences between crops. For our model, we use a single crop coefficient K_c to represent all characteristics that could distinguish a particular crop from the reference crop used to derive Equation (4-6). The characteristics embodied by the crop coefficient are crop height, albedo, canopy resistance, and evaporation from bare soil (Allen et al. 1998).

Since most crops require different amounts of water during different growth stages, the crop coefficient will vary over the growing period, as illustrated in Figure 4-12 and Figure 4-13. The growing period can be divided into four distinct stages: initial, crop development, mid-season, and late season. Figure 4-13 shows a generalized crop coefficient curve for a perennial crop. During the initial growth stage, the value of crop coefficient, $K_{c\ ini}$ is small. As crop starts to develop, its water demand is higher until it reaches the maximum development and the value of crop coefficient is at the maximum equal to $K_{c\ mid}$. Then the crop evapotranspiration begins to decrease until it reaches a lower value at the end of the growing period equal to $K_{c\ end}$.

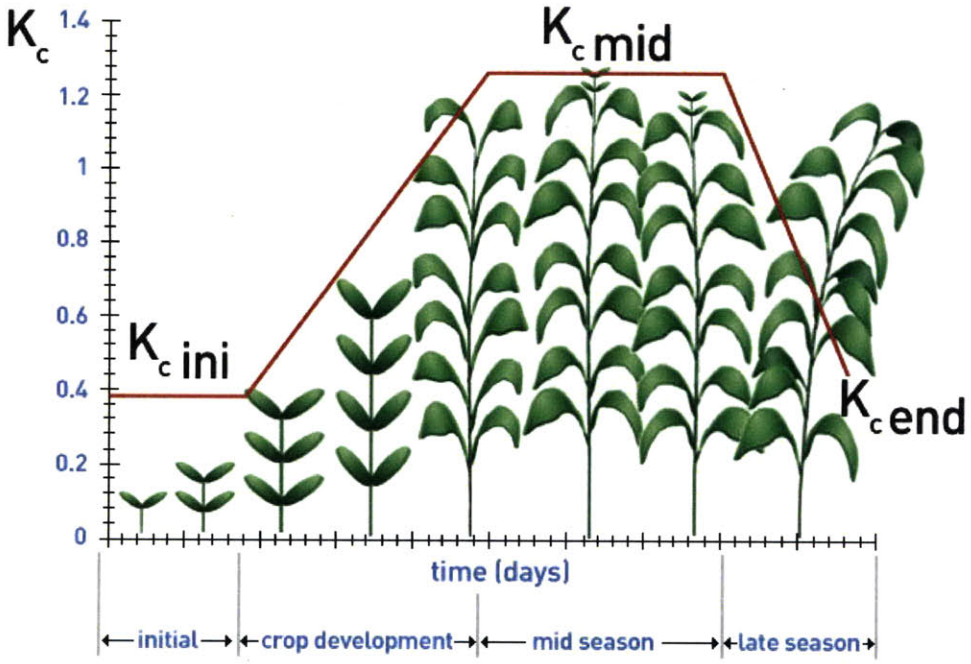

Figure 4-13: The generalized single crop coefficient curve for perennial crops from (Allen et al. 1998).

The crop coefficients for the model's seven crop categories and references are summarized in Table 4-5 below. Since crop water demand changes on a daily time scale, we calculate the crop

evapotranspiration accordingly. The fraction of time spent in each growing stage is summarized in Table 4-6. By multiplying the total growing period with the fraction of time, we arrive at the number of days spent in each stage.

There are two sets of crop evapotranspiration rates because we distinguish between irrigated and rainfed agriculture. For viable rainfed crop sequences, not only temperature requirements have to be met but water demand during growing season must also be met solely by precipitation. On the other hand, irrigated viable sequences are only subject to temperature requirements. Note that these viable crop sequences are only possible options. The optimization model will determine which sequences will produce the optimal result subject to all other constraints as presented in Chapter 3.

Table 4-5: Crop evapotranspiration adjustment coefficients for the seven model crop categories.

	K_c			Reference
	Initial	Mid	End	
Maize	0.50	1.20	0.90	(Kang et al. 2003)
Rice	1.05	1.20	0.75	(Allen et al. 1998)
Spring wheat	0.55	1.20	0.70	(Li et al. 2003)
Winter wheat	0.50	1.20	0.90	(Kang et al. 2003)
Tubers	0.50	1.10	0.95	(Allen et al. 1998)
Oil crops	0.35	1.15	0.35	(Allen et al. 1998)
Vegetables	0.70	1.05	0.95	(Allen et al. 1998)

Table 4-6: Fractional time spent in each growth stage for each model crop category.

	Fraction of Time Spent in Each Growth Stage				Reference
	Initial	Development	Mid	Late	
Maize	0.16	0.28	0.32	0.24	(Kang et al. 2003)
Rice	0.20	0.20	0.40	0.20	(Allen et al. 1998)
Spring wheat	0.20	0.17	0.33	0.30	(Li et al. 2003)
Winter wheat	0.44	0.31	0.13	0.13	(Kang et al. 2003)
Tubers	0.21	0.23	0.37	0.19	(Allen et al. 1998)
Oil crops	0.17	0.27	0.35	0.21	(Allen et al. 1998)
Vegetables	0.20	0.25	0.39	0.16	(Allen et al. 1998)

In addition to crop evapotranspiration, when a crop is not being grown on cultivated land, the model assumes the land is fallow and the surface is bare soil. Allen et al. (1998) reported that the K_c value of bare soil will be quite similar to the $K_{c\ ini}$ and its evapotranspiration rate depends on the frequency and amount of precipitation. Therefore, we assume a representative value of 0.5 for K_c for fallow. Water requirement does not need to be met for fallow land. If fallow evapotranspiration exceeds precipitation, it is set equal to precipitation.

4.2.3 Municipal and Industrial Water Use

Besides our focus on water use in agricultural section, we also take into account municipal and industrial water diversion and loss to evaporation. National Bureau of Statistics (2008) provides annual provincial M&I diversion data WP_v. The M&I diversion is the required amount of water for municipal and industrial water use. We downscale the provincial M&I diversion data to pixel scale using pixel population fraction (F_p). We use the latest available data for year 2007 and are shown in Figure 4-14. A portion of the M&I diversion will be lost to evaporation and the rest will be returned to outflow. To estimate the M&I loss to evaporation, we multiply the M&I diversion by (1-*effc*). By using the calibration model presented in Chapter 5 and defining the

efficiency as a decision variable, we found that the efficiency is relatively constant throughout the country at the value of 0.80.

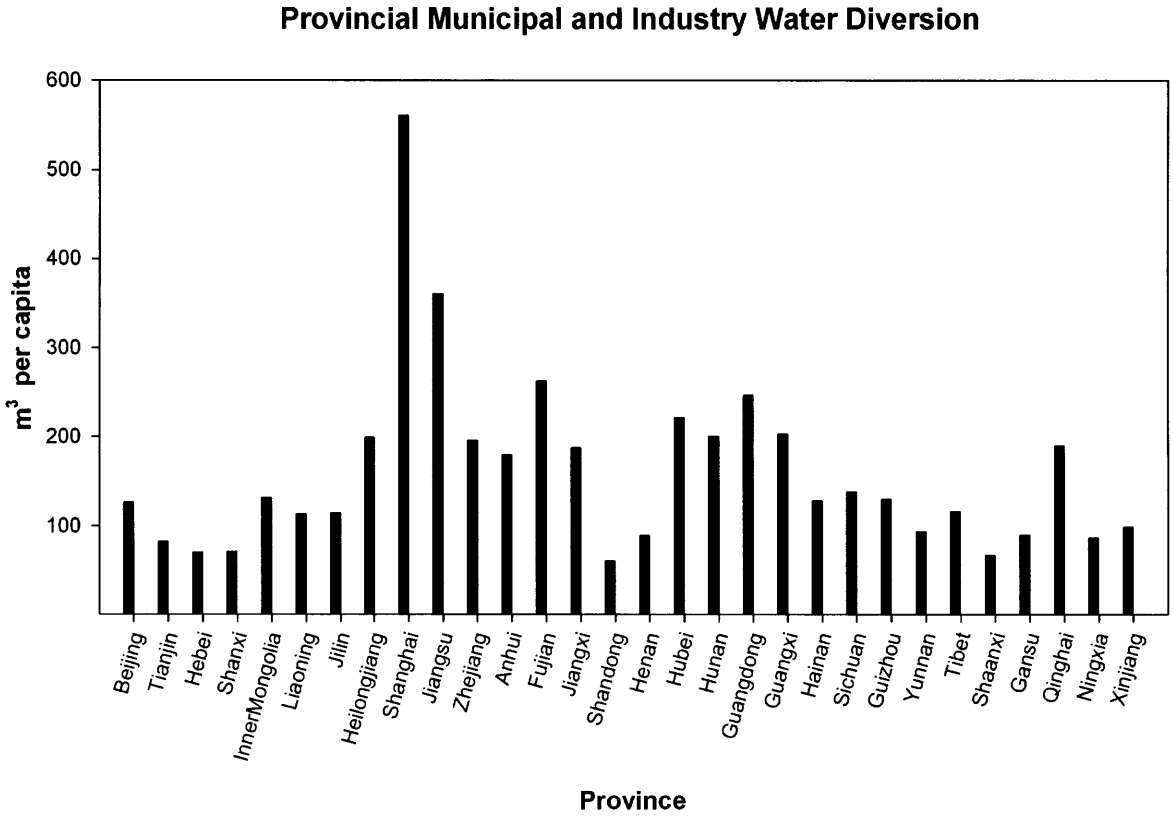

Figure 4-14: Provincial M&I water diversion per capita in 2007.

We calculated the pixel population fraction using data from the Gridded Population of the World (henceforth GPWv3) (CIESIN 2005). GPWv3 provides the spatial distribution of populations in 2005 across the globe at a resolution of 2.5 arc minutes. We aggregated the dataset to the level of 0.5^{o} x 0.5^{o} (Figure 4-15).

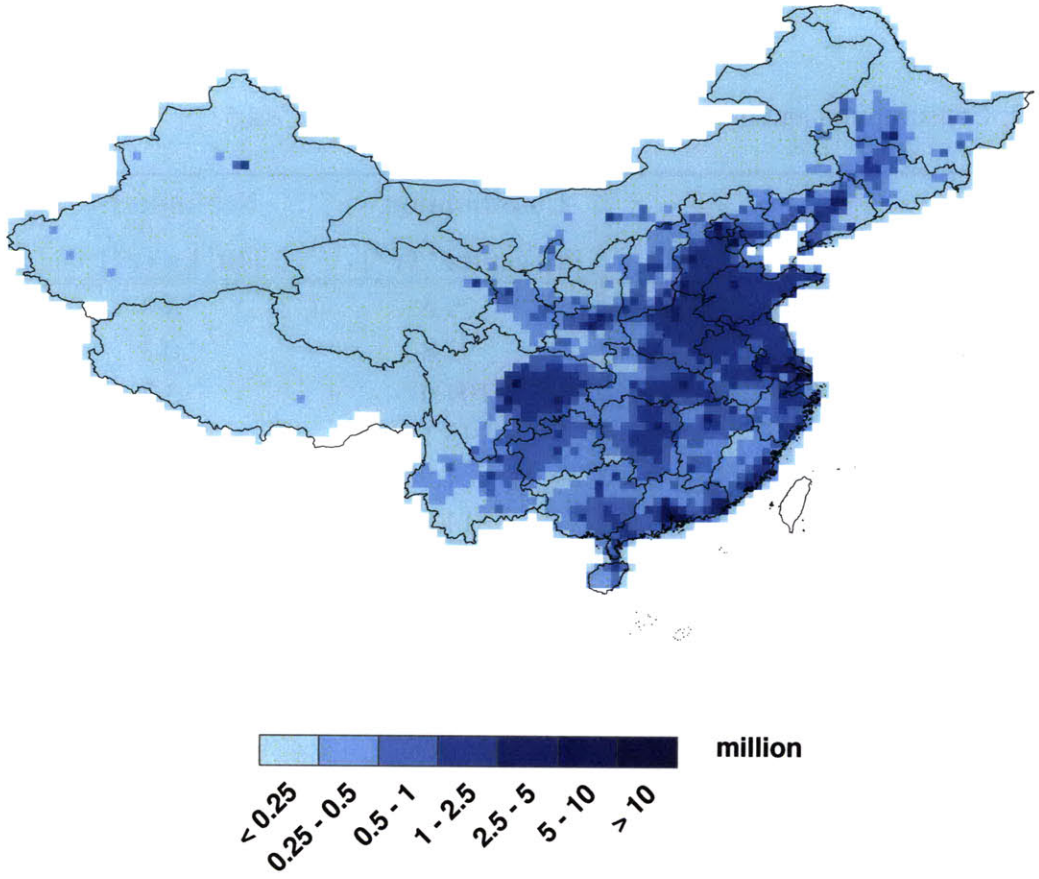

Figure 4-15: Population distribution over China in 2005 (CIESIN 2005). The legend shows number of people in each 0.5° pixel.

4.3 Production/Consumption-Related Inputs

For the production-consumption constraints, the required inputs are the consumption rate (C_c), the crop yield (M_c), and the net imports (S_c) as expressed in Equation (3-13). The Food Balance Sheets (FBS) from the Food and Agriculture Organization of the United Nations Statistical Databases (FAOSTAT) provides information for country's annual food production and consumption as well as import and export. The most recent available Food Balance Sheet for

China is in 2005 and we use this data for our baseline simulation. The consumption and net import for 2005 are summarized in Table 4-7 below (FAOSTAT 2009a).

Table 4-7: Consumption and net import for each crop category in 2005.

Crop	Consumption [kg capita^{-1} yr^{-1}]	Net import [10^9 kg yr^{-1}]
Spring and Winter Wheat	79.6	4.3
Rice	91.8	0.3
Maize	104.6	-3.7
Tubers	145.1	13.9
Oil crops	64.5	28.3
Vegetables	314.8	-7.6

For crop yield, the core production data from (FAOSTAT 2009b) provides the annual yield values, in units of mass per unit area (kg ha^{-1}), for most crops grown in a country. Figure 4-16 illustrates trend in annual crop yield of the model's seven crops (spring and winter wheat have same yield) from 1961-2008 except for rice and oil crops that yields are only available until 2005. Increasing trend is observed in yield values for maize, wheat, and oil crops. Therefore, we estimate yield values of maize, wheat, and oil crops by extrapolating their trends linearly to 2010. For rice, tubers, and vegetables, we assume their yields to take the most recent values available which are 2008 values for tubers and vegetables and 2005 value for rice. We also assume that yield is uniform over all of China.

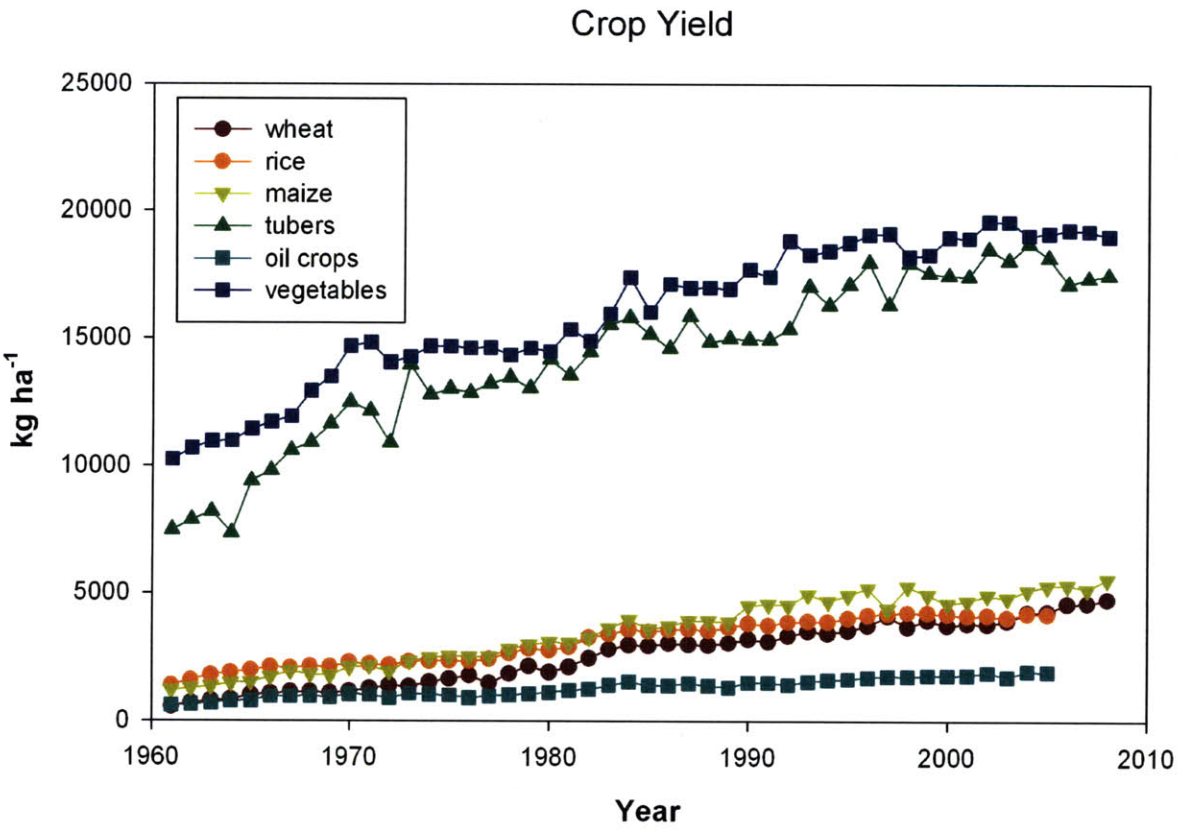

Figure 4-16: Trend in annual crop yield.

Table 4-8: Yield values for each crop category for baseline simulation and climate change alternatives.

Crop	Yield [kg ha^{-1}]
Spring and Winter Wheat	4841
Rice	4171
Maize	5943
Tubers	17452
Oil crops	2036
Vegetables	19009

Chapter 5

Input Estimation

In this chapter, we present a procedure to estimate three unavailable inputs that are not available in the literature: irrigated cropland for each pixel and crop sequence ($LI^{\circ}_{p,s}$), rainfed cropland for each pixel and crop sequence ($LD^{\circ}_{p,s}$), and noncrop evapotranspiration rate (E_N_p) for each pixel. This procedure identifies inputs that minimize the mean squared error (misfit) between predicted and observed values for several variables measured over the 1990-2000 calibration period. These variables are: total population, provincial crop production, annual basin runoff, total cropland in each pixel, and total irrigated cropland in each pixel. Apparently normalized misfits for each of these data sources are weighted equally.

5.1 Formulation of the Input Estimation Problem

The input estimation problem can be posed as a quadratic programming problem that uses the same constraints as those included in the optimization problem of Chapter 3. The only difference is the objective function, which penalizes the sum of normalized mean-squared differences (misfits) between predictions and measurements, as shown in Equation (5-1).

$$\underset{eLI_{p,s},eLD_{p,s},E_{p,nc}}{minimize} \quad \boldsymbol{F}(N,P_{v,c},R_b,eLI_{p,s},eLD_{p,s}) = \left(\frac{N^*-\hat{N}}{N^*}\right)^2$$

Population

$$+\frac{1}{N_v}\sum_{c\in all\ crops}\left(\sum_{v\in all\ provinces}\left(\frac{P^*_{v,c}-\hat{P}_{v,c}}{\left\langle P^*_{v,c}\right\rangle}\right)^2\right)$$

Provincial production

$$+\frac{1}{N_b}\sum_{b\in all\ basins}\left(\frac{R^*_b-\hat{R}_b}{\left\langle R^*_b\right\rangle}\right)^2$$

Basin runoff

$$+\frac{1}{N_p}\sum_{p\in all\ pixels}\left(\frac{L^*_p-\sum_{s\in viable\ sequences}(\widehat{eLI}_{p,s}+\widehat{eLD}_{p,s})}{\left\langle L^*_p\right\rangle}\right)^2$$

Total cropland

$$+\frac{1}{N_p}\sum_{p\in all\ pixels}\left(\frac{LI^*_p-\sum_{s\in viable\ sequences}\widehat{eLI}_{p,s}}{\left\langle LI^*_p\right\rangle}\right)^2$$

Total irrigated area

(5-1)

where * denotes measurements and ^ denotes predictions. The terms included in the objective function are the squared errors of:

1) the national population normalized by observed population
2) the provincial crop production for the model's six crop categories summing over all provinces normalized by mean observed provincial crop production and the number of provinces

3) the basin annual runoff for all of the model's basins normalized by mean observed basin runoff and the number of river basins
4) the total pixel crop area, which is the sum of irrigated and rainfed cropland, normalized by the mean pixel observed total crop area and the number of pixels
5) the total pixel irrigated area normalized by the mean pixel observed total irrigated area and the number of pixels

The constraints for this least squares problem are the same as those of the model presented in Chapter 3 except for the noncrop evapotranspiration constraints. If all constraints are linear, the least squares problem is a positive definite quadratic programming problem that has a unique global minimum. In the model of Chapter 3, the evapotranspiration is a product between the evapotranspiration rate and the corresponding area as shown in Equation (3-17).

$$E_p = \sum_{s \in viable\ sequences} \left[\left(E\_I_{p,s}\right)\left(LI_{p,s}\right) + \left(E\_D_{p,s}\right)\left(LD_{p,s}\right) \right] + \left(E\_N_p\right)\left(LN_p\right), \quad (3\text{-}17)$$

where, for the noncrop evapotranspiration, LN_p is a decision variable and E_N_p is an input. If E_N_p and LN_p are unknown, this constraint becomes nonlinear and the desirable global optimal properties of a quadratic programming formulation are lost. To assure that a solution to the constrained least-square problem is globally optimal, we need to define the entire term of $E_{p,nc} = \left(E\_N_p\right)\left(LN_p\right)$ as a decision variable. After minimizing (5-1), we can obtain the noncrop evapotranspiration rate E_N_p required in the model of Chapter 3 by dividing $E_{p,nc}$ by LN_p as follows:

$$E\_N_p = \frac{E_{p,nc}}{LN_p} \quad (5\text{-}2)$$

In order to ensure that the estimated noncropland evapotranspiration is physically reasonable, we need to add some additional constraints. We specify a lower bound on $E_{p,nc}$ to prevent the model from assigning zero or unrealistically low value to the evapotranspiration. This is particularly important in arid regions. We follow the crop coefficient approach to set a lower bound on $E_{p,nc}$, assuming the lower bound coefficient to be 0.1, which is above zero but lower than the value for the crop coefficient for fallow land of 0.5. The constraint can be expressed as follow

$$E_{p,nc} \geq 0.1 \times ET_{o,p} \times LN_p. \tag{5-3}$$

In addition, the available water for noncrop evapotranspiration is constrained by the amount of precipitation on noncrop land less evaporation from M&I. The upperbound on $E_{p,nc}$ can then be expressed as follow:

$$E_{p,nc} \leq (P_p \times LN_p) - W_p. \tag{5-4}$$

The resulting constrained least-square problem is a quadratic program that can be solved by the GAMS CPLEX solver. Its decision variables are $LI^{\circ}_{p,s}$, $LD^{\circ}_{p,s}$, and $E_{p,nc}$.

5.2 Data Used for Estimation of Unknown Model Inputs

5.2.1 Total Population

The average Chinese population during the 1990-2000 period reported in China Statistical Yearbook (National Bureau of Statistics 2000) is 1209 million people.

5.2.2 Provincial Crop Production ($P^*_{v,c}$)

Crop production data provide useful information for estimating China's cropland distribution. FAOSTAT, from which we obtained consumption, yield, and net import data, also provides China's total annual crop production data (FAOSTAT 2007b). However, the national amount is too coarse for our purposes because we want to estimate existing cropland distribution on a pixel scale. The China Statistical Yearbook available for the period 1997-2005 provides more detailed production at provincial level. We compared national crop production from these two data sources during the same period to see if they are consistent. Table 5-1 shows the comparison of average crop production for the model's six crop categories during the period 1997-2001 from FAOSTAT and the China Statistical Yearbook.

Table 5-1: The national annual crop production data from FAOSTAT and China Statistical Yearbook averaged during the period 1997-2001 for the model's seven crop categories (spring and winter wheat are combined).

	Total China Crop Production (1997-2001) [10^9 kg]	
Crop Categories	**FAOSTAT**	**China Statistical Yearbook**
Maize	117.31	120.49
Rice	129.78	187.45
Spring and Winter Wheat	108.08	101.48
Oil Crops	32.36	29.34
Tubers	180.81	34.25
Vegetables	291.93	80.43*

* Vegetables production data from China Statistical Yearbook are only available for seven provinces (Guangdong, Guangxi, Hainan, Sichuan, Guizhou, Yunnan, and Tibet).

We see that maize, wheat (spring and winter), and oil crops production data are consistent between the two data sources. However, there is a large discrepancy for rice, tubers, and

vegetables production data. Even though the Statistical Yearbook provides production data at the provincial level, it does not list which crop is included in tubers and vegetables categories, while FAOSTAT (2007b) explicitly specifies those. Moreover, the time period for available Statistical Yearbook is 1997-2005, which does not overlap with our calibration period of 1990-2000. In order to preserve consistency with dietary consumption rate, yield, and net imports, which are all from FAOSTAT, we adopt the national crop production data from FAOSTAT and use the Statistical Yearbook provincial data to downscale the FAOSTAT national amount to provincial values. Vegetable production must be handled differently because the Statistical Yearbook only provides data for seven provinces. Since most vegetables in China are consumed locally, we assume that their provincial production is proportional to population distribution and we use the provincial population density to downscale down national vegetable production. The resulting provincial production values for all crop categories are shown in Figure 5-1 below (with spring and winter wheat combined).

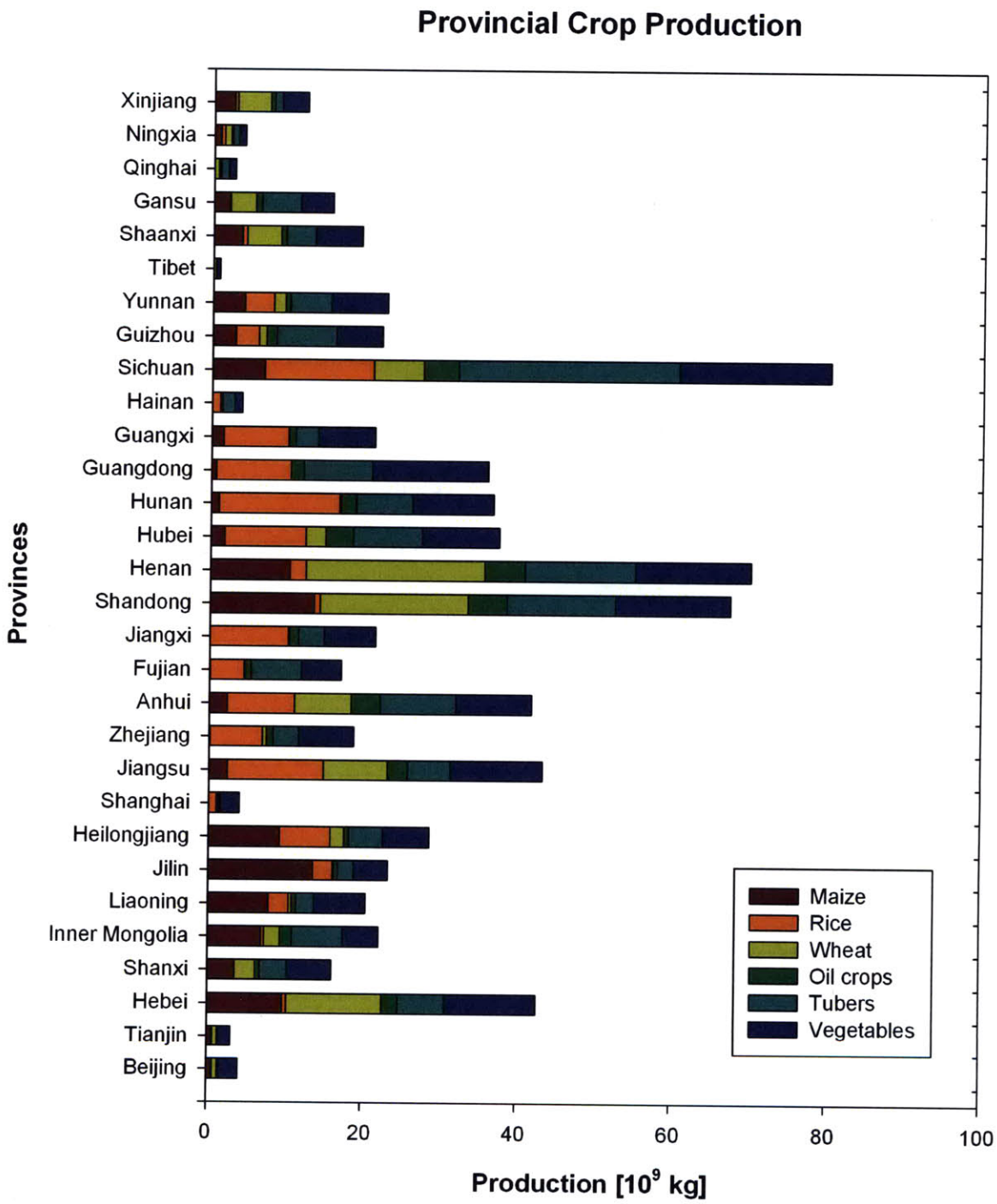

Figure 5-1: Average annual provincial crop production for the model's six crop categories during the period 1990-2000. The national amount is according to FAOSTAT and is scaled down to provincial level with data from China Statistical Yearbook (1997-2001).

5.2.3 Basin Runoff (R_b^*)

More than half of the total drainage area in China discharges to the ocean while the rest drains internally. There are about thirty major river basins. The Yangtze Basin is the largest, with the mean annual runoff of 950 km^3.

Basin runoff provides a validation of the model's water balance, and is an important source of information for estimating noncrop evapotranspiration. The Ministry of Water Resources, PRC provides a comprehensive assessment of water resources in China (Department of Hydrology, Ministry of Water Resources, PRC 1992). This assessment includes mean annual runoff over the period 1956-1979 for all major river basins in China, at the basin outlet summarized in Table 5-2.

Table 5-2: Mean annual runoff for all of the model's river basins (1956-1979).

River basins	Mean annual runoff (km^3)
Heilongjiang Region	116.6
Tumen River	5.1
Yalujiang River	16.2
Coastal Rivers in Liaoning Province	12.6
Liaohe River Basin	14.8
Luanhe River	5.97
Haihe River Basin	22.8
Yellow River Basin	66.1
Coastal Rivers in Shandong Province	11.9
HuaiHe River Basin	62.2
Yangtze River Region	951.3
Southeast Coastal Rivers	237.8
Pearl River Basin	333.8
Coastal Rivers in South Guangxi and West Guangdong, Hainan Island	88.9
Yuanjiang River	48.4

Lancang River	74
Nujiang River	68.9
Rivers in West Yunnan	31.4
Yarlung Zangbo River	165.4
Rivers in West Tibet	2.01
Ertix River	10
Inland Rivers in Inner Mongolia	1.17
Inland Rivers in Hexi	6.86
Inland Rivers in Qinghai	7.24
Inland Rivers in Junggar	12.5
Inland Rivers in Middle Asia	19.3
Tarim River	34.7
Inland Rivers in Qiangtang Area	24.6

Even though the time period of the available runoff data are earlier than our calibration period of 1990-2000, it provides annual runoff for all of the model's river basins and comparison of six basin runoffs with more recent data in year 2000 (National Bureau of Statistics 2000) shows that the runoffs in 2000 are generally higher than those from the period 1956-1979 except Haihe and Yellow River Basins. We therefore use the runoff data shown in Table 5-2 to calibrate the model with adjustment to lower runoff in Haihe River Basin to 12.5 km^3 (National Bureau of Statistics 2000) and in Yellow River Basin to 44.5 km^3 (Chunhui et al. 2004).

5.2.4 Total Cropland (L_p^*)

There is a considerable uncertainty in estimates relating to cropland in China. Heilig (2004) summarized various estimates of total cultivated land in China. The reported amount was ~95 Mha from the agricultural census and ~130 Mha from the land-use mapping and various studies. Frolking et al. (1999) compared estimates of total cropland area in China from land cover maps derived from optical remote sensing in 1992-1993 (1-km resolution NOAA AVHRR) and

county-level agricultural census data for 1990 and reported that the total cropland area estimated by remote sensing is 50-100% higher than reported in the agricultural census.

To our knowledge, there is no available information on the cropland distribution for all of China for individual crop sequences at 0.5° resolution. The most detailed data available on China's cropland is provided by Frolking et al. (2002). They combined remote sensing data from Landsat Thematic Mapper (TM) and county-scale agricultural census data to produce 0.5^{o} x 0.5^{o} resolution maps of total cropland areas and cropland devoted to major crops in China. The maps can be obtained from http://www.dndc.sr.unh.edu/Maps.html.

Although the Frolking et al. (2002) cropland distribution maps include several major crops and multiple crop rotations at the same resolution as our model, they did not include all of our model's crop categories and sequences, and the original data they used were from a period different than our calibration period of 1990-2000. The Landsat TM used by Frolking et al. (2002) was primarily from the years 1995-1996 and had 100-m spatial resolution. The agricultural census data are from the Eco-Environmental Database of the Research Center for Eco-Environmental Sciences, Chinese Academy of Sciences containing statistics on total cropland area and sown area of 17 major crops in 1990. As a result, we decided to use only the Frolking et al. (2002) total pixel crop area values in our input estimation model. Figure 5-2 shows the resulting map of total cropland at 0.5° resolution expressed as a percentage of total pixel area.

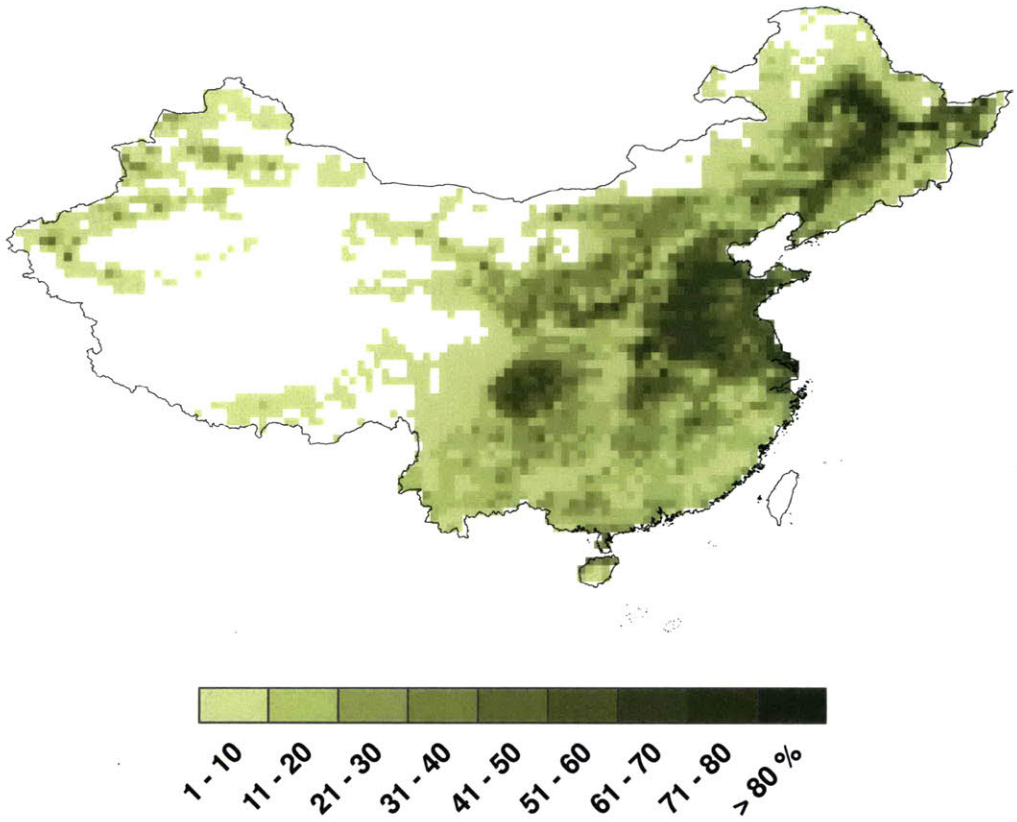

Figure 5-2: Distribution of total cropland areas in China. The map shows the fraction of total land devoted to cropland in at least one season in each 0.5° pixel (Frolking et al. 2002). White indicates negligible cropland.

5.2.5 Total Irrigated Cropland (LI_p^*)

There are several estimates regarding irrigated areas in China with different spatial resolution covering different time periods. For example, in the 1990 cropping season, there is a county-level inventory based on the agricultural census reporting a total irrigated area of 46 Mha (Skinner 1997). Another inventory based on a land-use atlas (Wu 1990) estimated the amount for the same year to be 68 Mha.

Siebert et al (2005) estimated the irrigated areas in China for the 2000 cropping season using three inventories. They assumed the irrigated area per province to be as given in the China Statistical Yearbook 2001, which gives a total irrigated area of 53.8 Mha. The provincial values were then downscaled to county values by combining the aforementioned two inventories (Skinner 1997 and Wu 1990). The resulting map was included as part of the Global Map of Irrigation Areas version 4.0.1 (Stefan et al. 2007). The resolution of the map is 0.0833°.

We aggregated the irrigated area of the Stefan et al. (2007) map to the resolution of our model and compared it to the cropland map from Frolking et al. (2002). We found that some pixels had more irrigated land than cropland. Since irrigated land should not exceed cropland, the irrigated area was modified where necessary to insure that irrigated area never exceeds cropland. The resulting irrigated cropland is shown in Figure 5-3, expressed as a percentage of total pixel area.

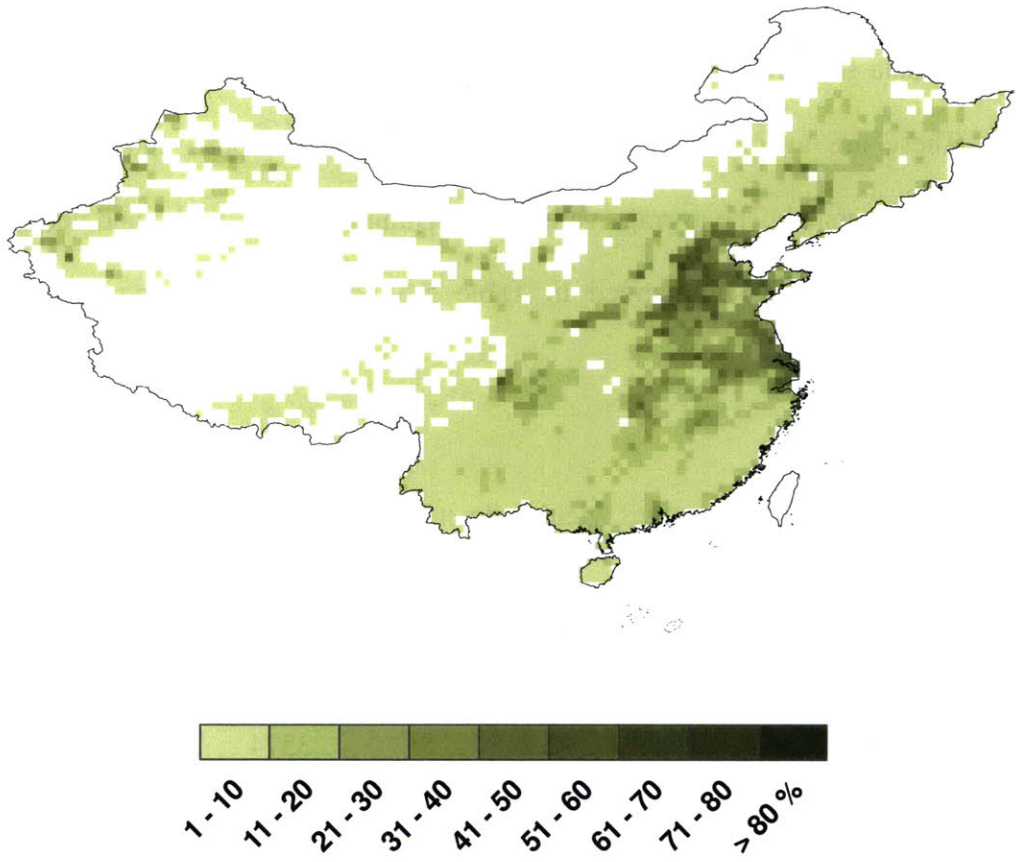

Figure 5-3: Map of fraction of irrigated area in 0.5° grid consistent with the cropland distribution. White indicates negligible irrigated area.

The four largest provincial irrigated areas in the 2000 cropping season were concentrated in the North China Plain and adjacent areas. These are: Shandong (4.8 Mha), Henan (4.7 Mha), Hebei (4.5 Mha), and Anhui (3.2 Mha). The irrigated areas in these provinces account for more than thirty percent of the country's total irrigated area (National Bureau of Statistics 2001). They are also the areas where the issue of groundwater depletion is most critical. The proposed middle and eastern routes of the North-to-South Water Diversion are expected to transfer about 10 billion m^3 of water for agriculture use to these areas (Nickum 2006).

5.2.6 Constraint-Related Inputs

In addition to five observations required in the objective function of the input estimation problem, four data sets are needed in the production-consumption constraint and water balance constraint. These are average consumption rates, yield, net import, and the municipal and industrial water diversion. The average values of consumption rates, yield, and net import during the calibration period are summarized in Table 5-3 below (with spring and winter wheat combined).

Table 5-3: Average consumption rates, yield and net import during the calibration period for the model's seven crop categories (spring and winter wheat combined).

Crop	Consumption [kg capita^{-1} yr^{-1}]	Yield [kg ha^{-1}]	Net import [10^9 kg yr^{-1}]
Spring and Winter Wheat	92.7	3574	7.7
Rice	103.9	4020	-0.7
Maize	89.8	4784	-0.1
Tubers	138.4	16628	2.2
Oil crops	38.3	1629	4.2
Vegetables	169.1	18458	-2.1

The provincial municipal and industrial water diversion is obtained from the China Environmental Statistical Yearbook ((National Bureau of Statistics 2005). The earliest available data set is in 2004 and we assume the 2004 values best proxy for average values during the calibration period. The per capita provincial M&I diversion is shown in Figure 5-4.

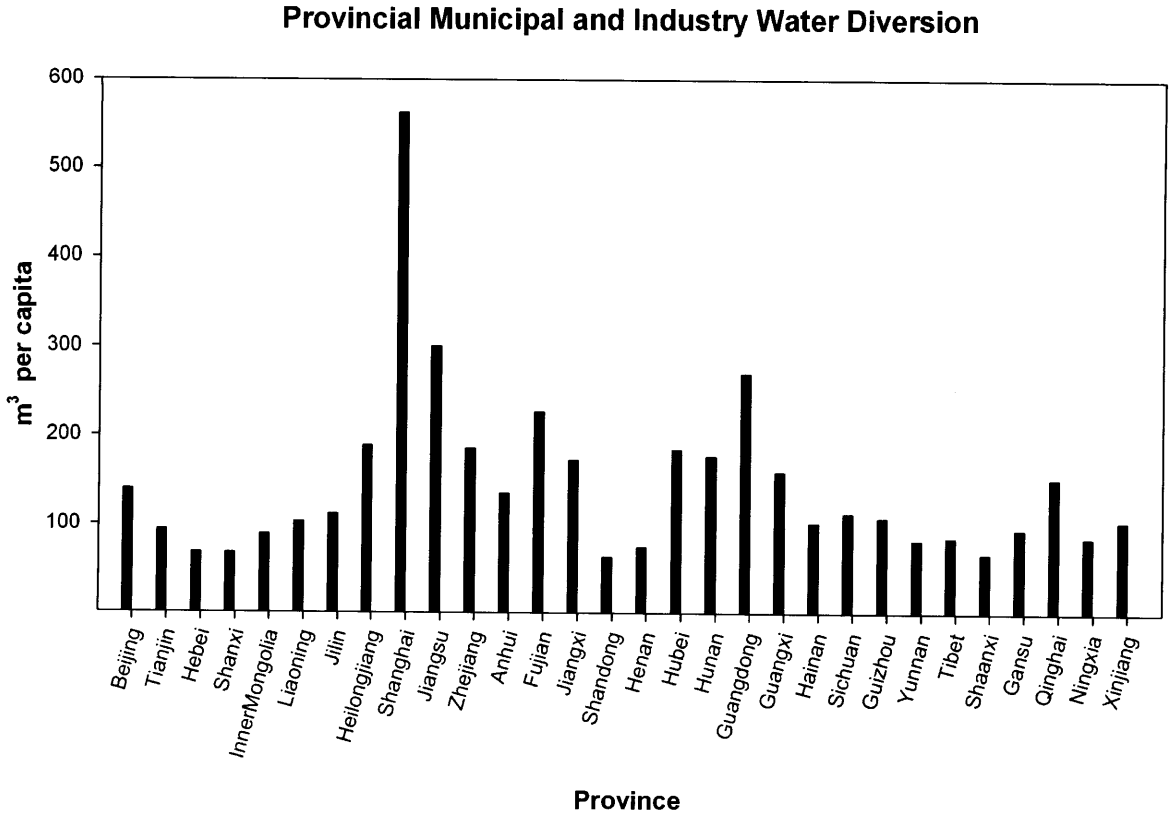

Figure 5-4: Provincial M&I water diversion per capita in 2004.

5.3 Estimates of Unknown Inputs

5.3.1 Estimated Cropland

The model inputs estimated in the least-squares procedure are irrigated cropland for each pixel and crop sequence ($LI^{\circ}_{p,s}$) and rainfed cropland for each pixel and crop sequence ($LD^{\circ}_{p,s}$). In order to facilitate graphical display of the estimated cropland, we show in Figures Figure 5-5 through Figure 5-7 aggregated displays of the detailed results. Figure 5-5 plots the total land area in each pixel devoted single, double, or triple cropping. In each case this total is obtained by summing crop areas over all sequences with one, two, or three non-fallow crop entries, respectively.

The single-cropping area spreads out over the country. The double-cropping area is concentrated in the North China Plain and the central coastal area as well as Sichuan province, where the crop production output is highest in China. Triple-cropping area occurs only in the water-abundant region in the south particularly in Henan, Anhui and Hubei provinces, where rice and tubers production are relatively high.

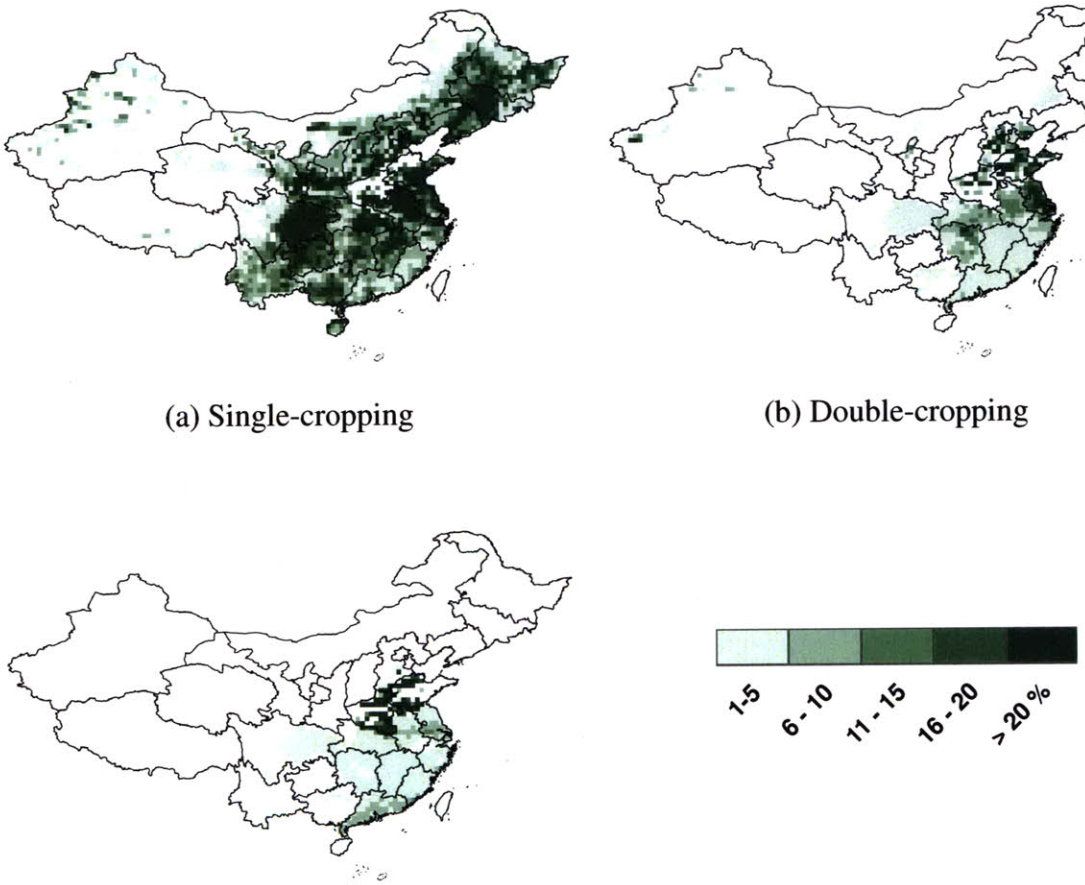

(a) Single-cropping

(b) Double-cropping

(c) Triple-cropping

Figure 5-5: Model's estimated crop area devoted to (a) single-cropping; (b) double-cropping; (c) triple cropping. The map shows a fraction of crop area as a percentage of the total pixel area.

Maps of total irrigated and rainfed cropland for individual crop category are shown in Figure 5-6 and Figure 5-7. The intensity of irrigated area is noticeably higher than rainfed crop area for all

major grains (maize, rice, and wheat). Maize agriculture occurs in most regions of China but is concentrated in the northeast. Rice is concentrated in the southeast while wheat is concentrated in the central region.

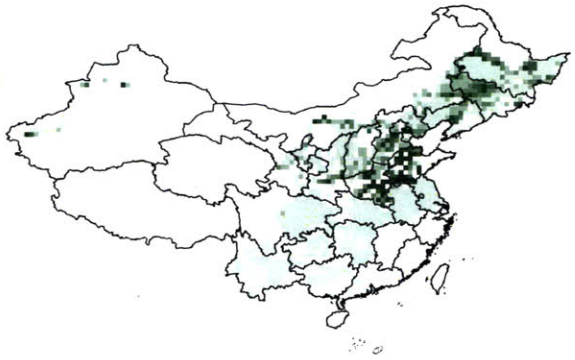

(a-1) Irrigated area of maize

(a-2) Rainfed crop area of maize

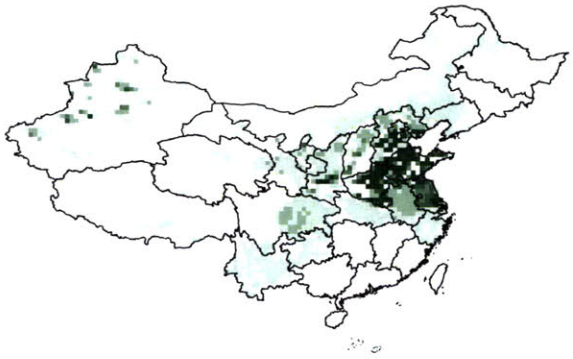

(b-1) Irrigated area of wheat

(b-2) Rainfed crop area of wheat

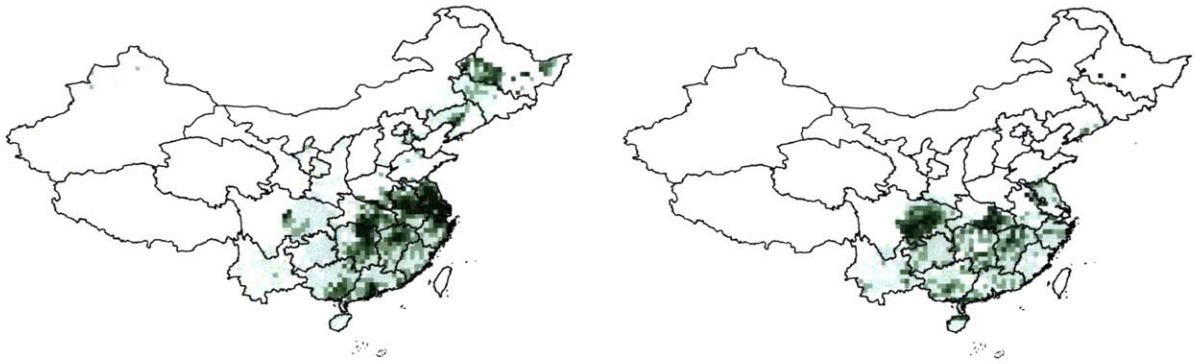

(c-1) Irrigated area of rice

(c-2) Rainfed crop area of rice

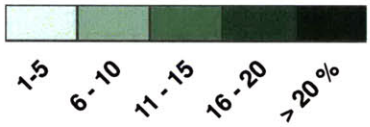

Figure 5-6: Model's estimated irrigated and rainfed crop area for (a) maize; (b) wheat; (c) rice. The left column is the irrigated area and the right column is the rainfed crop area. The map shows a fraction of crop area as a percentage of the total pixel area.

(a-1) Irrigated area of oil crops

(a-2) Rainfed crop area of oil crops

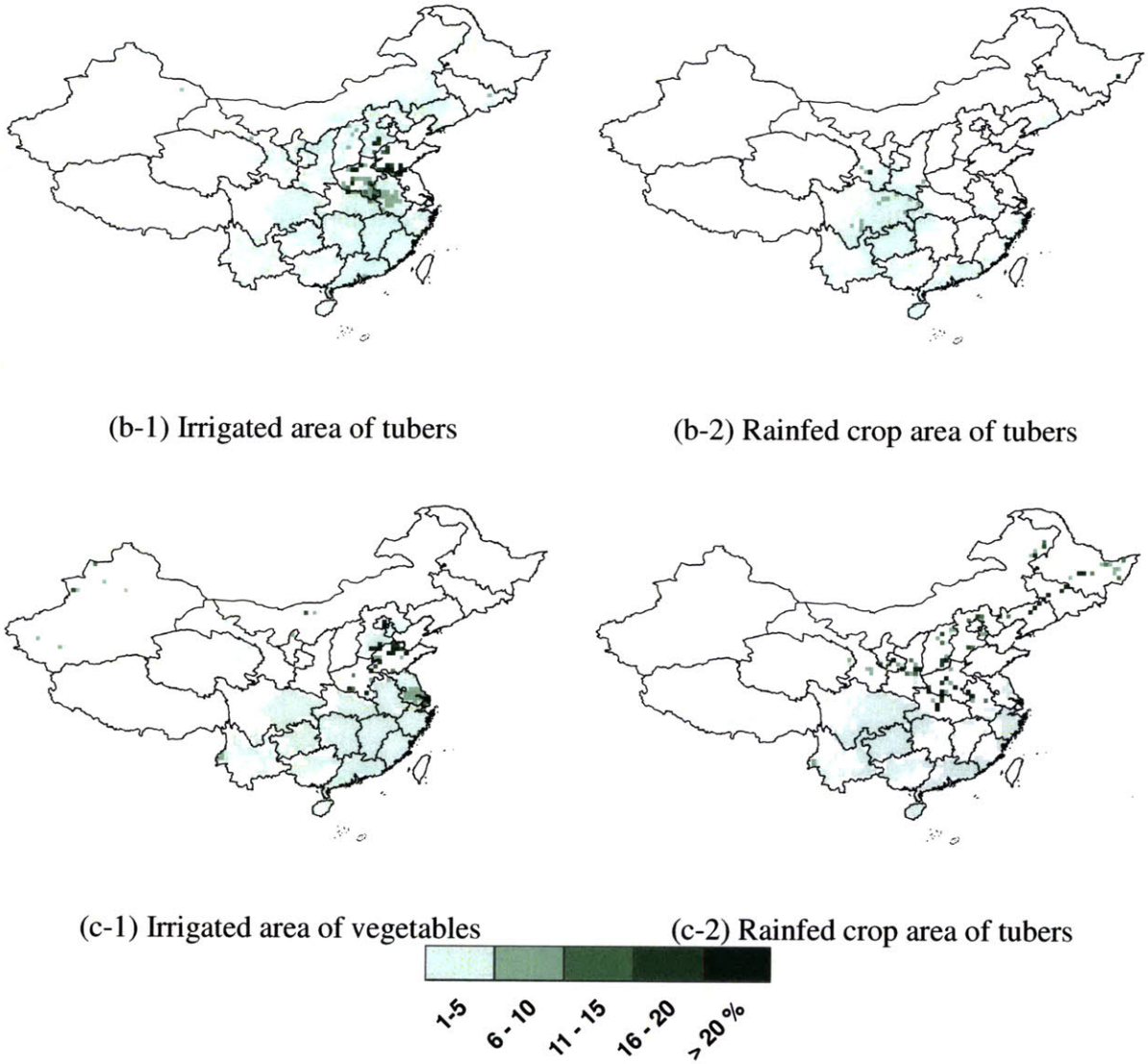

Figure 5-7: Model's estimated irrigated and rainfed crop area for (a) oil crops; (b) tubers; (c) vegetables. The left column is the irrigated area and the right column is the rainfed crop area. The map shows a fraction of crop area as a percentage of the total pixel area.

5.3.2 Estimated Noncrop Evapotranspiration Rate

The other important input for the detailed model is noncrop evapotranspiration rate. The estimate from the constrained least-square model is shown in Figure 5-8. The noncrop evapotranspiration shows a decreasing trend from the southern coastal area toward the arid northwestern region. This information on the noncrop evapotranspiration rates is generally unavailable in standard data sets.

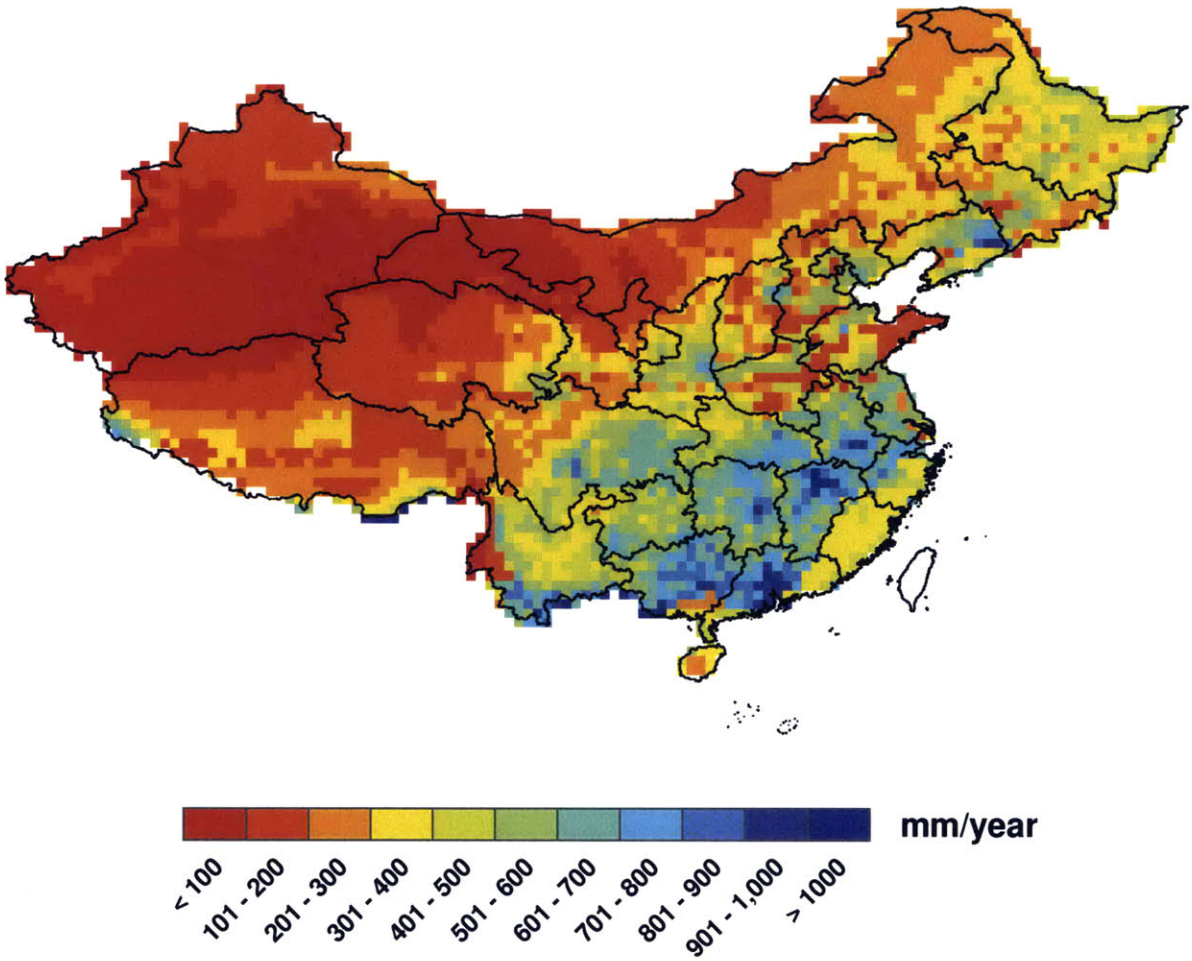

Figure 5-8: Estimated annual noncrop evapotranspiration rate.

5.4 Estimation Performance

In this section we compare the model predictions obtained from our input estimates with the observations. The number of unknowns in the problem is significantly larger than the number of observations. There are roughly over 120,000 unknown pixel irrigated areas, about 60,000 unknown pixel rainfed crop areas, and about 4,000 unknown pixel noncrop evapotranspiration values. By contrast, there are only about 8,200 observations: 4,000 pixel crop areas, 4,000 pixel irrigated areas, 180 provincial crop production values, 28 basin runoff values, and one average national population value for the calibration period. Nevertheless, the number of equality and inequality constraints in the input estimation problem is large enough to keep the problem reasonably well posed.

5.4.1 Total Population

In our model, the estimated average Chinese population during the 1990-2000 calibration period is 1223 million people, which is consistent with the reported value of 1209 million people.

5.4.2 Provincial Crop Production

Our provincial crop production estimates of all seven crop categories are very close to observations, as shown in Figure 5-9.

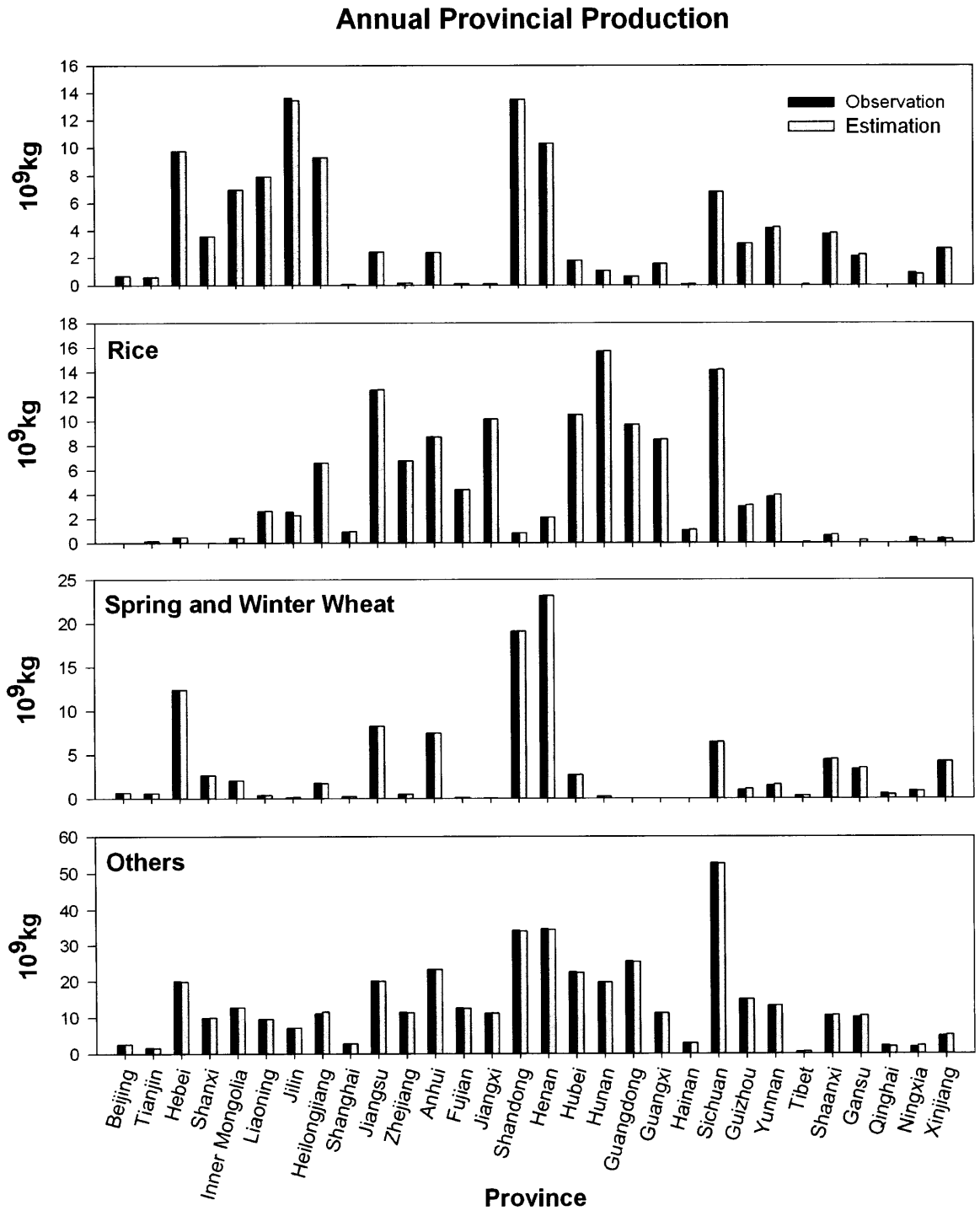

Figure 5-9: Comparison between model's estimate and observed provincial crop production.

5.4.3 Basin Runoff

Overall, our runoff estimates are very close to observations, as shown in Figure 5-10. Exceptions are significant underestimates of basin runoff for the Ertix River, inland Rivers such as the IliHe and the Tarim River. All of these rivers are located in the northwestern region of China where it is extensively arid. The largest discrepancy is observed in the Ertix Basin. The annual mean reference evapotranspiration in the basin is ~1500 mm/year; while the annual mean precipitation is almost ten times lower (~160 mm/year). The model's average estimated actual evaporation rate for Ertix Basin is close to precipitation resulting in a small amount of runoff.

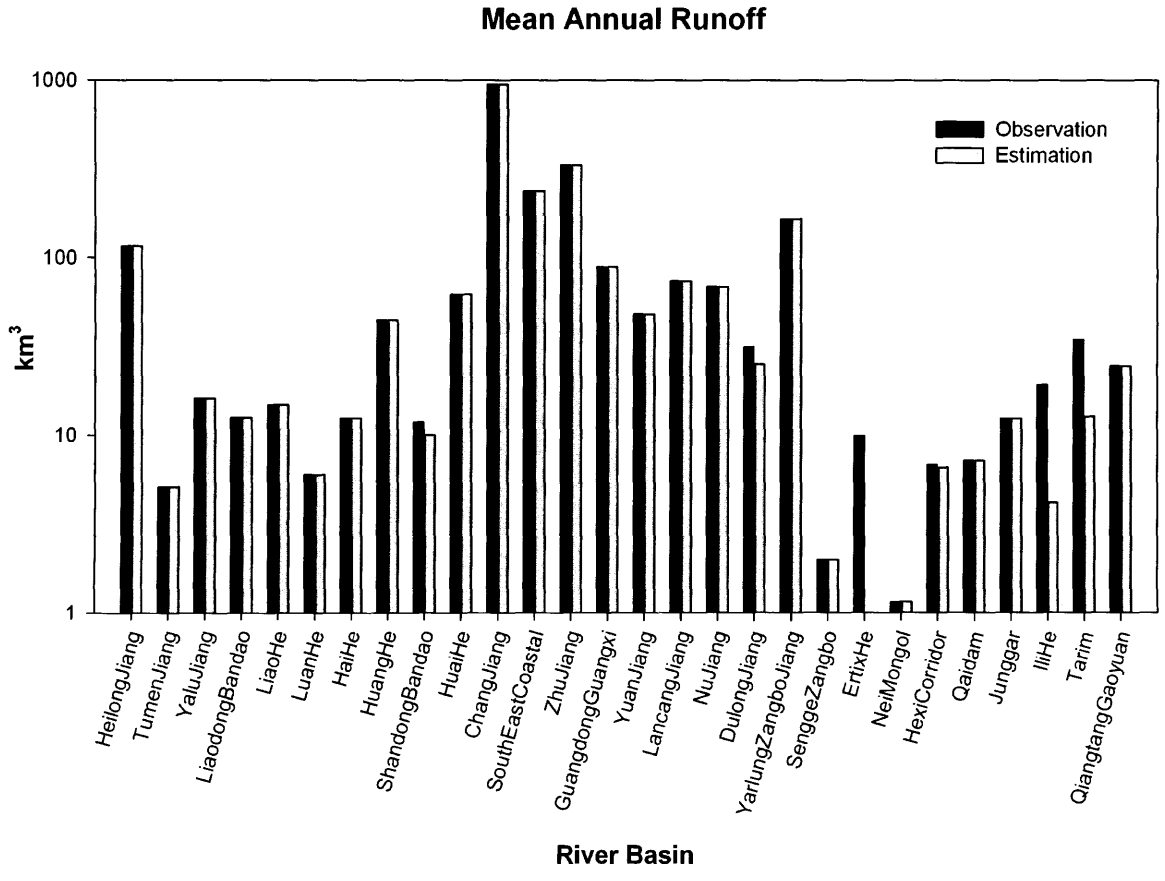

Figure 5-10: Basin runoff comparison between the model's estimates and observations.

5.4.4 Total Cropland

Comparison of our total cropland estimates to those derived by (Frolking et al. 2002) indicates that model tends to underestimate cropland in most regions, as shown in

Figure 5-11. A discrepancy of over 30% of the total pixel area is observed in portions of Heilongjiang province. Agriculture in this area and most part of the northeast region is water limited. This discrepancy might be due to the mismatch between the average values computed over our calibration period (1990-2000) and the values that applied during the year the observation took place (1995/1996). The mismatch may imply that cropland in Heilongjiang was expanded during the 1990's.

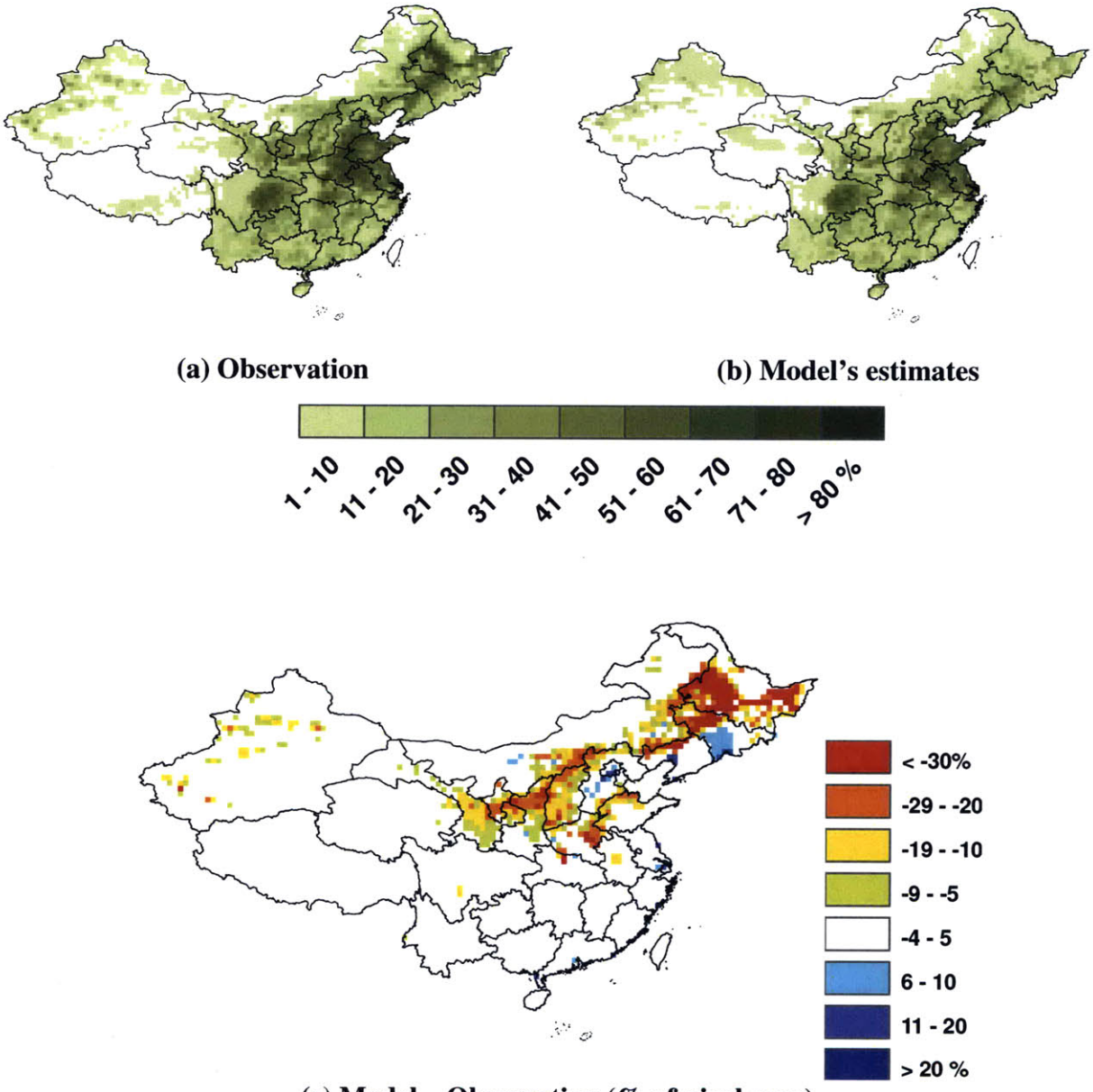

Figure 5-11: Cropland distribution as a fraction of total area in 0.5°grid from (a) observation; and (b) model's estimates. The third figure is the difference between model's estimates and observation in percent to the total pixel area.

5.4.5 Total Irrigated Cropland

Our irrigation area estimates are close those derived by (Stefan et al. 2007) with some overestimates in certain area as shown in Figure 5-12 below.

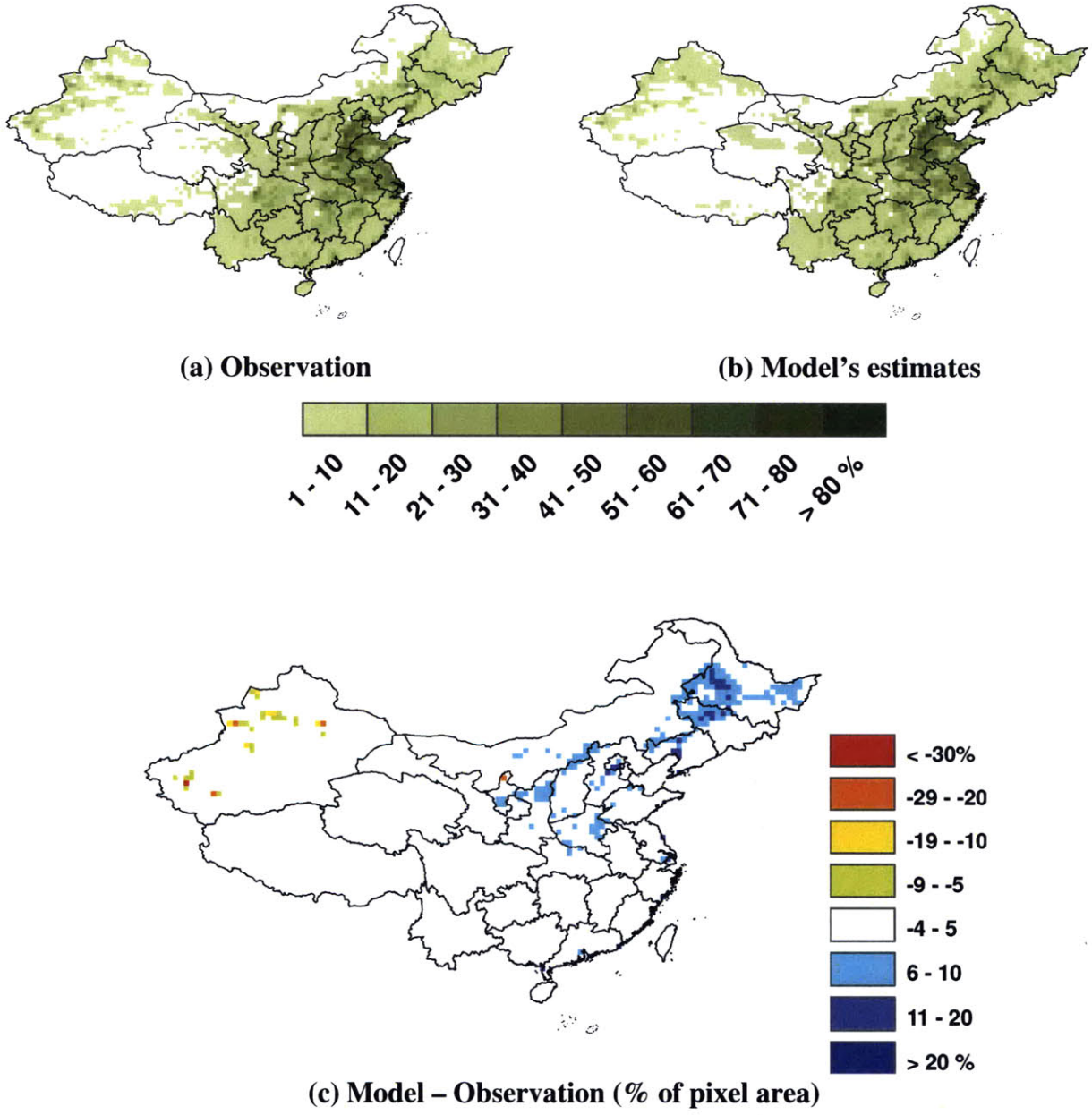

Figure 5-12: Irrigated area as a fraction of total area in 0.5°grid from (a) observation; and (b) model's estimates. The third figure is the difference between model's estimates and observation in percent of the total pixel area.

Chapter 6

Scenario Analysis under Nominal and Changed Climates

In this chapter, we use the model presented in Chapter 3 with the data and inputs discussed in Chapter 4 and 5 to study China's food production capacity. The results presented in here describe sustainable food production strategy. This chapter consists of two main parts. The first part is a baseline simulation for year 2010 with nominal climate. The second part is an impact study of South-to-North Water Diversion Project and climate change for the future period of 2046-2065. We consider future climates produced by several general circulation models (GCMs). These alternative climates span a range of diverse seasonal and regional patterns. Because GCM outputs typically lack the spatial and temporal resolution needed for our model, they are incorporated in the form of relative change factors. Understanding the sensitivity of agriculture to climate change on a national scale will be critical for meeting future food requirements.

6.1 Baseline Solution

The objective function of the model of Chapter 3 is a tradeoff that seeks to maximize people fed and to minimize the normalized mean-squared deviation (misfit) between optimized and nominal crop sequence areas. Misfit minimization is incorporated in the maximization problem by subtracting rather than adding the misfit term. A weighting factor α is used to control the tradeoff between these two contributions to the composite objective functions, as indicated below:

$$\underset{LI_{p,s},LD_{p,s},N}{\text{minimize}} \quad \boldsymbol{F}(N, LI_{p,s}, LD_{p,s}) =$$

$$N - \alpha\left(\sum_{p,s}\left\|\frac{LI_{p,s} - LI^{o}_{p,s}}{\left\langle LI^{o}_{p}\right\rangle}\right\|^{2} + \sum_{p,s}\left\|\frac{LD_{p,s} - LD^{o}_{p,s}}{\left\langle LD^{o}_{p}\right\rangle}\right\|^{2}\right). \tag{3-1}$$

The decision variables are people fed (N), pixel irrigated cropland for each crop sequence ($LI_{p,s}$), and pixel rainfed cropland for each crop sequence ($LD_{p,s}$). The two crop area terms are normalized by the mean nominal crop area per pixel. Note that the exact value of α does not have any physical meaning related to the solution; its purpose is to make it possible to examine the tradeoff between maximizing people fed and crop area misfit. In the baseline simulation, we assume that the climate remains unchanged from the meteorological period of 1951-1990. A plot between people fed and pixel land use change in percentage for the baseline simulation is shown in Figure 6-1.

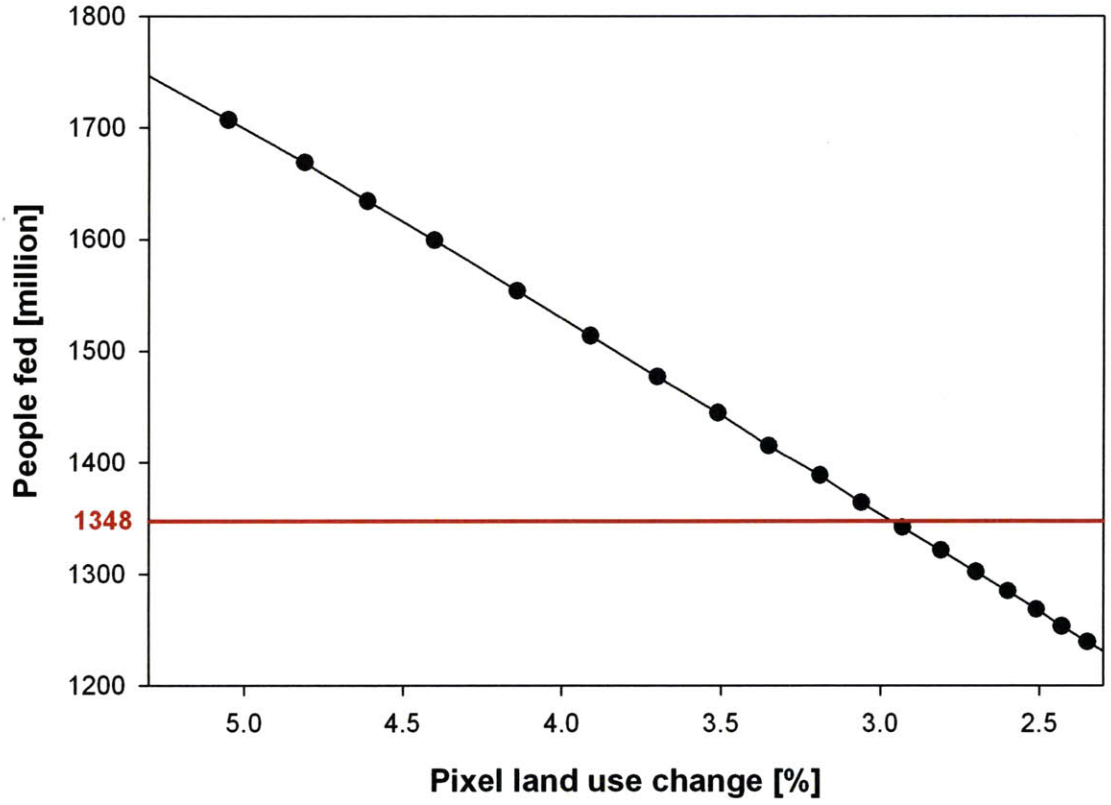

Figure 6-1: Model's baseline people fed versus land use change in percentage.

The pixel land use change is defined as follows:

$$Pixel\ land\ use\ change = \frac{100}{\left\langle L_p^* \right\rangle} \times \sqrt{\frac{1}{P}\sum_p \sum_s \left(LI_{p,s} - LI_{p,s}^{\circ} \right)^2 + \frac{1}{P}\sum_p \sum_s \left(LD_{p,s} - LD_{p,s}^{\circ} \right)^2}, \quad (6\text{-}1)$$

where P is the total number of pixels in China and $\left\langle L_p^* \right\rangle$ is the average observed total cropland in a pixel [ha]. The sums of squared deviation are over all crop sequences and all pixels in China for irrigated cropland and rainfed cropland, respectively. The pixel land use change denotes the

deviation from nominal land use expressed as a percentage of the average observed total cropland in a pixel.

As shown in Figure 6-1, China can potentially support quite a large number of populations up to about 1750 million people for the baseline solution. The expansion in land use reaches the maximum value of about 5.5 percents. This land use changed is bounded by water limitations. The U.S. Census Bureau estimates number of population in China in 2010 to be about 1348 million people (superimposed as a reference in Figure 6-1); the pixel land use change needs to be about 3 percents more than nominal cropland to support this level of population. To investigate how much these changes are in each land use category, we compare baseline solution with the nominal condition from the period 1990-2000. Table 6-1 summarizes area devoted to agriculture for different cases of land use change. The table includes number of people fed, sown area, cropland, irrigated cropland, and cropland devoted to single-, double-, and triple-cropping. If cropland is double-cropped, the sown area will be twice of the cropland. We see that it requires a large increase in the total sown area in order to support more people.

Table 6-1: Comparison of people fed and agricultural area between nominal condition and three levels of land use change from baseline solution.

		Nominal condition	Land use change 3%	4%	5%
People fed	[million]	1223.8	1342	1553.6	1706.7
Sown area	[Mha]	132.0	174.6	190.2	205.0
Cropland	[Mha]	99.3	115.8	121.9	127.7
Irrigated cropland	[Mha]	57.8	69.4	73.8	77.9
Single cropping	[Mha]	76.0	77.1	77.6	78.0
Double cropping	[Mha]	13.9	18.6	20.5	22.2
Triple cropping	[Mha]	9.4	20.1	23.9	27.5

Figure 6-2 shows changes (increase) in sown area, cropland, and irrigated cropland. Since cropland consists of irrigated and rainfed agriculture, it is interesting to see that most of the increase in cropland are from the increase in irrigated cropland. Moreover, to be able to feed 1.7 billion people (land use change of 5 percents), there needs to a large increase in sown area. The increase in sown area is about three times higher than the increase in crop area. This implies that there must be an increase in land devoted to multiple-cropping. Shown in Figure 6-3 is an increase in area devoted to single-, double-, and triple-cropping. As expected, the increase in double- and triple-cropping area for all three cases is dominant over the increase in single-cropping. If China is to feed more people, an increase in multiple-cropping area will be needed.

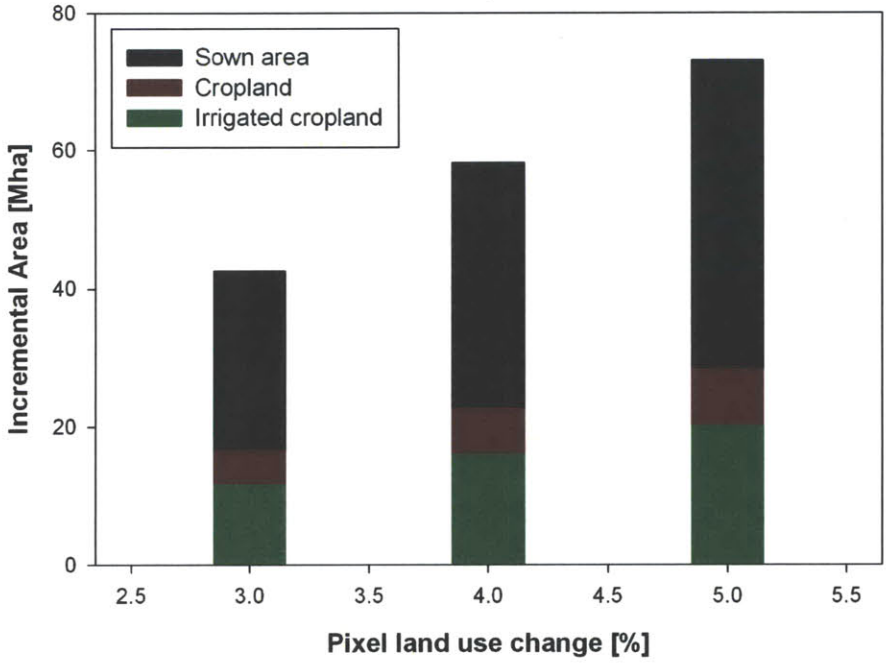

Figure 6-2: Increase in sown area, crop area, and irrigated area for three cases of land use change compare to the nominal condition.

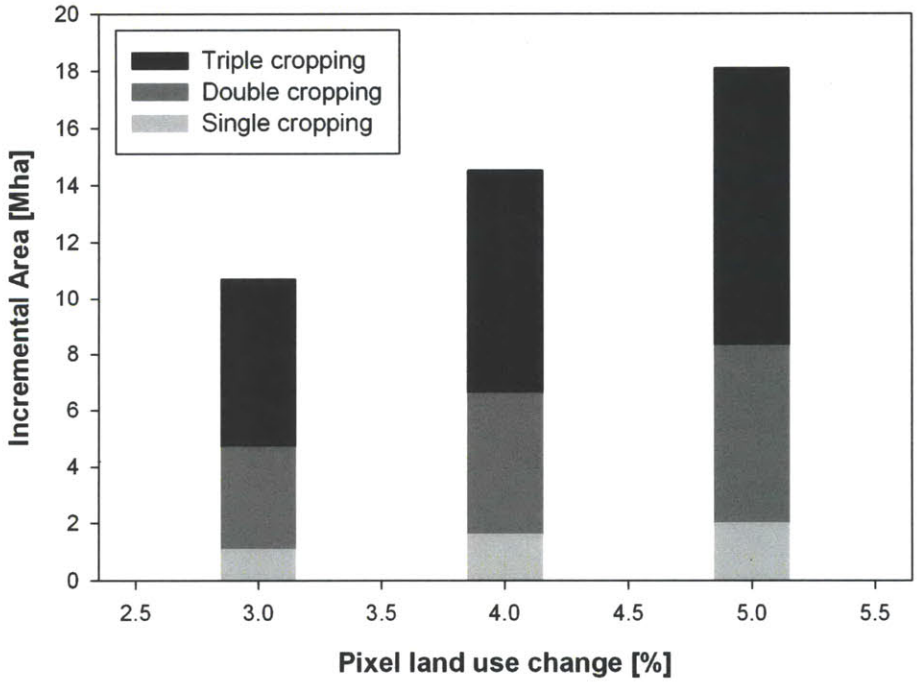

Figure 6-3: Increase in single-, double-, and triple cropping area for three cases of land use change compare to the nominal condition.

In summary, we find that irrigation and multiple-cropping will be keys to enhancing food production capacity in China if the climate remains relatively similar to what was observed in the past. Potentially, China will be able to support the increasing population if land use is allowed to change in the general way described here.

6.2 Scenario Analysis with South-to-North Water Diversion and Climate Change

In this section, we investigate how the South-to-North Water Diversion Project and climate change could affect the future food production capacity of China. The model's solutions presented here describe a sustainable food production strategy for the period 2046-2065. We apply the model developed in Chapter 3 modified to include the South-to-North Water Diversion Project with the climate alternatives selected from a subset of GCMs. We assume the other model's parameters except meteorological inputs to be at the same level as in baseline simulation. We make no attempt to predict future trends in these parameters. We will compare changes between the baseline simulation and 'changed' climate scenarios.

6.2.1 South-to-North Water Diversion

The South-to-North Water Diversion project is designed to transfer water from the Yangtze River to the Yellow River to relieve water shortages in over ten provinces in north and northwest China. The total amount of water diverted is expected be about 44.8 billion m^3 $year^{-1}$ by 2050, which is equivalent to the annual runoff of the Yellow River (Nickum 2006). The project consists of three diversion projects: Eastern Route Project (ERP), Middle Route Project (MRP), and Western Route Project (WRP). ERP and MRP are intended to be finished by 2020; while

WRP is still in a preliminary study stage and expected to be completed by 2050. The general layout of the three routes is shown in Figure 6-4 below.

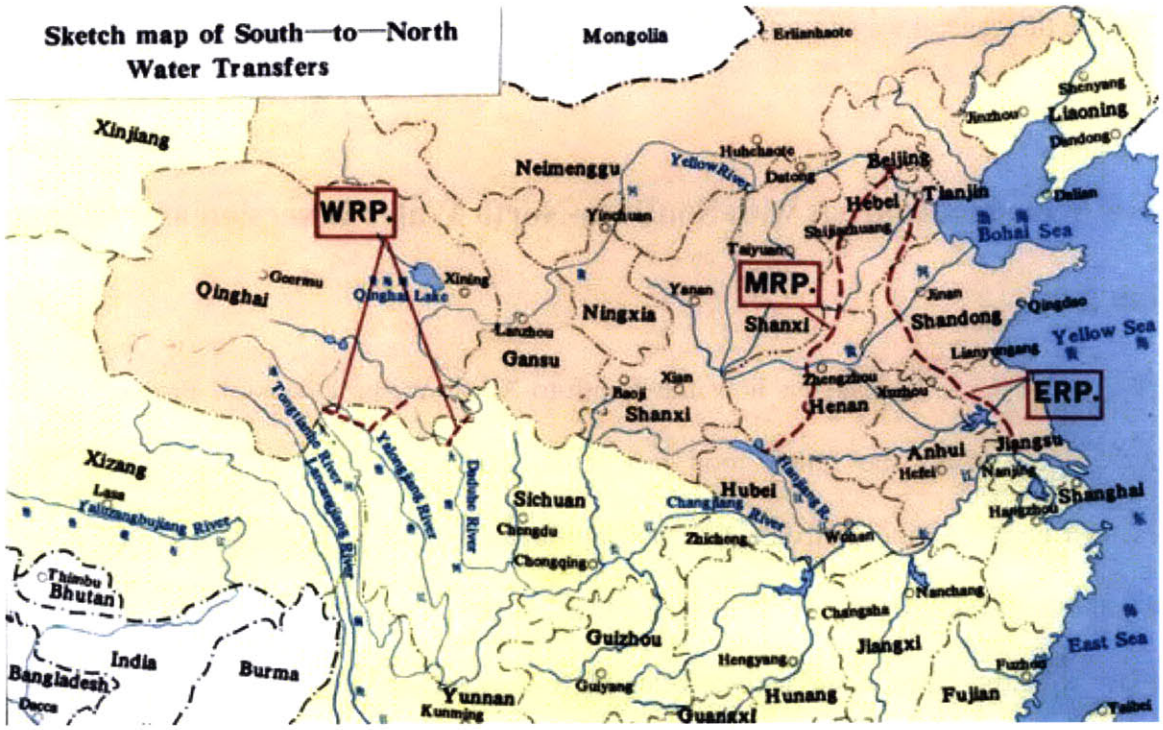

Figure 6-4: The general layout of the South-to-North Water Diversion Project (Source: www.yellowriver.gov.cn).

ERP will transfer water from the lower reaches of the Yangtze River to the eastern Huang-Huai-Hai Plain. MRP will divert water from the Danjiangkou reservoir on the Hanjiang, a tributary of the Yangtze River to Beijing. For WRP, there are three proposed routes diverting water from upper reach and tributaries of the Yangtze to replenish the upper reach Yellow River. These are the Yalongjiang, Tongtianhe, and Daduhe Routes.

To include the impacts of the South-to-North Water Diversion in our model, we implement the following steps:

1) Identify pixels that are sources of water for each route.
2) Identify the water receiving area.
3) Include the transferred amount into water balance constraints at both pixel and basin scales.
4) Assume that the transferred water is distributed among pixels proportional to population density since the main purpose of the project is to supply water for municipal and industrial water use.
5) Distinguish between M&I and agricultural water deliveries.

In the following sections, we describe the three projects, the transferred amount of water and how much of it will be contributed to agriculture and municipal and industrial water use, and the service area.

Eastern Route Project (ERP)

There will be two diversion locations for ERP: (1) Sanjiangying where the Huaihe River enters the Yangtze and (2) Gaogang where Beijing-Hangzhou Grand Canal crosses the Yangtze with the termination in Tianjin. The layout of ERP is shown in Figure 6-5. ERP will be built on the existing diversion project in Jiangsu Province, Beijing-Hangzhou Grand Canal, Huaihe projects and other related projects.

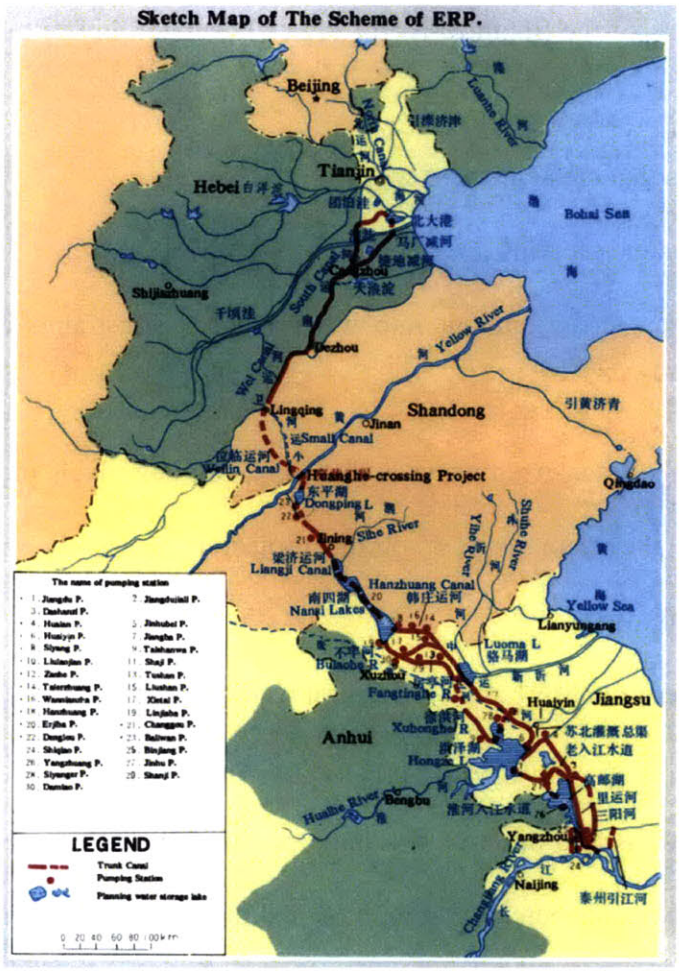

Figure 6-5: The layout of ERP.

The project will supply an additional 14.33 billion m^3 $year^{-1}$ to Jiangsu, Anhui, Shandong, Hebei Provinces and Tianjin Municipality (Nickum 2006). The cost of diverted water will be very high due to the scale and complication of the project; therefore, agriculture has lower priority, even though it accounts for a significant fraction of the total diversion. According to (Nickum 2006), agriculture is projected to receive 7.68 out of 14.33 billion m^3 $year^{-1}$, with the remaining 6.66 billion m^3 $year^{-1}$ of water go to urban, industrial, and navigation uses.

Middle Route Project (MRP)

MRP will divert water from Danjiangkou Reservoir on the Hanjiang in Hubei, which is a tributary of the Yangtze River. MRP will be an important facility for mitigating water crises in North China because the water is plentiful, has good quality, and can be transferred by gravity. One of the key components of MRP is the heightening of the Danjiangkou dam to raise water storage from 157 m to 170 m (www.nsbd.gov.cn). MRP will supply additional 3 billion m^3 $year^{-1}$ for agriculture and 6.4 billion m^3 $year^{-1}$ for municipal and industrial water use in Beijing, Tianjing, Hebei, Henan, and Hubei (Lei et al. n.d.). Water will be transferred from Danjiangkou Reservoir to Beijing through canals to be built along Funiu and Taihang Mountains. The layout of MRP is shown in Figure 6-6.

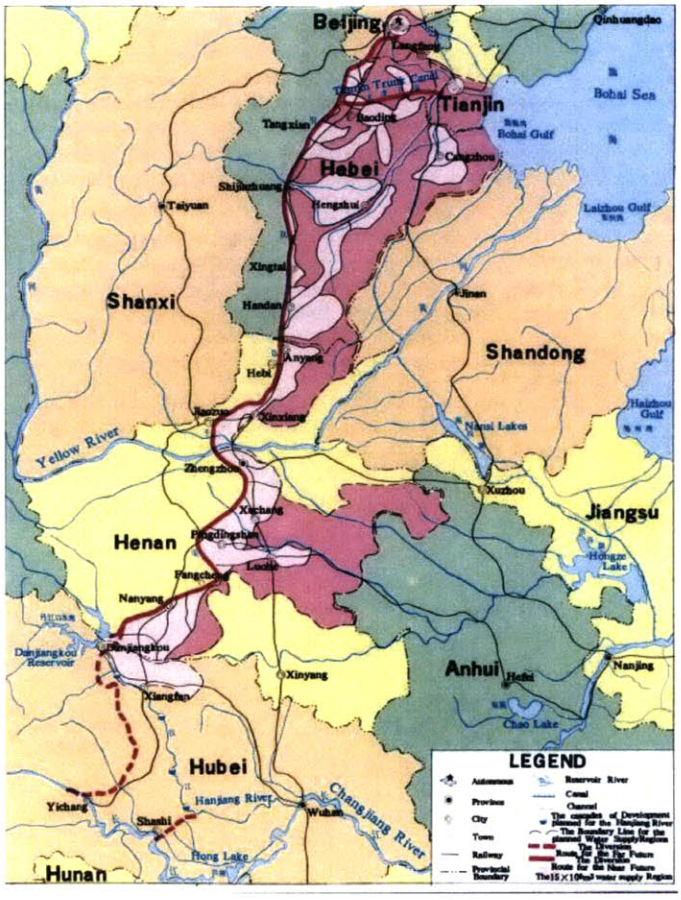

Figure 6-6: The layout of MRP.

Western Route Project (MRP)

WRP will divert water from the upper reach of the Yangtze River into the Yellow River to mitigate water shortages in northwest and north China. WRP is still in the preliminary study stage. The Yellow River Conservancy Commission (YRCC) has focused on three transfer routes from Tongtianhe, Yalongjiang, and Daduhe Rivers, as shown in Figure 6-7. The project requires construction of a high dam and pumping stations since Bayankala Mountain lies between the Yellow River and the Yangtze River, and the elevation of the bed of the Yellow River is higher than that of the corresponding section of the Yangtze River (www.yellowriver.gov.cn).

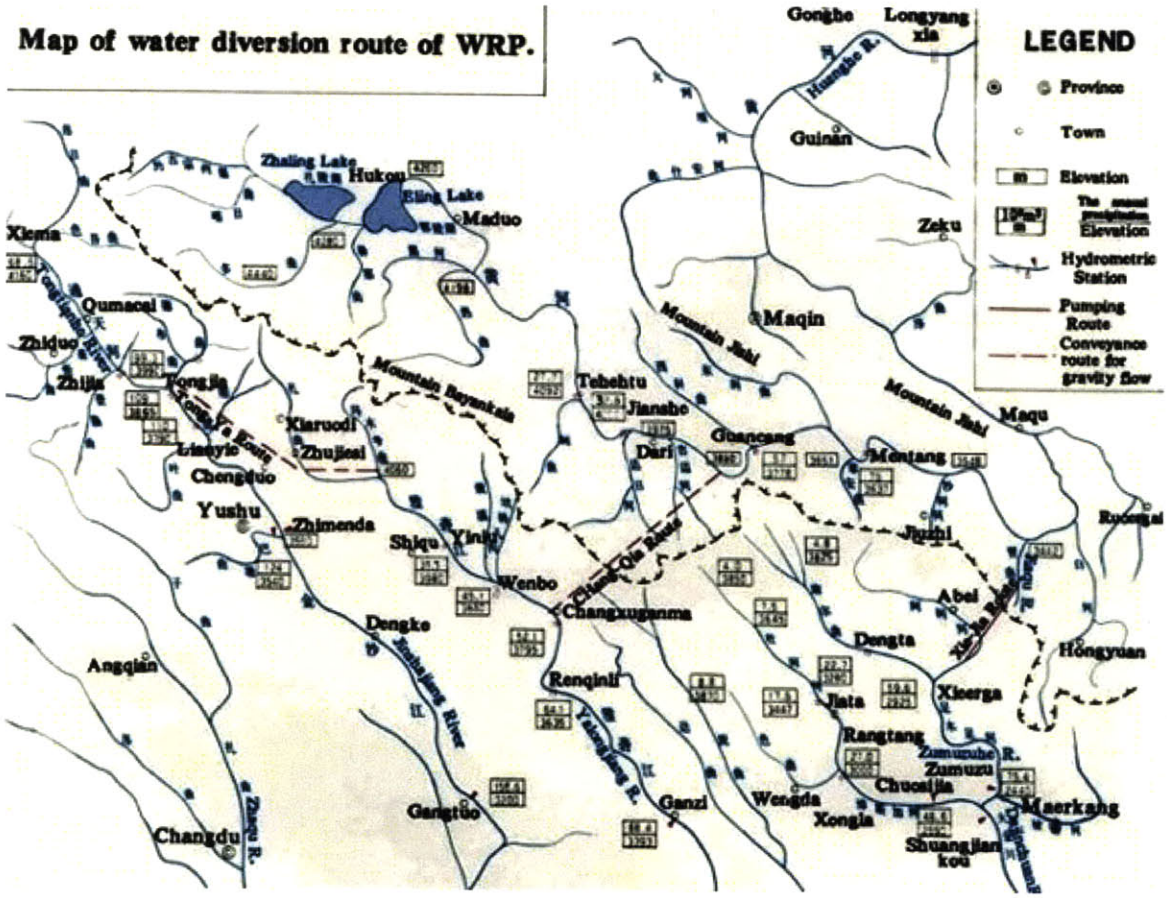

Figure 6-7: The layout of WRP.

WRP is expected to divert 20 billion m^3 $year^{-1}$ of water from these three rivers to supply 9 billion m^3 $year^{-1}$ for municipal and industrial water use and the remaining 11 billion m^3 $year^{-1}$. This will increase the irrigated area in Qinghai, Gansu, Shanxi, Shaanxi, Ningxia, and Inner Mongolia by a total of 2 Mha. The contribution to the transferred water will be 10 billion m^3 $year^{-1}$ from Tongtianhe River, 5 billion m^3 $year^{-1}$ from Yalongjiang, and 5 billion m^3 $year^{-1}$ from Daduhe River (Lei et al. n.d.). The Tongtianhe diversion route is a combined development with the Yalongjiang diversion route, in which the water will be diverted by gravity from Tongtianhe to Yalongjiang.

6.2.2 Climate Alternatives from GCMs

To quantify climate changes we consider predictions from 24 general circulation models (GCMs) participating in the World Climate Research Programme's (WCRP's) Coupled Model Intercomparison Project phase 3 (CMIP3) multi-model dataset*. We have selected a subset of these GCMs to provide a range of possible changes. In particular, we will look at changes in the three climatological inputs: precipitation, temperature, and reference evapotranspiration

Most of models predict that China's climate will be warmer during this century with the projected changes in annual temperature for the Tibetan Plateau to be 3.8° C and for East Asia to be 3.3° C (Christensen et al. 2007). Predictions of precipitation are different in sign and magnitude in different regions and seasons. Figure 6-8 shows the number of models with A1B scenario that agree precipitation will increase in any given pixel, during winter and summer. In this case, the changes are between 1970-1989 and 2080-2099. We can see that there is a strong consensus that winter precipitation will increase in the northern half of China. However, there is

greater uncertainty in predicted changes in winter rainfall in the south and in summer rainfall over most of the country.

* *We acknowledge the modeling groups, the Program for Climate Model Diagnosis and Intercomparison (PCMDI) and the WCRP's Working Group on Coupled Modelling (WGCM) for their roles in making available the WCRP CMIP3 multi-model dataset. Support of this dataset is provided by the Office of Science, U.S. Department of Energy.*

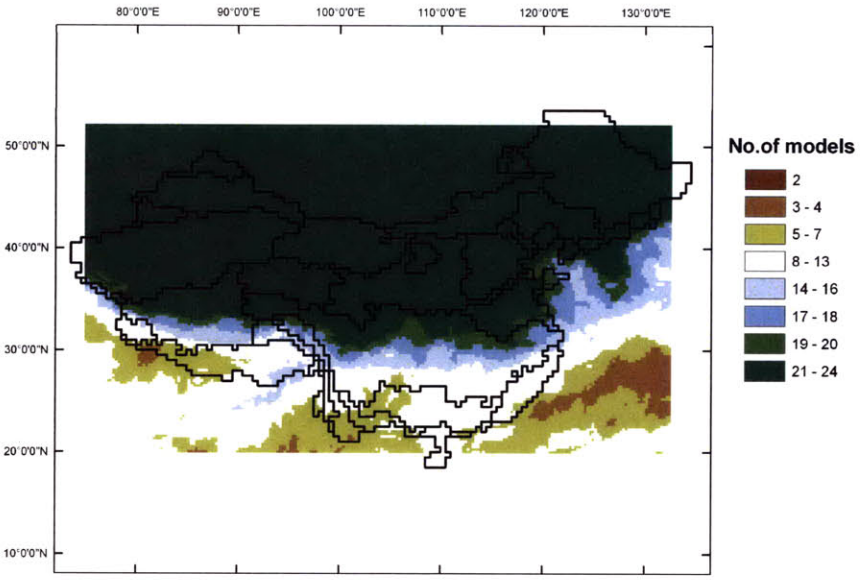

(a) Winter (DJF)

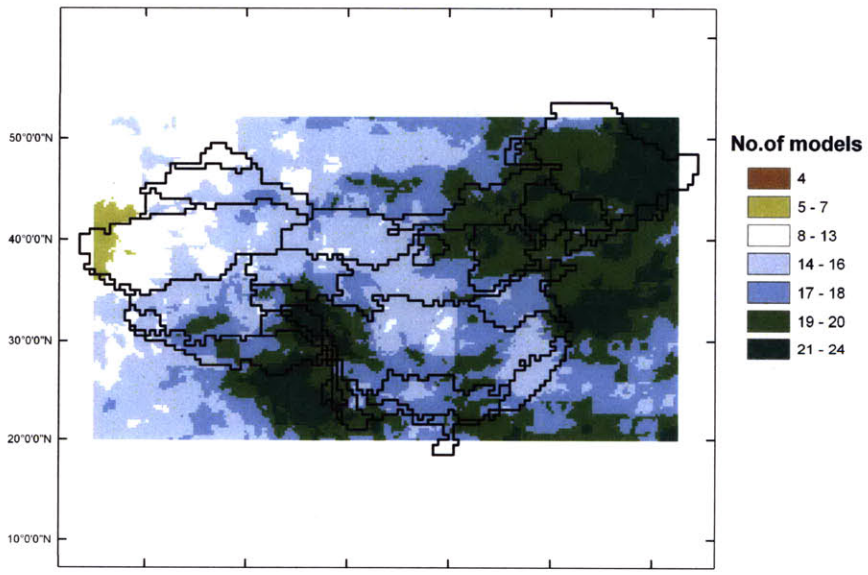

(b) Summer (JJA)

Figure 6-8: Number of models out of 24 GCMs that project increases in (a) winter precipitation and (b) summer precipitation over China for A1B scenario. Precipitation change between 1970-1989 and 2080-2099.

Figure 6-9 shows annual precipitation change in percent over China between the period 2080-2099 and 1970-1989 from all 24 GCMs. These predictions are based on the A1B scenario, which is defined as *"a future world of very rapid economic growth, global population that peaks in mid-century and declines thereafter, and the rapid introduction of new and more efficient technologies. The energy system will be balanced across all sources (where balanced is defined as not relying too heavily on one particular energy source, on the assumption that similar improvement rates apply to all energy supply and end use technologies)"* (SRES 2000).

Since changes in precipitation from the CMIP3 dataset are more diversified among the GCMs than changes in temperature, we will select a subset of GCMs that exhibit diverse seasonal and regional precipitation patterns. Predicted changes in precipitation differ seasonally and geographically. Moreover, it is important for our study to focus on changes where cropland is concentrated. When selecting candidate models and alternatives we will consider both the temporal and spatial distribution of precipitation.

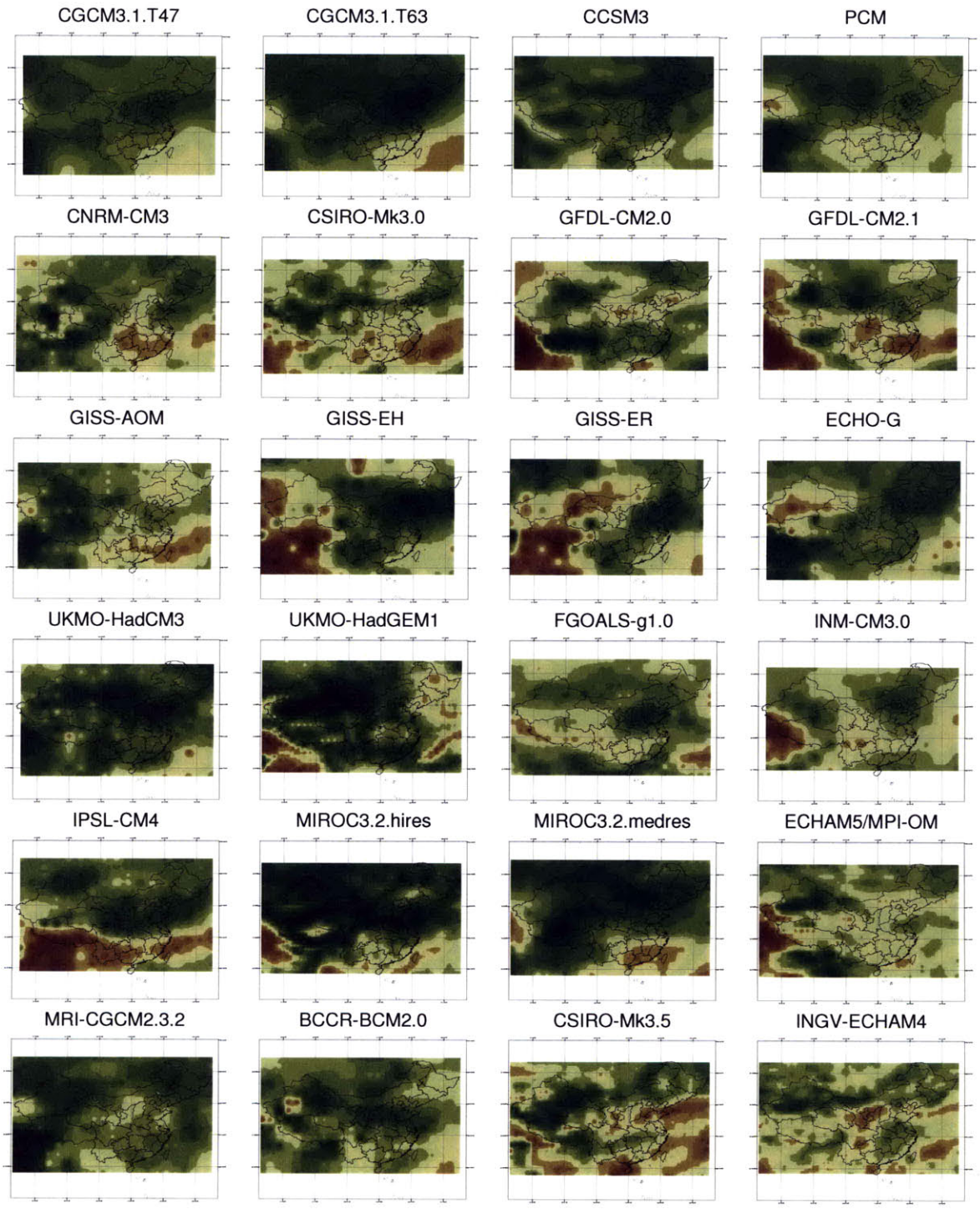

Figure 6-9: Precipitation change (%) from the years 1970-1989 to 2080-2099 for A1B scenario from 24 GCMs.

Since cropland distribution is highly correlated to regional climate, we divide China's climates into six distinct regions (Figure 6-10). The northwestern regions are steppe (as indicated by BS in the map) and desert (BW), while the northern and central parts are temperate continental (Dc). The southern part is subtropical wet (Cr) and summer rain (CW), and the southern island, Hainan, is tropical wet and dry (Aw). For consistency and simplicity, we modify the climatic boundaries to coincide with the river basins (as shown in Figure 6-10) and aggregate parts of the northwestern region to obtain four climatic regions. Then we calculate an average precipitation change for each climatic region for winter (December, January, February), summer (June, July, August), and annual precipitation.

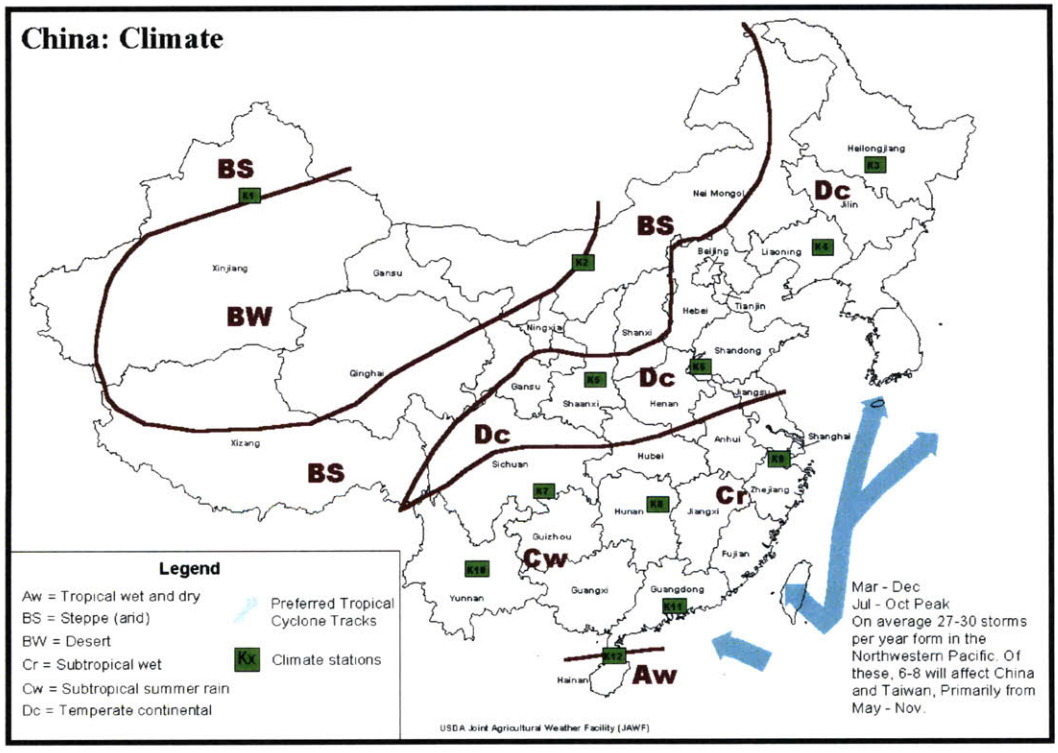

Figure 6-10: Climatic regions in China. (Source: USDA Joint Agricultural Weather Facility)

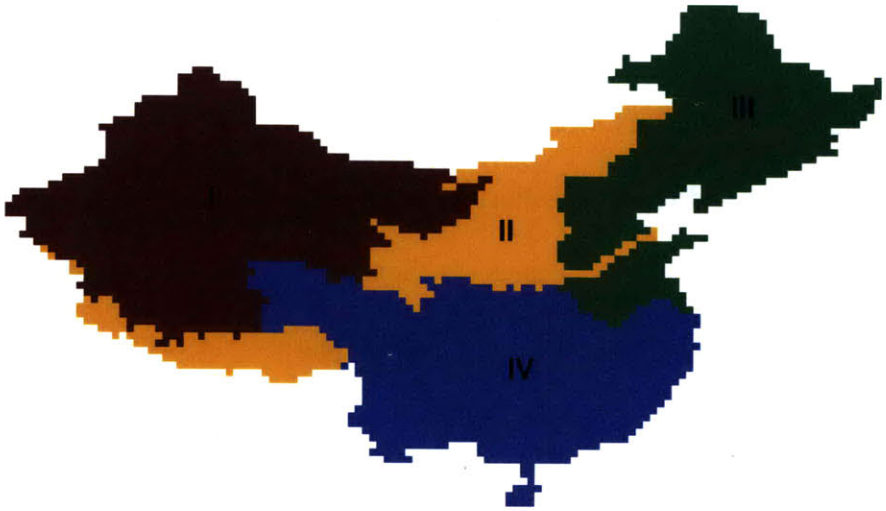

Figure 6-11: Modified climatic regions to coincide with the river basins. Region I: steppe and desert; Region II: steppe; Region III: temperate continental; Region IV: subtropical wet, summer rain, and tropical wet and dry.

Table 6-2 summarizes spatially average changes for each of four climate regions. The average changes in precipitation over all GCMs are positive in both summer and winter. However, if we look closely into each region and season, the predicted changes are different among GCMs. For example, ECHAM5/MPI-OM (Germany) predicts decreasing precipitation in three regions, while more than half of GCMs predict that there will be more precipitation. Predictions are more consistent for winter precipitation, since all of the GCMs predict positive changes for Regions I, II, and IV. However, for the south (Region IV), eight out of 24 GCMs predict negative changes with a wide range in magnitude.

Table 6-2: Precipitation changes (%) between 2080-2099 and 1970-1989. Numbers in red indicate decreases in change. GCMs highlighted with yellow color are selected alternatives.

	ANNUAL					SUMMER					WINTER				
Model ID and countries	**I**	**II**	**III**	**IV**	**rmse**	**I**	**II**	**III**	**IV**	**rmse**	**I**	**II**	**III**	**IV**	**rmse**
BCCR-BCM2.0, Norway	16	16	8	8	0.07	3	4	5	8	0.09	73	45	34	16	0.45
CCSM3, USA	13	14	23	10	0.11	15	15	25	12	0.19	22	22	30	7	0.16
CGCM3.1(T47), Canada	15	16	15	11	0.06	7	15	15	6	0.07	28	26	36	14	0.11
CGCM3.1(T63), Canada	20	23	27	12	0.19	5	23	26	6	0.20	39	18	27	12	0.19
CNRM-CM3, France	14	11	12	0	0.07	16	16	15	4	0.13	35	46	70	(4)	0.36
CSIRO-Mk3.0, Australia	15	4	7	(1)	0.13	17	2	5	(4)	0.19	24	15	20	(2)	0.26
CSIRO-Mk3.5, Australia	17	7	5	3	0.11	10	4	3	5	0.11	48	25	41	(27)	0.35
ECHAM5/MPI-OM, Germany	9	1	6	3	0.15	(6)	(8)	(6)	3	0.28	21	20	46	(1)	0.17
ECHO-G, Germany/Korea	0	15	20	11	0.17	(15)	16	19	12	0.23	16	34	63	16	0.32
FGOALS-g1.0, China	7	7	11	3	0.10	3	4	11	(7)	0.16	23	22	18	6	0.25
GFDL-CM2.0, USA	10	12	7	12	0.09	(12)	18	2	14	0.22	37	17	41	7	0.12
GFDL-CM2.1, USA	9	9	7	(3)	0.13	(25)	11	10	6	0.30	24	5	20	(23)	0.42
GISS-AOM, USA	18	9	3	2	0.12	(10)	13	6	4	0.16	32	14	11	11	0.33
GISS-EH, USA	1	9	19	12	0.16	4	5	9	12	0.08	14	26	70	20	0.39
GISS-ER, USA	(3)	(2)	15	9	0.23	(10)	0	18	7	0.20	9	21	36	10	0.26
INGV-ECHAM4, Italy	10	0	7	3	0.15	(3)	0	8	7	0.14	30	15	20	(5)	0.26
INM-CM3.0, Russia	6	5	11	2	0.12	4	0	5	5	0.12	19	25	33	(2)	0.17
IPSL-CM4, France	10	9	16	(1)	0.10	3	4	10	5	0.07	38	16	34	(12)	0.22
MIROC3.2(hires), Japan	37	33	22	13	0.33	38	31	12	13	0.39	59	47	67	5	0.42
MIROC3.2(medres), Japan	25	26	21	6	0.19	27	21	7	6	0.24	26	50	74	4	0.41
MRI-CGCM2.3.2, Japan	19	10	15	9	0.06	2	1	6	7	0.11	25	18	32	3	0.15
PCM, USA	13	13	11	3	0.05	4	19	15	9	0.10	20	33	33	6	0.16
UKMO-HadCM3, UK	23	22	22	16	0.18	17	20	23	10	0.20	65	74	82	36	0.77
UKMO-HadGEM1, UK	43	19	6	18	0.32	32	17	6	20	0.31	69	32	17	21	0.46
AVERAGE	14	12	13	7		5	10	11	7		33	28	40	5	

Since the emphasis of our study is the crop production, we will consider scenarios, in which climate changes affect summer rainfall in single-crop areas with concentrated cropland (Region II, III, and IV), summer rainfall, and both summer and winter rainfall in heavily cultivated multiple cropping areas (Region IV). Table 6-3 summarizes four alternatives that display the mention criteria. The numbers in Table 6-3 are average precipitation changes in percentage between specified period and 1970-1989.

Table 6-3: Selected climate alternatives from GCMs with precipitation changes (%) for two time periods compare to 1970-1989. Numbers in red indicate decrease in change.

		Anuual				**Summer**				**Winter**			
Scenarios	**Year\Region**	1	2	3	4	1	2	3	4	1	2	3	4
CGCM-T47													
Average over all	2081-2100	14	16	15	11	4	13	14	7	29	25	33	16
models	2046-2065	12	18	18	7	2	14	16	5	26	14	17	15
ECHAM5													
Slightly drier in	2081-2100	8	2	12	4	(23)	(7)	2	6	30	26	48	3
summer	2046-2065	6	3	7	3	(8)	1	0	4	10	6	16	16
GFDL-2.1													
Dry summer in NW	2081-2100	4	8	2	1	(14)	13	4	9	17	4	33	(14)
and dry winter in SE	2046-2065	8	4	(5)	(3)	(8)	7	(7)	2	17	(1)	14	(18)
MIROC3.2 (hires)													
High summer	2081-2100	37	33	22	13	38	31	12	13	60	48	72	5
rainfall everywhere	2046-2065	27	26	14	13	29	25	9	13	37	34	45	11

The CGCM3.1(T47) model is used to approximate the overall average condition across all 24 GCMs. It predicts an increase in precipitation for all of the regions. The ECHAM5/MPI-OM model predicts a reduction in summer rainfall in all regions except in the south. The GFDL-CM2.1 predicts the driest alternative among the four GCMs in Table 6-3, while the MIROC3.2(hires) model predicts the wettest alternative. Note that precipitation changes shown in Table 6-3 are spatially averaged over each region and used only to facilitate in alternative

selection. For model simulations, we apply changes on a finer scale, which will be further explained in the following section.

6.2.3 Downscaling GCM Predictions

Since the resolution of GCMs is still at a coarser spatial scale than our model grid, typically of the order of 200 km on a side, we need to downscale their predictions in order to use them as model inputs. This can be achieved by two approaches: dynamical downscaling or statistical downscaling. Even though sophisticated dynamical downscaling methods are based on physical concepts, they do not give much better results than simpler statistical downscaling (Wood et al. 1997). Therefore, we employ the simplest method of statistical downscaling for our study, which is to apply GCM-scale projections in the form of change factors (CFs) (Prudhomme et al. 2002). First, we calculate a change factor by comparing predictions from GCM for the future period of 2046-2065 with the nominal climate of 1970-1989 simulated by the same GCM. The precipitation and reference evapotranspiration change factors are multiplicative while the temperature change factors are additive. We apply the monthly calculated change factors to the monthly observed climate at 0.25° resolution for the period 1970-1989 from (Thomas 2007) and (Thomas 2008). We calculate the change factors at a monthly time scale due to the limited reliability of GCM results at finer temporal resolution, especially for precipitation.

In order to make downscaled reference evapotranspiration consistent with our crop coefficient approach, we need to calculate reference evapotranspiration values from other variables predicted by the GCM, using the FAO Penman-Monteith equation. The FAO Penman-Monteith expression from Equation (4-2) is:

$$ET_o = \frac{0.408\Delta(R_n - G) + \gamma \frac{900}{T+273} u_2 (e_s - e_a)}{\Delta + \gamma(1 + 0.34u_2)} \quad (4\text{-}2)$$

Figure 6-12 (a)-(d) show examples of predicted changes in precipitation, reference evapotranspiration, and temperature in the month of June from the four selected GCMs. In general, changes in reference evapotranspiration are more subtle than those in precipitation. All four GCMs predict warmer conditions in June over all of China.

(a) CGCM3.1.T47

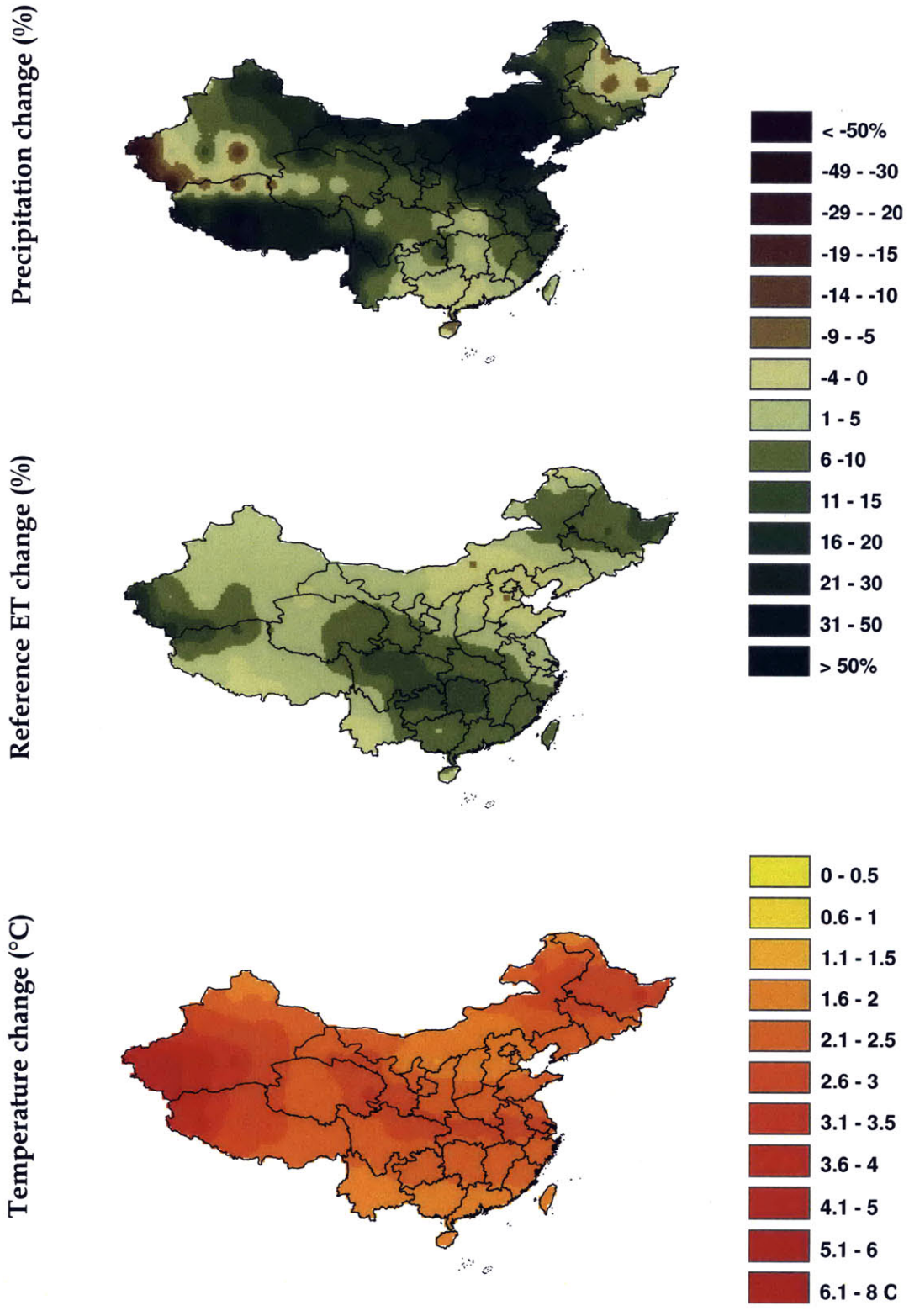
Precipitation change (%)
Reference ET change (%)
Temperature change (°C)
< -50%
-49 - -30
-29 - - 20
-19 - -15
-14 - -10
-9 - -5
-4 - 0
1 - 5
6 -10
11 - 15
16 - 20
21 - 30
31 - 50
> 50%
0 - 0.5
0.6 - 1
1.1 - 1.5
1.6 - 2
2.1 - 2.5
2.6 - 3
3.1 - 3.5
3.6 - 4
4.1 - 5
5.1 - 6
6.1 - 8 C

(b) ECHAM5/MPI-OM

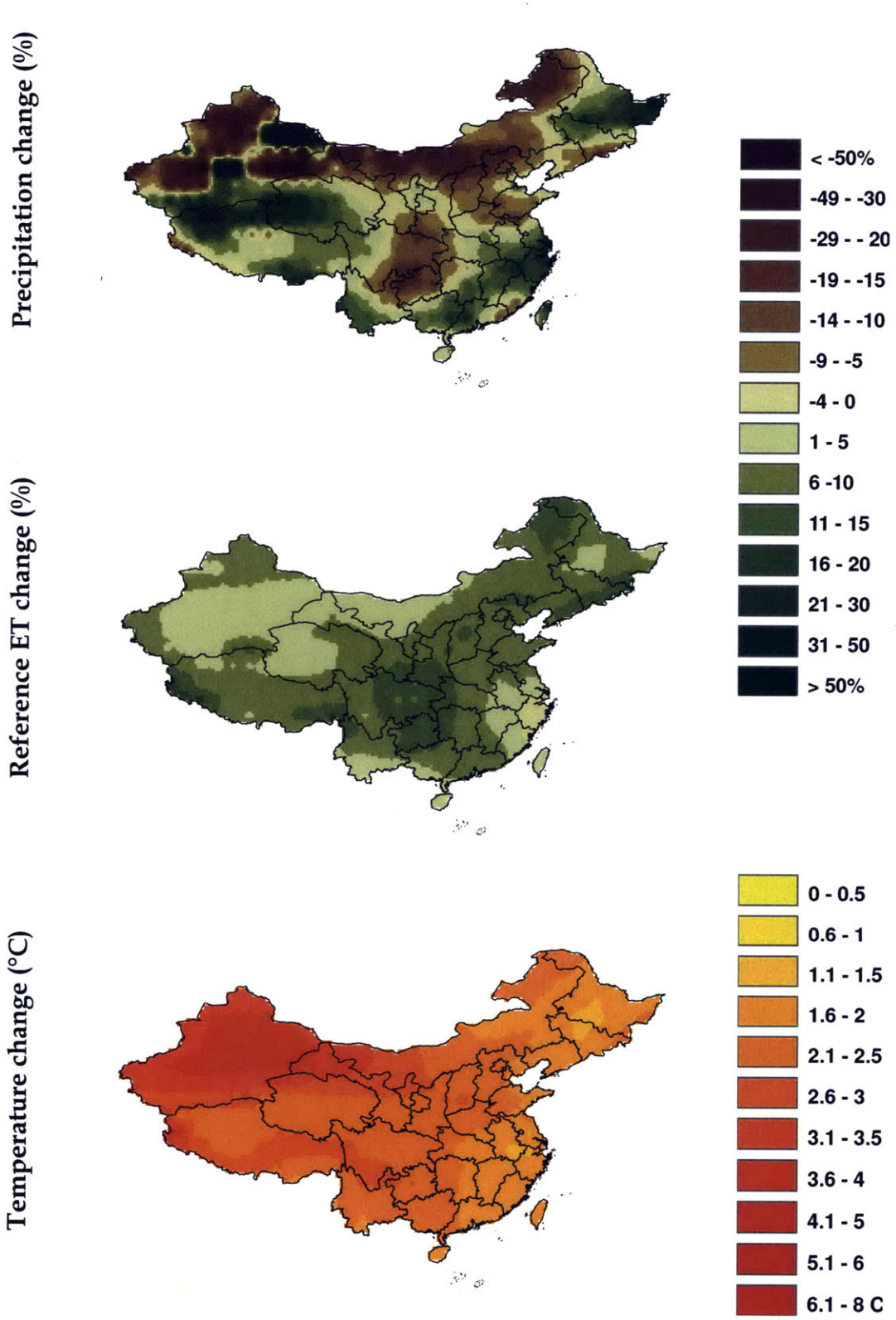

(c) GFDL-CM2.0

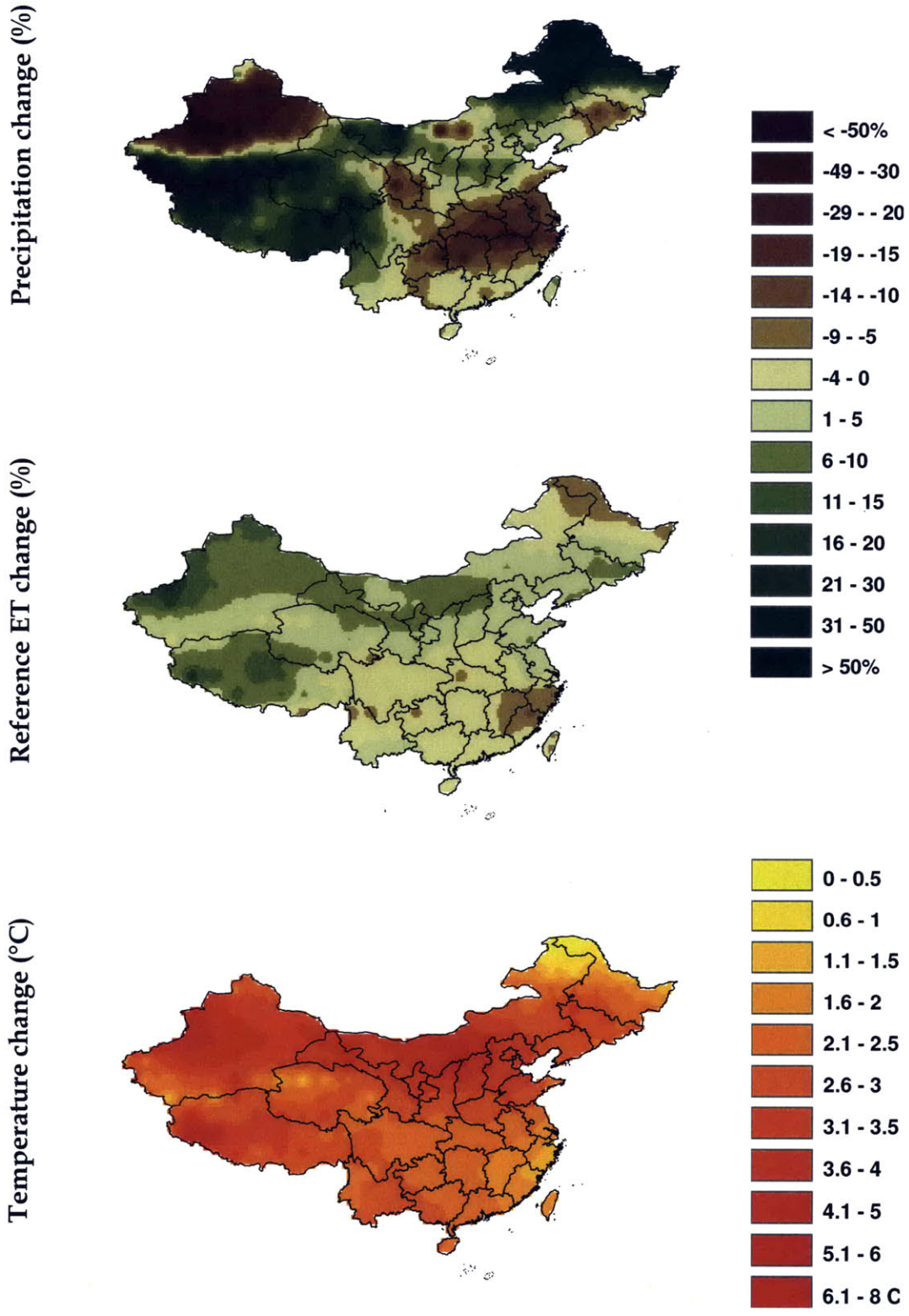
Precipitation change (%)
< -50%
-49 - -30
-29 - - 20
-19 - -15
-14 - -10
-9 - -5
-4 - 0
1 - 5
6 -10
11 - 15
16 - 20
21 - 30
31 - 50
> 50%
Reference ET change (%)
Temperature change (°C)
0 - 0.5
0.6 - 1
1.1 - 1.5
1.6 - 2
2.1 - 2.5
2.6 - 3
3.1 - 3.5
3.6 - 4
4.1 - 5
5.1 - 6
6.1 - 8 C

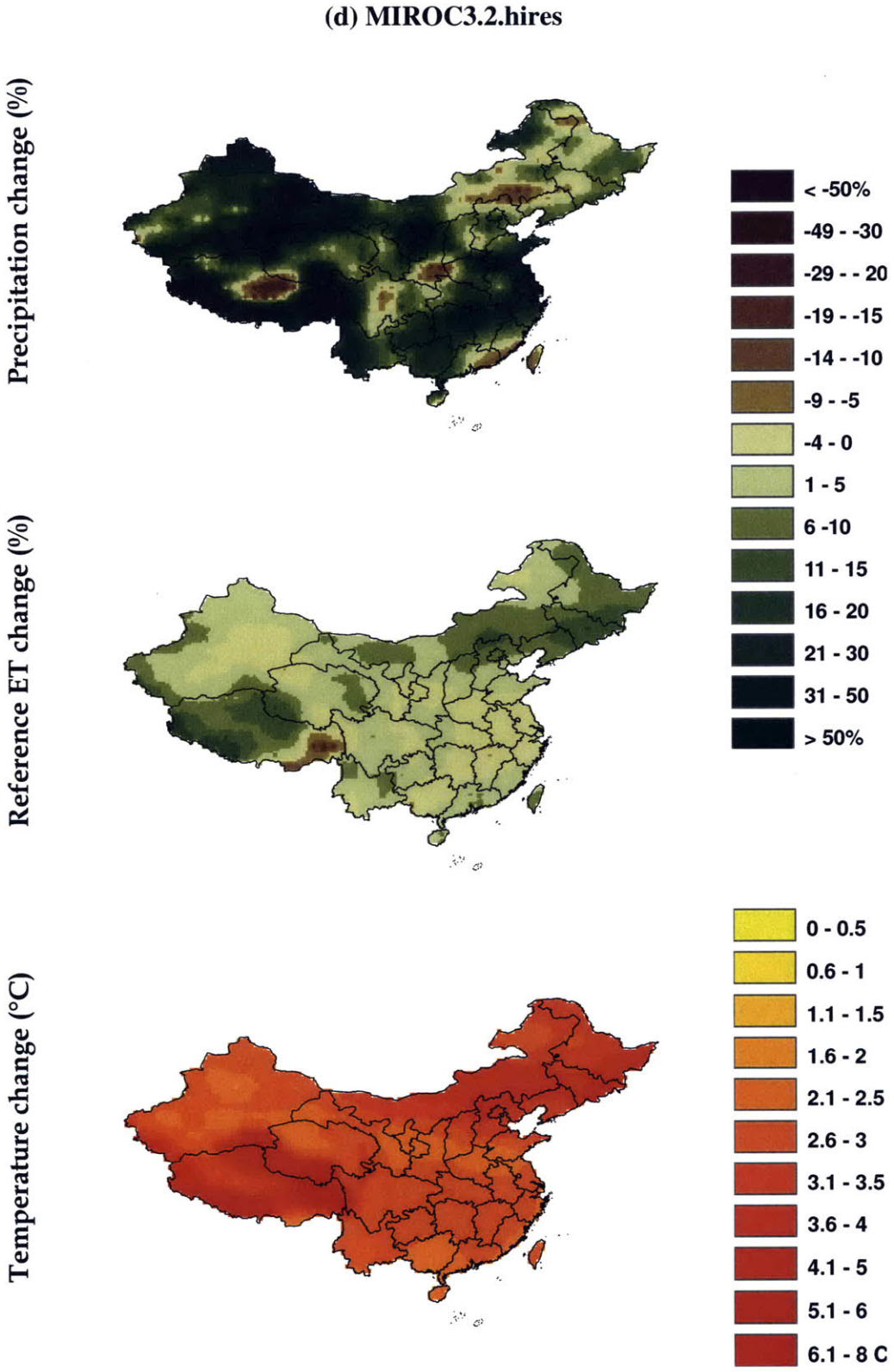

Figure 6-12 (a-d): The predicted changes in precipitation, temperature, and reference evapotranspiration in June from the years 1970-1989 to 2046-2065 under the A1B scenario from selected GCMs.

6.2.4 Model Solutions for Climate Alternatives

CGCM3.1(T47) (Average over all models)

The CGCM3.1(T47) alternative represents an average over all 24 GCMs, with an increase in annual, summer and winter precipitation over each climatic region. The resulting value for people fed is shown in Figure 6-13. The solutions under this alternative are close to the baseline solution until the land use change reaches about 5.5 percents where the CGCM3.1(T47) alternative could support more people but the baseline simulation reaches maximum land use change (shown as a dash line in Figure 6-13).

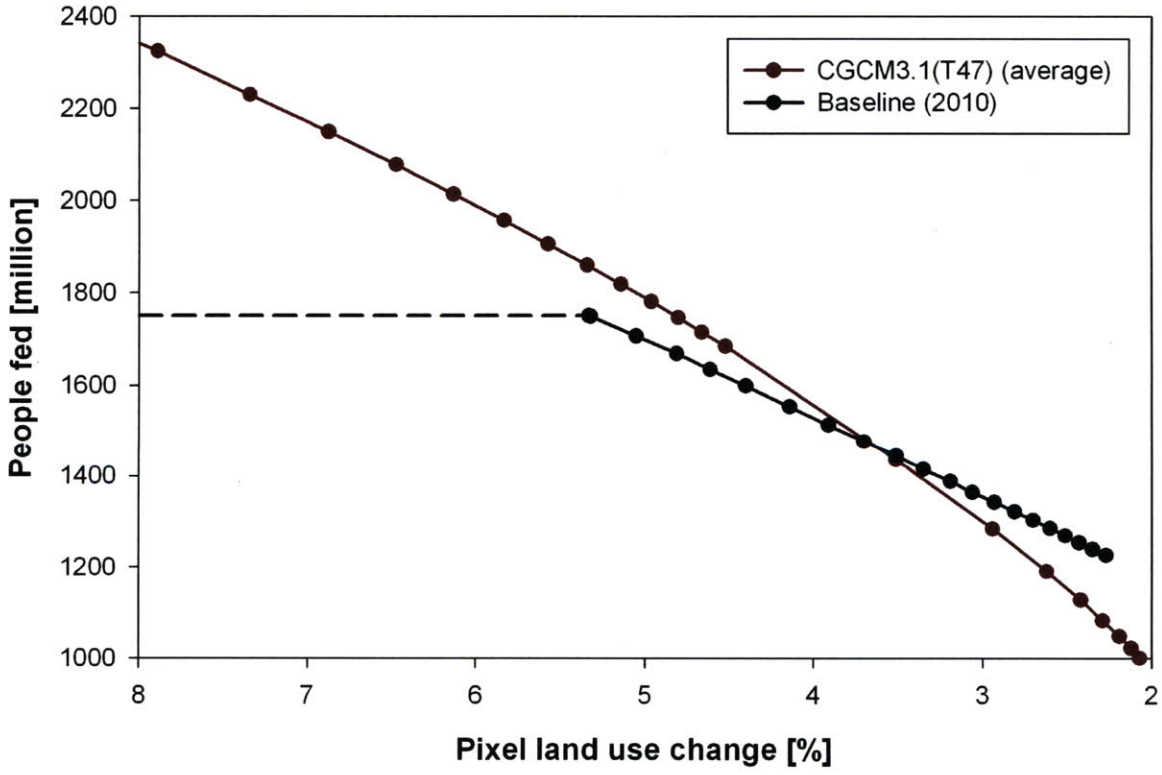

Figure 6-13: Model's people fed versus land use change for the period 2045-2065 with the CGCM3.1(T47) alternative (average over all models) compare with the baseline solution.

Table 6-4 summarizes the land devoted to different agricultural land categories for three cases of misfit. The solution for this alternative expands triple-cropping area to a value greater than is possible with nominal climate. For the case of land use change of 5 percents, the triple-cropping area is 27.5 Mha for baseline simulation, but 34.4 Mha for the CGCM3.1(T47) alternative.

Table 6-4: People fed and agricultural areas from three levels of land use change from the CGCM3.1(T47) alternative.

		Land use change		
		3.5%	**4.5%**	**5.5%**
People fed	[million]	1436.3	1684.6	1882.3
Sown area	[Mha]	179.7	201.9	224.0
Cropland	[Mha]	115.7	124.1	132.5
Irrigated cropland	[Mha]	69.6	75.3	81.1
Single cropping	[Mha]	74.4	74.9	75.3
Double cropping	[Mha]	18.5	20.7	22.8
Triple cropping	[Mha]	22.7	28.6	34.4

ECHAM5/MPI-OM (Slightly drier in summer)

The ECHAM5/MPI-OM alternative predicts a reduction in summer rainfall in all regions except in the south (Region IV), where summer rainfall is predicted to increase slightly (3%). Annual and winter precipitation changes are positive for all the regions except for a slight decrease in winter rainfall in the south (1%). Figure 6-14 shows that the people fed value obtained under the ECHAM5/MPI-OM alternative is less than the baseline until the land use change reaches 6.5 percents. The solution obtained for this alternative is lowest among the four alternatives. The largest change is observed in the triple cropping area. The ability to increase triple cropping in the ECHAM5/MPI-OM alternative makes it possible to support more people. When the land use

change equal to 5 percents, the areas devoted to single- and double-cropping under this alternative are less than those of the baseline, but the triple-cropping area is 10 Mha higher. In addition, the irrigated area under this alternative is almost 7 Mha higher. This increase in irrigated cropland is responsible for much of the increase in the total cropland.

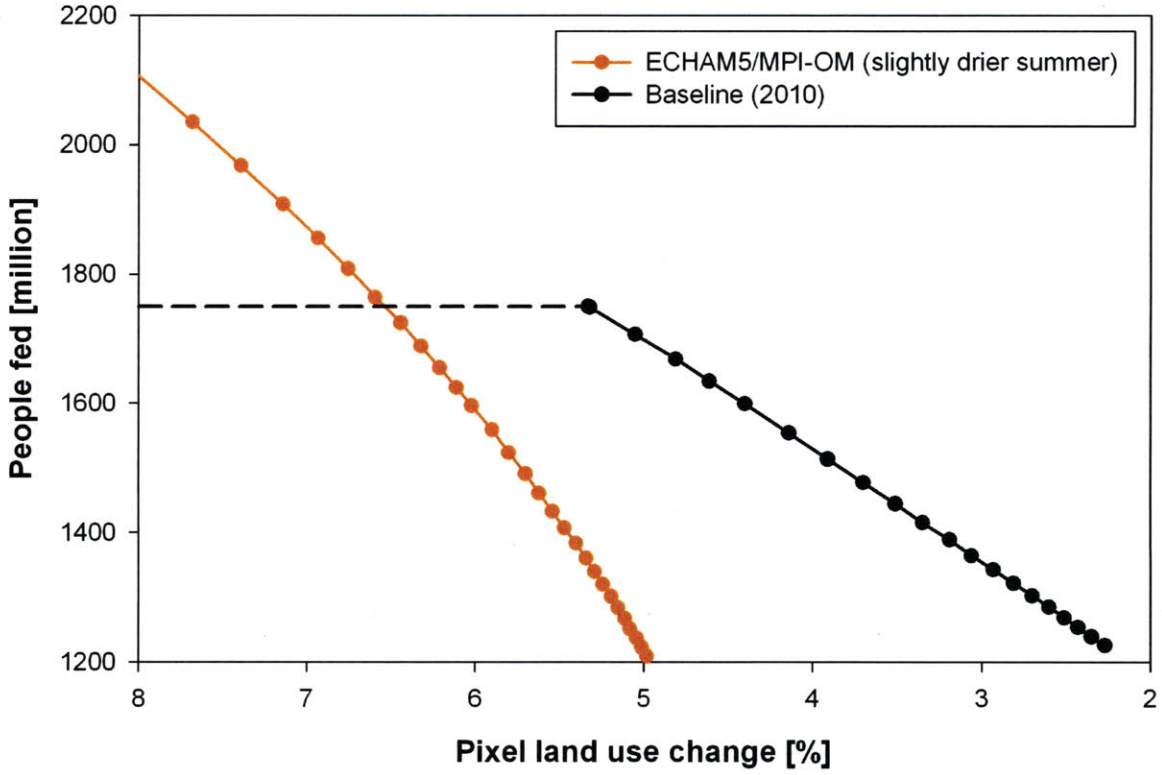

Figure 6-14: Model's people fed versus land use change for the period 2045-2065 with the ECHAM5/MPI-OM alternative (Slightly drier in summer) compare with the baseline solution.

Table 6-5: People fed and agricultural areas from three levels of land use change from the ECHAM5/MPI-OM alternative.

		Land use change		
		5%	6%	7%
People fed	[million]	1266.9	1595.9	1908.2
Sown area	[Mha]	167.3	192.7	227.7
Cropland	[Mha]	107.4	116.9	130.0
Irrigated cropland	[Mha]	68.1	74.9	84.6
Single cropping	[Mha]	68.7	69.1	69.7
Double cropping	[Mha]	17.5	19.9	23.0
Triple cropping	[Mha]	21.2	28.0	37.4

GFDL-CM2.1 (Dry summer in Northwest and dry winter in Southeast)

The GFDL-CM2.1 alternative is the driest among the four climate change alternatives. The GFDL-CM2.1 model predicts a 25% reduction in summer rainfall in the northwestern region (Region I) and a 23% reduction in winter rainfall in the south/southeastern region (Region IV), where most triple-cropping occurs. A comparison with the baseline solution is shown in Figure 6-15. The number of people fed of the GFDL-CM2.1 alternative is lower than the baseline. When the land use change equal to 4 percents, the GFDL-CM2.1 alternative only supports 1266 million people while the baseline's people fed are 1553.6 million people. However, the land use can be expanded more under the GFDL-CM2.1 alternative. When the land use change reaches 6 percents, the triple-cropping area and number of people fed are both higher under the GFDL-CM2.1 alternative.

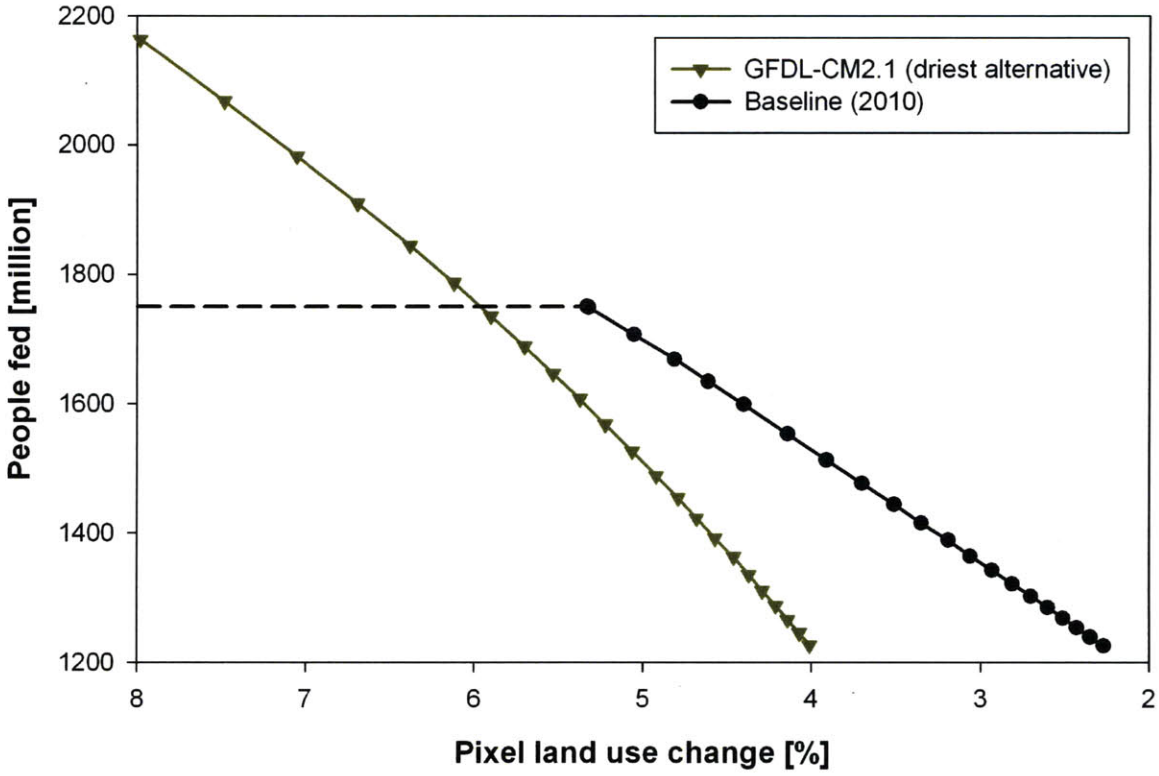

Figure 6-15: Model's people fed versus land use change for the period 2045-2065 with the GFDL-CM2.1 alternative (Dry summer in Northwest and dry winter in Southeast) compare with the baseline solution.

Table 6-6: People fed and agricultural areas from three levels of land use change from the GFDL-CM2.1 alternative.

		Land use change		
		4%	5%	6%
People fed	[million]	1266.1	1507.5	1786.7
Sown area	[Mha]	164.8	184.9	214.6
Cropland	[Mha]	104.0	111.5	122.7
Irrigated cropland	[Mha]	69.8	75.6	84.3
Single cropping	[Mha]	64.5	64.8	65.3
Double cropping	[Mha]	18.1	20.1	22.9
Triple cropping	[Mha]	21.4	26.6	34.5

MIROC3.2.hires (High summer rainfall everywhere)

The MIROC.hires alternative predicts the largest percentage increase in summer rainfall in almost all regions among all 24 GCMs. Nevertheless, the number of people fed for this alternative can be slightly lower than the baseline when land use change is relative small. This could be due to the significant spatial variation in precipitation changes by the MIROC3.2.hires GCM. Even though the average change over a given region may be positive, there are scattered patches where precipitation is lower. Figure 6-12 (d) confirms that the predicted change in June rainfall from the MIROC.hires model is not positive everywhere. More specifically, the change over the northeastern region, where cropland is concentrated, is negative. In addition, if the increase in rainfall occurs over a region that is not suitable for crop or crop area cannot be expanded because of arability constraints, the excess precipitation will not be able to produce more crops.

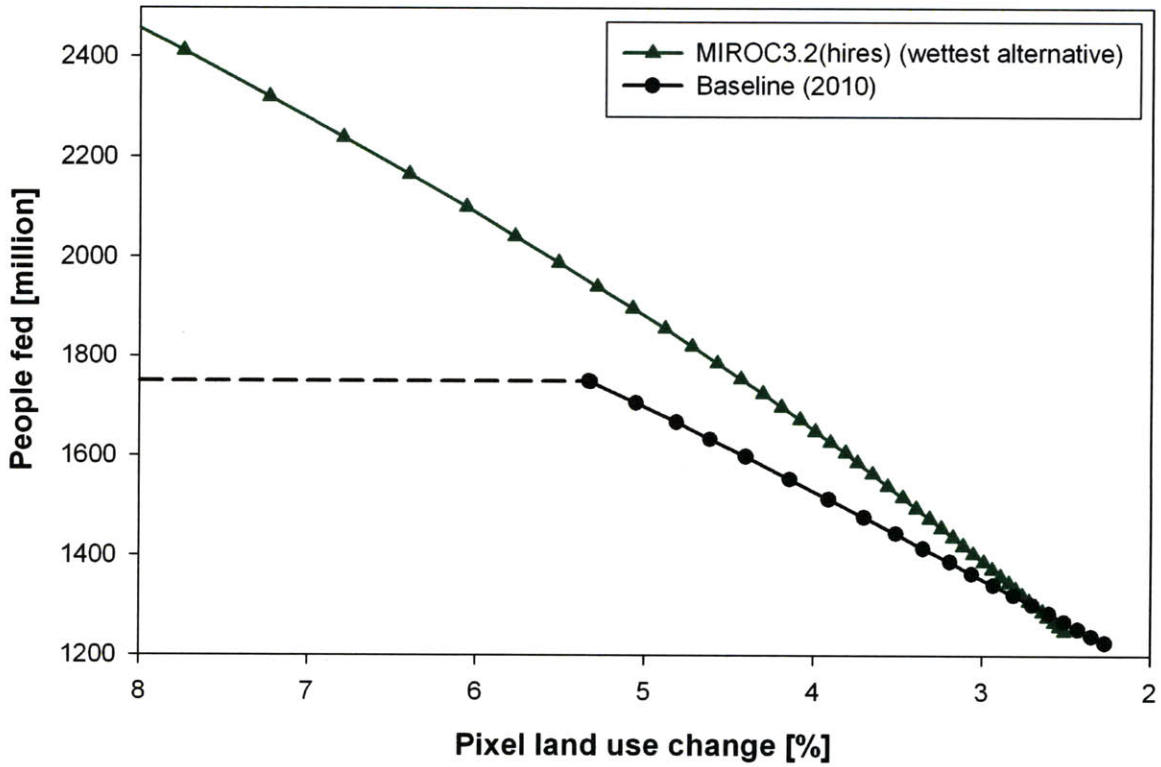

Figure 6-16: Model's people fed versus land use change for the period 2045-2065 with the MIROC3.2.hires alternative (High summer rainfall everywhere) compare with the baseline solution.

Table 6-7: People fed and agricultural areas from three levels of land use change from the MIROC3.2.hires alternative.

		Land use change		
		3%	4%	5%
People fed	[million]	1388.4	1650	1876.1
Sown area	[Mha]	171.9	194.6	219.9
Cropland	[Mha]	111.7	120.3	129.8
Irrigated cropland	[Mha]	67.2	72.7	78.9
Single cropping	[Mha]	72.6	73.0	73.4
Double cropping	[Mha]	18.2	20.3	22.7
Triple cropping	[Mha]	21.0	27.0	33.7

Summary of All Alternatives

Figure 6-17 summarizes the people fed vs. land use change tradeoff for all of the alternatives. The peak population of 1462 million people in 2032 predicted by the U.S. Census Bureau is superimposed as a reference. All of the alternatives predict fewer people fed than the peak population until certain percentage in land use expansion occur. The people fed solution obtained for the MIROC3.2(hires) is the highest among all alternatives. The people fed solutions for the GFDL-CM2.1 and ECHAM5/MPI-OM are lower than the baseline until land use expansion reaches about 6 and 6.5 percents, respectively. Required agricultural land use for all of the five alternatives to be able to feed 1462 million people is summarized in Table 6-8 below. For all alternatives, the amount of total cropland is lower than the baseline. However, the amount of triple cropping areas is higher with the two drier alternatives (GFDL-CM2.1 and ECHAM5/MPI-OM). When comparing predictions with nominal land use (1990-2000), notably increase in irrigated area contributes mainly to the increase in the total crop area as well as the triple-cropping area mainly contributes to the increase in the total sown area.

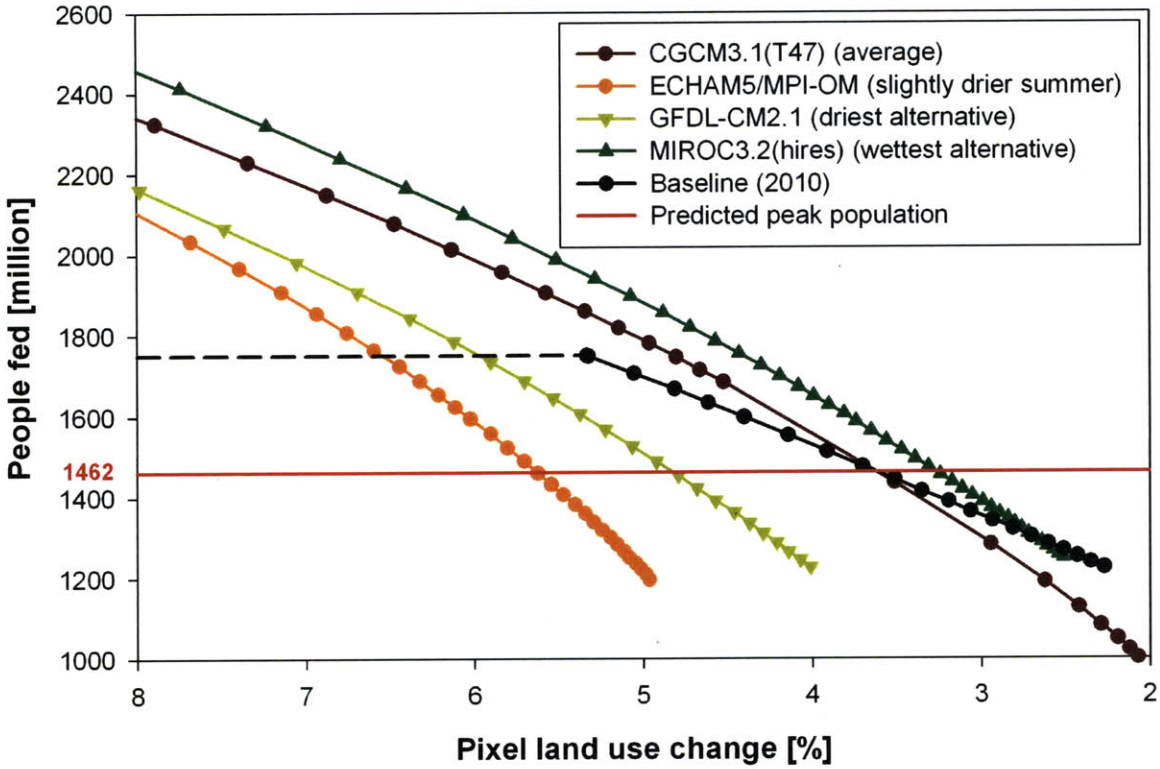

Figure 6-17: Model's predicted people fed versus land use change for the period 2045-2065 under climate alternatives compare with result from the baseline and the predicted peak population of 1462 million people.

Table 6-8: Agricultural land use from all alternatives to feed predicted peak population of 1462 million people and nominal land use from the period 1990-2000.

		Nominal	Baseline	CGCM3.1 (T47)	ECHAM5/ MPI-OM	GFDL-CM2.1	MIROC3.2 (hires)
Land use change	[%]		3.7	3.6	5.6	4.9	3.3
People fed	[million]	1223.8	1477.1	1457.1	1460.7	1471.3	1474.9
Sown area	[Mha]	132.0	184.6	181.3	182.3	181.6	178.6
Cropland	[Mha]	99.3	119.7	116.3	113.0	110.3	114.3
Irrigated cropland	[Mha]	57.8	72.2	70.0	72.1	74.6	68.8
Single cropping	[Mha]	76.0	77.4	74.5	68.9	64.8	72.3
Double cropping	[Mha]	13.9	19.8	18.7	18.9	19.8	18.8
Triple cropping	[Mha]	9.4	22.5	23.1	25.2	25.7	22.8

Chapter 7

Conclusions

This thesis proposes a systematic approach to investigate how natural resources (land and water) constrain food production. The developed approach is applied to China as a case study. By formulating an optimization problem to determine which resource is a limiting factor at a fine scale (0.5° by 0.5°), crop production and the corresponding people fed can be estimated under observed and changed climates. Major results and original contributions from this study are summarized below.

7.1 Summary of Results

Arable land is abundant in the North, while water is concentrated in the South

By formulating a simplified optimization (Chapter 2) with basic principles of a balance between available natural resources and crop resource requirements, a limiting factor for the northern and southern regions can be determine. It is found that water is a limiting resource in the north, while land limits crop production in the south. In addition, the simplified optimization model predicts a number of people fed to be around 2 billion people. This prediction shows significant potential

for increasing food production in China, yet it is in ways that could involve dramatic changes in land use. As a consequence, the nominal cropland is included in the objective function to provide realistic constrain and allow us to infer how much changes in cropland from nominal condition are expected.

Irrigation and triple-cropping are keys to enhancing food production to support increasing population

China's population is predicted to reach its peak of 1462 million people in the year 2032. Using the detailed optimization model of Chapter 3 and assuming future climate remains unchanged from what was observed during the years 1951-1990, significant increase in irrigated and triple-cropping areas are needed to support the increase in population of 250 million more people. The predicted increase from the nominal condition (1990-2000) in irrigated area is about 12 Mha (21% increase from nominal irrigated cropland). For triple-cropping area, the required expansion is more pronounce. The increase is estimated to about 13 Mha or more than doubles the nominal amount of 9.4 Mha.

Predicted changes in future precipitation are diversified seasonally and regionally resulting in wide range of people fed

All of the climate models predict a warmer scenario over all China in the next fifty years; however, changes in precipitation subject to considerable uncertainty. Relative changes in reference evapotranspiration are also varied, but relatively subtle than changes in precipitation. Based on average climate prediction over all available GCMs, people fed are close to what obtained under nominal climate. For two drier alternatives considered, people fed are less than

those under nominal climate unless there is quite a significant change in agricultural land use (ranging between 50 to 60 Mha increases in the total sown area compare to the nominal sown area during the period of 1990-2000). To support the predicted peak population, the expected increase in the total cropland is less than the baseline solution for all of the considered alternatives.

7.2 Original Contributions

Developed a consistent framework for analyzing how water and land resources constraint food production and for studying how agricultural system responds to climate change

The consistent framework developed in this thesis is the first that can reproduce existing agricultural as well as hydrological conditions. The model's calibration process results in the estimation of uncertain and unobserved inputs, which are consistent with historical observations of provincial crop production, basin annual runoff, crop area, and irrigated area. These inputs are pixel total crop area, pixel irrigated area, and noncrop evapotranspiration. Specifically, the estimated total crop area and irrigated area serve as additional physical constraints for realistic prediction and provide base line to infer how much change in agricultural land use would be required to meet future's food production demand from increasing population.

Incorporated the impacts of the South-to-North Water Diversion project in scenario analysis

The main propose of the diversion project is to alleviate the problem arising from the mismatch between the location of water resources, and available land and population. The project will

transfer water from the Yangtze River to the water scarce regions in the NCP, northwestern and northern regions. Including the impacts of the project is important for our future prediction since the water demand in those water scarce regions are predicted to increase due to increase in population, per capita M&I water use, and irrigated area.

Identified key requirements in meeting future demand of food production

By comparing future predictions with the existing condition derived from the calibrated optimization model, we are able to identify where significant changes in agricultural land use are required to support future population. As discussed in the Summary of Results section, irrigation and triple-cropping are keys in increasing China's food production capacity.

Studied the potential impacts of climate change on China's food production capacity

Understanding the sensitivity of agriculture to climate change is critical for meeting future food requirements. Using the calibrated model, incorporated with the diversion project, with predicted climate scenarios from GCMs provided insights into how changed climates could potentially impact food production capacity and estimated required changes to support increasing food demand.

7.3 Future Research

Some possible extensions of this work are outlined here.

Dynamic analysis of inter annual variability

The optimization model developed in this study presents an average long term analysis. However, inter annual variability in climates play a significant role in agricultural planning and unquestionably affecting agricultural production outputs. Importantly, the dynamic analysis entails the need of comprehensive datasets of climatological time series and changes in grain reserves over the same period. Also, computational load will be critical for the dynamic study. The results from this steady-state study could serve as an initial condition for the dynamic analysis.

Explicit consideration of groundwater component

Our climatological analysis considers long-term average conditions. Thus, the change in water storage is negligible in the steady-state conditions for water balance, yet significant changes (notably decrease) in water tables have been observed in several groundwater basins, especially those in the North China Plain. Including a component of groundwater flux in the model will allow a direct investigation into how increase in population and food demand will affect the groundwater resources and vice versa. This poses a very critical question, yet requires a complex modeling of groundwater flux movement. In addition, the optimization model developed in this study needs to be modified to allow dynamic analysis as discussed above before the effect of changes in water tables can be considered.

Appendix

GAMS Optimization Model

```
* GAMS China crop allocation problem

* Primary decision variables:
*       land(pixel,sequence) -- land devoted to each crop sequence in pixel (Mha)


$offsymxref
$offsymlist
$offlisting
$onempty

option
      limrow=10
      limcol=10           ;
option sysout = off;
option QCP = Cplex;
option iterlim = 999999 ;
option reslim = 10000 ;

sets
$include china_pixels.txt

alias (pixel,n)

sets
basin /HeilongJiang, SuifenHe, LiaoningHebei, TumenJiang, YaluJiang, LiaodongBandao, LiaoHe,
    LuanHe, HaiHe, HuangHe, ShandongBandao, HuaiHe, ChangJiang,
    SouthEastCoastal, ZhuJiang, GuangdongGuangxi, YuanJiang, LancangJiang,
    NuJiang, DulongJiang, YarlungZangboJiang, SenggeZangbo, ErtixHe, NeiMongol,
    HexiCorridor, Qaidam, Junggar, IliHe, Tarim, QiangtangGaoyuan/ ;


parameter pop_frac(basin)      Fraction of nation's population in each basin
$include basin_pop_frac.txt

parameter pop_dens(pixel)      Fraction of nation's population in each pixel [CIESIN 2005]
```

```
$include pop_dens.txt

sets
* pixel set for each tributary
$include trib_def.txt
trib(n,pixel);
$include trib_table.txt

set
* pixel set for each basin
$include basinpixel_def.txt
basinpixel(basin,pixel);
$include basinpixel_table.txt

set
* dryland crop sequence set for each pixel
$include sequence.txt
$include pixelsequence_dry_def.txt
pixelsequence_dry(pixel,sequence);
$include pixelsequence_dry_table.txt

set
* irrigated crop sequence set for each pixel
$include pixelsequence_irr_def.txt
pixelsequence_irr(pixel,sequence);
$include pixelsequence_irr_table.txt

parameters
$include et_irr.txt
$include et_dry.txt
$include natet.txt
$include precip.txt
$include pet.txt
*$include aet.txt
$include yieldMz.txt
$include yieldWt.txt
$include yieldHw.txt
$include yieldRc.txt
$include yieldVg.txt
$include yieldTu.txt
$include yieldOl.txt
$include china_area.txt
$include croplandqp.txt
$include irr_area.txt
$include china_onecrop.txt
$include china_twocrop.txt
$include china_thrcrop.txt

*Read in nominal cropland from calibration model parameters
landqp_irr(pixel,sequence), landqp_dry(pixel,sequence);

Execute_Load 'qpsolutions.gdx', landqp_irr=land_irr_qp.l, landqp_dry=land_dry_qp.l;

sets
        prov /Beijing, Tianjin, Hebei, Shanxi, InnerMongolia, Liaoning,
        Jilin, Hei, Shanghai, Jiangsu, Zhejiang, Anhui, Fujian,
```

```
      Jiangxi, Shandong, Henan, Hubei, Hunan, Guangdong, Guangxi, Hainan,
      Sichuan, Guizhou, Yunnan, Tibet, Shaanxi, Gansu, Qinghai, Ningxia,
      Xinjiang/

set
* pixels set for each province
$include provpixel_def.txt
provpixel(prov,pixel);
$include provpixel_table.txt

parameter
$include prov_frac.txt

set
upstrm(pixel)
$include upstream_pixel.txt
downstrm(pixel);

downstrm(pixel) = yes;
downstrm(pixel) = not upstrm(pixel) ;

parameter effc(pixel) ;
effc(pixel)$upstrm(pixel) = 1.0 ;
effc(pixel)$downstrm(pixel) = 0.4 ;

set
single(sequence)
double(sequence)
triple(sequence)
$include singleseq.txt
$include doubleseq.txt
$include tripleseq.txt

set
$include rsingle.txt
$include rdouble.txt
$include msingle.txt
$include mdouble.txt
$include wsingle.txt
$include wdouble.txt
$include osingle.txt
$include odouble.txt
$include tsingle.txt
$include tdouble.txt
$include vsingle.txt
$include vdouble.txt
$include hsingle.txt

*Consumption rate 2005 from FBS
develmaizepc   kg per person per yr /104.64/
develwheatpc   kg per person per yr /79.62/
develricepc    kg per person per yr  /91.80/
develvegepc    kg per person per yr  /314.78/
develtubepc    kg per person per yr  /145.13/
develoilpc     kg per person per yr   /64.51/
```

```
**** Import Data [billion kg/year] 2005****
import_rice     /0.25/
import_wheat    /4.30/
import_maize    /-3.72/
import_vege     /-7.62/
import_tube     /13.88/
import_oil      /28.29/
;

* conversion from (10^6 ha)(mm yr^-1) to (10^6 m^3 yr^-1)
conv1 conversion factor 1     /10/
* conversion from (10^9 kg yr^-1) to (10^6 people)(kg person^-1 yr^-1)
conv2 conversion factor 2     /1000/
* conversion from (sq kilometers) to (10^6 ha)
conv3 conversion factor 3     /0.0001/
* conversion from (10^6 m^3 per yr) to (km^3 per yr)
conv4 conversion factor 4       /0.001/
* conversion from (10^6 ha) to (km^2)
conv5 conversion factor 5     /10000/

set
crop_seq(sequence)   all crop sequences except 'nnn';
crop_seq(sequence) = yes ;   crop_seq('nnn') = no ;

parameters
cropland_nat  total cropland in the country [km^2]
irrland_nat   total irrigated area from PD [km^2]
onecrop_nat   total cropland devoted to single rotations [km^2]
twocrop_nat   total cropland devoted to double rotations [km^2]
thrcrop_nat   total cropland devoted to triple rotations [km^2];

cropland_nat = sum(pixel, croparea(pixel));
irrland_nat = sum(pixel, irr_area(pixel));
onecrop_nat = sum(pixel, onecrop(pixel));
twocrop_nat = sum(pixel, twocrop(pixel));
thrcrop_nat = sum(pixel, thrcrop(pixel));

set
$include rseq.txt
$include mseq.txt
$include wseq.txt
$include hseq.txt
$include oseq.txt
$include tseq.txt
$include vseq.txt

parameters
$include maize_arable.txt
$include wheat_arable.txt
$include rice_arable.txt

parameter p_landqpirr(pixel), p_landqpdry(pixel), index_irr, index_dry;
scalar alpha, i, meanqp_irr, n_irr, meanqp_dry, n_dry;
p_landqpirr(pixel) = sum(sequence$(crop_seq(sequence)), landqp_irr(pixel,sequence));
p_landqpdry(pixel) = sum(sequence$(crop_seq(sequence)), landqp_dry(pixel,sequence));
index_irr(pixel) = 1$(p_landqpirr(pixel) <> 0);
```

```
index_dry(pixel) = 1$(p_landqpdry(pixel) <> 0);
n_irr = sum(pixel, index_irr(pixel));
n_dry = sum(pixel, index_dry(pixel));
meanqp_irr = sum(pixel,sum(sequence$(crop_seq(sequence)), landqp_irr(pixel,sequence)))/n_irr;
meanqp_dry = sum(pixel,sum(sequence$(crop_seq(sequence)), landqp_dry(pixel,sequence)))/n_dry;
display n_irr,n_dry,meanqp_irr,meanqp_dry;

*Municipal and industrial water diversion
parameter
$include develmipc07.txt
*m^3 per capita
;
scalars irr_term, dry_term, rmse ;

positive variables
land_irr(pixel,sequence)        irrigated land use in pixel for sequence (ha)
land_dry(pixel,sequence)        land use in pixel for sequence (ha)
total_irr(pixel)                total irrigated cropland in pixel (ha)
total_dry(pixel)                total dryland cropland in pixel (ha)
total_cropland(pixel)           total cropland in pixel (km^2)
total_onecrop(pixel)            total cropland devoted to single rotations (km^2)
total_twocrop(pixel)            total cropland devoted to double rotations (km^2)
total_thrcrop(pixel)            total cropland devoted to triple rotations (km^2)
total_sown                      total sown area (count double cropping twice) (km^2)
total_crop                      total cropland (km^2)
total_irri                      total irrigated area (km^2)
total_single                    total single cropping area (km^2)
total_double                    total double cropping area (km^2)
total_triple                    total triple cropping area (km^2)
irr_upper_bound(pixel)          total irrigated land in each pixel (km^2)
arableland_basin(basin)         total arable land in each basin (km^2)
etpixel_nnn(pixel)              ET in each pixel for sequence nnn (10^6 m^3 per yr)
etpixel_irr(pixel)              ET in each pixel from irrigated agriculture (10^6 m^3 per yr)
etpixel_dry(pixel)              ET in each pixel from dryland agriculture (10^6 m^3 per yr)
etpixel(pixel)                  ET in each pixel for all sequences except nnn (10^6 m^3 per yr)
runoff(basin)                   runoff water of each basin (10^6 m^3 per year)
mandi(basin)                    m and i water of each basin (10^6 m^3 per yr)
tot_maize                       total maize yield (10^9 kg per yr)
tot_wheat                       total wheat yield (10^9 kg per yr)
tot_rice                        total rice yield (10^9 kg per yr)
tot_vege                        total vege yield (10^9 kg per yr)
tot_tube                        total tuber yield (10^9 kg per yr)
tot_oil                         total oil yield (10^9 kg per yr)
ET_tot_arable                   total volume of water evapotranspired by arable land (km^3 per yr)
ET_tot_nnn                      total volume of water evapotranspired by non-arable land (km^3 per yr)
Precip_tot                      total precipitation (km^3 per yr)
yieldmaize(pixel)               total maize yield from each pixel (1000 kg per yr)
yieldwheat(pixel)               total wheat yield from each pixel (1000 kg per yr)
yieldw_wt(pixel)                total winter wheat yield from each pixel (1000 kg per yr)
yieldrice(pixel)                total rice yield from each pixel (1000 kg per yr)
yieldvege(pixel)                total vege yield from each pixel (1000 kg per yr)
yieldtube(pixel)                total tuber yield from each pixel (1000 kg per yr)
yieldoil(pixel)                 total oil yield from each pixel (1000 kg per yr)
precipbasin(basin)              Precip over an entire basin (10^6 m^3 per yr)
precipbasin_arable(basin)       Arable Precip over an entire basin (10^6 m^3 per yr)
etbasin(basin)                  Arable ET over an entire basin (10^6 m^3 per yr)
```

```
etbasin_nnn(basin)          Non-arable ET over an entire basin (10^6 m^3 per yr)
mzyieldprov(prov)           provincial maize production (10^9 kg per yr)
olyieldprov(prov)           provincial oil crops production (10^9 kg per yr)
rcyieldprov(prov)           provincial rice production (10^9 kg per yr)
tuyieldprov(prov)           provincial tubers production (10^9 kg per yr)
vgyieldprov(prov)           provincial vegetables production (10^9 kg per yr)
wtyieldprov(prov)           provincial wheat production (10^9 kg per yr)
upstrm_area(pixel)          Upstream catchment area of each pixel (km^2) - not include itself
discharge(pixel)            Runoff from each pixel (km^3 per year)
chinafed                    People fed (million people)
rland(pixel)                Cropland devoted to rice (km^2)
mland(pixel)                Cropland devoted to maize (km^2)
wland(pixel)                Cropland devoted to spring wheat (km^2)
hland(pixel)                Cropland devoted to winter wheat (km^2)
oland(pixel)                Cropland devoted to oil crops (km^2)
tland(pixel)                Cropland devoted to tubers (km^2)
vland(pixel)                Cropland devoted to vegetables (km^2)
nat_rland                   Total cropland devoted to rice (km^2)
nat_mland                   Total cropland devoted to maize (km^2)
nat_wland                   Total cropland devoted to spring and winter (km^2)
nat_oland                   Total cropland devoted to oil crops (km^2)
nat_tland                   Total cropland devoted to tubers (km^2)
nat_vland                   Total cropland devoted to vegetables (km^2)
mandiused(pixel)            The municipal and industrial water loss to evaporation (10^6 m^3 per yr)
;

free variables
obj_fcn          People fed and the mean-squared deviation from nominal condition
;

equations
totalland(pixel)            'total land use in each pixel'
irr_land(pixel)             'set irrigated land devoted to nnn to zero'
pixelet_nnn(pixel)          'ET in each pixel for the nnn sequence'
pixelet_irr(pixel)          'ET in each pixel from irrigated agriculture (crop only)'
pixelet_dry(pixel)          'ET in each pixel from dryland agriculture (crop only)'
pixelet(pixel)              'ET in each pixel for all sequences except nnn (crop only)'
pixelet_dry_up(pixel)       'pixelet_dry must be met by annual precip in case of removing the water demand check in
preprocessor'
maizeyield(pixel)           'maize yield in each pixel'
wheatyield(pixel)           'wheat yield in each pixel'
w_wtyield(pixel)            'winter wheat yield in each pixel'
riceyield(pixel)            'rice yield in each pixel'
vegeyield(pixel)            'vegetable yield in each pixel'
tubeyield(pixel)            'tuber yield in each pixel'
oilyield(pixel)             'oil yield in each pixel'
mandiwater(basin)           'm and i water use in each basin'
basinbalance(basin)         'basin-wide water balance'
basinprecip(basin)          'Volumetric precip in each basin'
basinprecip_arable(basin)   'Volumetric arable precip in each basin'
basinet(basin)              'Volumetric et in each basin'
basinet_nnn(basin)          'Non-arable volumetric et in each basin'
runoff_limit(basin)         'ensure minimum river flow'
maizeused                   'maize used directly and indirectly for food'
wheatused                   'wheat used for food'
riceused                    'rice used for food'
```

```
vegeused                'vegetable used for food'
tubeused                'tubers used for food'
oilused                 'oil used for food'
irr_total(pixel)        'total irrigated cropland in pixel'
dry_total(pixel)        'total dryland cropland in pixel'
cropland_total(pixel)   'total cropland in pixel'
onecrop_total(pixel)    'total cropland devoted to single rotations in pixel'
twocrop_total(pixel)    'total cropland devoted to double rotations in pixel'
thrcrop_total(pixel)    'total cropland devoted to triple rotations in pixel'
sown_total              'total sown area'
crop_total              'total cropland'
irri_total              'total irrigated cropland'
single_total            'total single cropping area'
double_total            'total double cropping area'
triple_total            'total triple cropping area'
basin_arableland(basin) 'total arable land in basin'
people_lim              'Limit population to something feasible'
t_maize                 'total maize yield (10^9 kg per yr)'
t_wheat                 'total wheat yield (10^9 kg per yr)'
t_rice                  'total rice yield (10^9 kg per yr)'
t_vege                  'total vege yield (10^9 kg per yr)'
t_tube                  'total tuber yield (10^9 kg per yr)'
t_oil                   'total oil yield (10^9 kg per yr)'
prov_maize(prov)        'provincial maize production (10^9 kg per yr)'
prov_twheat(prov)       'provincial wheat production (10^9 kg per yr)'
prov_rice(prov)         'provincial rice production (10^9 kg per yr)'
prov_vege(prov)         'provincial vege production (10^9 kg per yr)'
prov_tube(prov)         'provincial tube production (10^9 kg per yr)'
prov_oil(prov)          'provincial oil production (10^9 kg per yr)'
et_volume               'total volume of ET from arable land (km^3 per yr)'
et_nnn                  'total volume of ET from non arabe land (km^3 per yr)'
tot_precip              'total precipitation'
catchment(pixel)        'catchment area'
pixel_wbalance(pixel)   'discharge from each pixel'
dryland_check(pixel)    'check how much water is available for dryland agriculture and natural land'
rland_total(pixel)      'aggregate cropland devoted to rice (km^2)'
mland_total(pixel)      'aggregate cropland devoted to maize (km^2)'
wland_total(pixel)      'aggregate cropland devoted to spring wheat (km^2)'
hland_total(pixel)      'aggregate cropland devoted to winter wheat (km^2)'
oland_total(pixel)      'aggregate cropland devoted to oil crops (km^2)'
tland_total(pixel)      'aggregate cropland devoted to tubers (km^2)'
vland_total(pixel)      'aggregate cropland devoted to vegetables (km^2)'
riceupb(pixel)          'rice arable land (km^2)'
maizeupb(pixel)         'maize arable land (km^2)'
wheatupb(pixel)         'wheat arable land (km^2)'
rland_nat               'total cropland devoted to rice (km^2)'
mland_nat               'total cropland devoted to maize (km^2)'
wland_nat               'total cropland devoted to spring and winter wheat (km^2)'
oland_nat               'total cropland devoted to oil crops (km^2)'
tland_nat               'total cropland devoted to tubers (km^2)'
vland_nat               'total cropland devoted to vegetables (km^2)'
usedmandi               'the municipal and industrial water loss to evaporation (10^6 m^3 per yr)'
objective               'objective function'
;

**************************************************************************
```

```
* Land balance
totalland(pixel)..          sum(sequence$pixelsequence_irr(pixel,sequence), land_irr(pixel,sequence))
                    + sum(sequence$pixelsequence_dry(pixel,sequence), land_dry(pixel,sequence))=e=
area(pixel)*100 ;

* set land_irr(pixel,'nnn') to zero
irr_land(pixel)..           land_irr(pixel,'nnn') =e= 0;

* municipal and industrial water loss to evaporation
usedmandi(pixel)..          mandiused(pixel) =e= 0.2*sum(prov$provpixel(prov,pixel),
develmipc(prov)*prov_frac(pixel,prov)*pop_dens(pixel)*chinafed);

* compute et in each pixel for 'nnn' sequence (noncrop area)
pixelet_nnn(pixel)..        etpixel_nnn(pixel) =e= natet(pixel)*land_dry(pixel,'nnn')/1e5 ;

* compute et in each pixel seperately from irrigated and rainfed agriculture of all sequences except 'nnn'
pixelet_irr(pixel)..        etpixel_irr(pixel) =e= sum(sequence$pixelsequence_irr(pixel,sequence),
land_irr(pixel,sequence)*et_irr(pixel,sequence)/1e5);

pixelet_dry(pixel)..        etpixel_dry(pixel) =e=
sum(sequence$(pixelsequence_dry(pixel,sequence)$(crop_seq(sequence))),
land_dry(pixel,sequence)*et_dry(pixel,sequence)/1e5);

pixelet_dry_up(pixel)..     etpixel_dry(pixel) =l= precip(pixel)*area(pixel)/1000 ;

* compute et in each pixel from all except the 'nnn' sequences
pixelet(pixel)..            etpixel(pixel) =e= etpixel_irr(pixel) + etpixel_dry(pixel);

* water balance for area tributary to pixel n (excess can only go downstream)
catchment(n)..              upstrm_area(n) =e= sum(pixel$trib(n,pixel), area(pixel)) + area(n);

pixel_wbalance(n)..             sum(pixel$trib(n,pixel), precip(pixel)*area(pixel)/1000 - mandiused(pixel) -
etpixel(pixel) - etpixel_nnn(pixel))+
                        (precip(n)*area(n)/1000 - mandiused(n) - etpixel(n)/1 - etpixel_nnn(n)) - discharge(n) =e= 0
;

dryland_check(pixel)$(irr_area(pixel) eq 0)..   precip(pixel)*area(pixel)/1000 - mandiused(pixel) - etpixel(pixel)/1
- etpixel_nnn(pixel) =g= 0;

* basin water balance
mandiwater(basin)..         mandi(basin) =e= sum(pixel$basinpixel(basin,pixel), mandiused(pixel)) ;

basinbalance(basin)..       sum(pixel$basinpixel(basin,pixel), (precip(pixel)*area(pixel)/1000)
                    - etpixel(pixel)- etpixel_nnn(pixel)) - mandi(basin) - runoff(basin) =e= 0 ;

* water per basin
basinprecip(basin)..        precipbasin(basin) =e= sum(pixel$basinpixel(basin,pixel),
precip(pixel)*area(pixel)/1000) ;
basinet(basin)..            etbasin(basin) =e= sum(pixel$basinpixel(basin,pixel), etpixel(pixel)) ;
basinet_nnn(basin)..        etbasin_nnn(basin) =e= sum(pixel$basinpixel(basin,pixel), etpixel_nnn(pixel)) ;
runoff_limit(basin)..       runoff(basin) =g= flow_frac*precipbasin(basin);
basinprecip_arable(basin).. precipbasin_arable(basin) =e= sum(pixel$basinpixel(basin,pixel),
precip(pixel)*(area(pixel)-(land_irr(pixel,'nnn')-land_dry(pixel,'nnn'))/100))/1000;

* compute yield from each pixel for each crop
```

```
maizeyield(pixel)..          yieldmaize(pixel)
=e=(sum(sequence$pixelsequence_irr(pixel,sequence),land_irr(pixel,sequence)*Mzyield(sequence))

+sum(sequence$pixelsequence_dry(pixel,sequence),land_dry(pixel,sequence)*Mzyield(sequence)));
wheatyield(pixel)..          yieldwheat(pixel)
=e=(sum(sequence$pixelsequence_dry(pixel,sequence),land_dry(pixel,sequence)*Wtyield(sequence))

+sum(sequence$pixelsequence_irr(pixel,sequence),land_irr(pixel,sequence)*Wtyield(sequence)));
w_wtyield(pixel)..           yieldw_wt(pixel)
=e=(sum(sequence$pixelsequence_dry(pixel,sequence),land_dry(pixel,sequence)*Hwyield(sequence))

+sum(sequence$pixelsequence_irr(pixel,sequence),land_irr(pixel,sequence)*Hwyield(sequence)));
riceyield(pixel)..           yieldrice(pixel)
=e=(sum(sequence$pixelsequence_irr(pixel,sequence),land_irr(pixel,sequence)*Rcyield(sequence))

+sum(sequence$pixelsequence_dry(pixel,sequence),land_dry(pixel,sequence)*Rcyield(sequence)));
vegeyield(pixel)..           yieldvege(pixel)  =e=
sum(sequence$pixelsequence_irr(pixel,sequence),land_irr(pixel,sequence)*Vgyield(sequence))

+sum(sequence$pixelsequence_dry(pixel,sequence),land_dry(pixel,sequence)*Vgyield(sequence));
tubeyield(pixel)..           yieldtube(pixel)  =e=
sum(sequence$pixelsequence_irr(pixel,sequence),land_irr(pixel,sequence)*Tuyield(sequence))

+sum(sequence$pixelsequence_dry(pixel,sequence),land_dry(pixel,sequence)*Tuyield(sequence)) ;
oilyield(pixel)..            yieldoil(pixel)   =e=
yieldcoeff(pixel)*(sum(sequence$pixelsequence_irr(pixel,sequence),land_irr(pixel,sequence) *Olyield(sequence))
                    +sum(sequence$pixelsequence_dry(pixel,sequence),land_dry(pixel,sequence)
*Olyield(sequence)));

*total crop production
t_maize.. tot_maize =e=  sum(pixel, yieldmaize(pixel))/1e6  ;
t_wheat.. tot_wheat =e=  sum(pixel, yieldwheat(pixel) + yieldw_wt(pixel))/1e6  ;
t_rice..  tot_rice =e=   sum(pixel, yieldrice(pixel))/1e6  ;
t_vege..  tot_vege =e=   sum(pixel, yieldvege(pixel))/1e6  ;
t_tube..  tot_tube =e=   sum(pixel, yieldtube(pixel))/1e6  ;
t_oil..   tot_oil =e=    sum(pixel, yieldoil(pixel))/1e6  ;

* production-consumption balance
maizeused..   chinafed*develmaizepc =e= (tot_maize + import_maize)*1000  ;
wheatused..   chinafed*develwheatpc =e= (tot_wheat + import_wheat)*1000  ;
riceused..    chinafed*develricepc  =e= (tot_rice + import_rice)*1000  ;
vegeused..    chinafed*develvegepc  =e= (tot_vege + import_vege)*1000  ;
tubeused..    chinafed*develtubepc  =e= (tot_tube + import_tube)*1000  ;
oilused..     chinafed*develoilpc   =e= (tot_oil + import_oil)*1000  ;

* Aggregate cropland from all sequences except 'nnn' for each pixel
irr_total(pixel)..           total_irr(pixel) =e=
sum(sequence$(pixelsequence_irr(pixel,sequence)$(crop_seq(sequence))), land_irr(pixel,sequence))/100;
dry_total(pixel)..           total_dry(pixel) =e=
sum(sequence$(pixelsequence_dry(pixel,sequence)$(crop_seq(sequence))), land_dry(pixel,sequence))/100;
cropland_total(pixel)..      total_cropland(pixel) =e= (total_irr(pixel) + total_dry(pixel));
onecrop_total(pixel)..       total_onecrop(pixel)   =e=
(sum(sequence$(pixelsequence_irr(pixel,sequence)$single(sequence)), land_irr(pixel,sequence))

+sum(sequence$(pixelsequence_dry(pixel,sequence)$single(sequence)),land_dry(pixel,sequence)))/100;
```

```
twocrop_total(pixel)..        total_twocrop(pixel)   =e=
(sum(sequence$(pixelsequence_irr(pixel,sequence)$double(sequence)), land_irr(pixel,sequence))

+sum(sequence$(pixelsequence_dry(pixel,sequence)$double(sequence)),land_dry(pixel,sequence)))/100;
thrcrop_total(pixel)..        total_thrcrop(pixel)   =e=
(sum(sequence$(pixelsequence_irr(pixel,sequence)$triple(sequence)), land_irr(pixel,sequence))

+sum(sequence$(pixelsequence_dry(pixel,sequence)$triple(sequence)),land_dry(pixel,sequence)))/100;
sown_total..              total_sown =e= sum(pixel, total_onecrop(pixel) + 2*total_twocrop(pixel) +
3*total_thrcrop(pixel));
crop_total..              total_crop =e= sum(pixel, total_cropland(pixel));
irri_total..              total_irri =e= sum(pixel, total_irr(pixel));
single_total..            total_single =e= sum(pixel, total_onecrop(pixel));
double_total..            total_double =e= sum(pixel, total_twocrop(pixel));
triple_total..            total_triple =e= sum(pixel, total_thrcrop(pixel));
basin_arableland(basin)..     arableland_basin(basin) =e= sum(pixel$basinpixel(basin,pixel), total_cropland(pixel));

* Aggregate total cropland for each crop
rland_total(pixel)..        rland(pixel) =e= (sum(sequence$(pixelsequence_irr(pixel,sequence)$rseq(sequence)),
land_irr(pixel,sequence))
                                +sum(sequence$(pixelsequence_dry(pixel,sequence)$rseq(sequence)),
land_dry(pixel,sequence)))/100;
mland_total(pixel)..        mland(pixel) =e= (sum(sequence$(pixelsequence_irr(pixel,sequence)$mseq(sequence)),
land_irr(pixel,sequence))
                                +sum(sequence$(pixelsequence_dry(pixel,sequence)$mseq(sequence)),
land_dry(pixel,sequence)))/100;
wland_total(pixel)..        wland(pixel) =e= (sum(sequence$(pixelsequence_irr(pixel,sequence)$wseq(sequence)),
land_irr(pixel,sequence))
                                +sum(sequence$(pixelsequence_dry(pixel,sequence)$wseq(sequence)),
land_dry(pixel,sequence)))/100;
hland_total(pixel)..        hland(pixel) =e= (sum(sequence$(pixelsequence_irr(pixel,sequence)$hseq(sequence)),
land_irr(pixel,sequence))
                                +sum(sequence$(pixelsequence_dry(pixel,sequence)$hseq(sequence)),
land_dry(pixel,sequence)))/100;
oland_total(pixel)..        oland(pixel) =e= (sum(sequence$(pixelsequence_irr(pixel,sequence)$oseq(sequence)),
land_irr(pixel,sequence))
                                +sum(sequence$(pixelsequence_dry(pixel,sequence)$oseq(sequence)),
land_dry(pixel,sequence)))/100;
tland_total(pixel)..        tland(pixel) =e= (sum(sequence$(pixelsequence_irr(pixel,sequence)$tseq(sequence)),
land_irr(pixel,sequence))
                                +sum(sequence$(pixelsequence_dry(pixel,sequence)$tseq(sequence)),
land_dry(pixel,sequence)))/100;
vland_total(pixel)..        vland(pixel) =e= (sum(sequence$(pixelsequence_irr(pixel,sequence)$vseq(sequence)),
land_irr(pixel,sequence))
                                +sum(sequence$(pixelsequence_dry(pixel,sequence)$vseq(sequence)),
land_dry(pixel,sequence)))/100;

rland_nat..               nat_rland =e= sum(pixel, rland(pixel));
mland_nat..               nat_mland =e= sum(pixel, mland(pixel));
wland_nat..               nat_wland =e= sum(pixel, (wland(pixel)+hland(pixel)));
oland_nat..               nat_oland =e= sum(pixel, oland(pixel));
tland_nat..               nat_tland =e= sum(pixel, tland(pixel));
vland_nat..               nat_vland =e= sum(pixel, vland(pixel));

* arable land constraints
riceupb(pixel)..          rland(pixel) =l= rice_arable(pixel);
```

```
maizeupb(pixel)..          mland(pixel) =l= maize_arable(pixel);
wheatupb(pixel)..          wland(pixel)+hland(pixel) =l= wheat_arable(pixel);

* Population less than 3 billion
people_lim..    chinafed =l= 3000 ;

* Total volume of water evapotranspired from each pixel (both irrigated and dry land) [km^3 per yr]
et_nnn..        ET_tot_nnn=e=sum(pixel, etpixel_nnn(pixel))/1000 ;
et_volume..     ET_tot_arable =e= sum(pixel, etpixel(pixel))/1000 ;
tot_precip..    Precip_tot =e= sum(pixel, precip(pixel)*area(pixel))/1e6 ;

* Provincial crop production
prov_maize(prov)..    mzyieldprov(prov) =e= sum(pixel$provpixel(prov,pixel),
yieldmaize(pixel)*prov_frac(pixel,prov))/1e6;
prov_oil(prov)..      olyieldprov(prov) =e= sum(pixel$provpixel(prov,pixel),
yieldoil(pixel)*prov_frac(pixel,prov))/1e6;
prov_rice(prov)..     rcyieldprov(prov) =e= sum(pixel$provpixel(prov,pixel),
yieldrice(pixel)*prov_frac(pixel,prov))/1e6;
prov_tube(prov)..     tuyieldprov(prov) =e= sum(pixel$provpixel(prov,pixel),
yieldtube(pixel)*prov_frac(pixel,prov))/1e6;
prov_vege(prov)..     vgyieldprov(prov) =e= sum(pixel$provpixel(prov,pixel),
yieldvege(pixel)*prov_frac(pixel,prov))/1e6;
prov_twheat(prov)..   wtyieldprov(prov) =e= sum(pixel$provpixel(prov,pixel), (yieldwheat(pixel)+
yieldw_wt(pixel))*prov_frac(pixel,prov))/1e6;

* The objective function to maximize people fed and minimize the misfit

objective..          obj_fcn      =e= chinafed  -
(alpha)*(sum(pixel,sum(sequence$(pixelsequence_irr(pixel,sequence)$(crop_seq(sequence))),
sqr((landqp_irr(pixel,sequence) - land_irr(pixel,sequence))/meanqp_irr))) +

sum(pixel,sum(sequence$(pixelsequence_dry(pixel,sequence)$(crop_seq(sequence))),
sqr((landqp_dry(pixel,sequence) - land_dry(pixel,sequence))/meanqp_dry))));

model china /all/  ;

for (i = 10 to 20,
alpha = i;
solve china maximizing obj_fcn using QCP ;

irr_term = sqrt((1/card(pixel))*sum(pixel,sum(sequence$(pixelsequence_irr(pixel,sequence)$(crop_seq(sequence))),
sqr(landqp_irr(pixel,sequence) - land_irr.l(pixel,sequence)))));
dry_term =
sqrt((1/card(pixel))*sum(pixel,sum(sequence$(pixelsequence_dry(pixel,sequence)$(crop_seq(sequence))),
sqr(landqp_dry(pixel,sequence) - land_dry.l(pixel,sequence)))));
*percentage of land use change (per pixel) by avg cropland (499.74 km^2)
rmse = 100*(irr_term + dry_term)/49974;
display irr_term, dry_term, rmse, irr_term2, dry_term2, rmse2;
)
```

Bibliography

Allen, R.G. et al., 1998. Crop evapotranspiration - Guidelines for computing crop water requirements - FAO Irrigation and drainage paper 56.

Angima, S.D., 2003. Growing Degree Days what exactly do they mean? Ag Newsline. , 1(2).

Bradley, S.P., Hax, A.C. & Magnanti, T.L., 1977. *Applied Mathematical Programming*, Addison-Wesley Publishing Company, Inc.

Christensen, J. et al., 2007. Regional Climate Projections. In: Climate Change 2007: The Physical Science Basis. Contribution of Working Group I to the Fourth Assessment Report of the Intergovernmental Panel on Climate Change [Solomon, S., D. Qin, M. Manning, Z. Chen, M. Marquis, K.B. Averyt, M. Tignor and H.L. Miller (eds.)].

Chuang, L., Xurong, Y. & Lavely, W., 1996. China Administrative Regions GIS Data: 1:1M, County Level, 1 July 1990. Available at: ftp://ftpserver.ciesin.org/pub/data/China/adm_bnd/CTSAR90.bnd9071/.

Chunhui, L., Zhifeng, Y. & Xuan, W., 2004. Trends of Annual Natural Runoff in the Yellow River Basin. *Water International*, 29(4), 447-454.

CIESIN, 2005. Gridded Population of the World Version 3 (GPWv3): Population Grids. Available at: http://sedac.ciesin.columbia.edu/gpw/ [Accessed December 29, 2007].

Cui et al., 1984. Atlas of phenology for major crops in China. [In Chinese].

Department of Hydrology, Ministry of Water Resources, PRC, 1992. *Water Resources Assessment for China*, China Water and Power Press.

Doll, P. & Siebert, S., 1999. A Digital Global Map of Irrigated Areas. Available at: http://www.geo.uni-frankfurt.de/ipg/ag/dl/f_publikationen/1999/doell_siebert_kwws1.pdf [Accessed December 28, 2007].

FAO/IIASA/ISRIC/ISS-CAS/JRC, 2008. Harmonized World Soil Database (version 1.0).

FAOSTAT, 2007a. "Nutritional Data - Food Balance Sheets". Available at:

http://faostat.fao.org/site/354/default.aspx [Accessed November 15, 2007].

FAOSTAT, 2007b. "Agricultural Data: Agricultural Production - Crops Primary." Available at: http://faostat.fao.org/site/567/default.aspx#ancor [Accessed November 15, 2007].

FAOSTAT, 2009a. "Nutritional Data - Food Balance Sheets". Available at: http://faostat.fao.org/site/354/default.aspx [Accessed November 28, 2009].

FAOSTAT, 2009b. "Agricultural Data: Agricultural Production - Crops Primary." Available at: http://faostat.fao.org/site/567/default.aspx#ancor [Accessed November 28, 2009].

Frolking, S. et al., 2002. Combining remote sensing and ground census data to develop new maps of the distribution of rice agriculture in China. *Global Biogeochemical Cycles*, 16(4), 1091.

Frolking, S. et al., 1999. Agricultural land-use in China: a comparison of area estimates from ground-based census and satellite-borne remote sensing. *Global Ecology & Biogeography*, 8(5), 407-416.

Heilig, G.K., Fischer, G. & van Velthuizen, H., 2000. Can China feed itself? -- An analysis of China's food prospects with special reference to water resources. *International Journal of Sustainable Development & World Ecology*, 7(3), 153.

Intergovernmental Panel on Climate Change (IPCC), 2007. IPCC Fourth Assessment Report: Climate Change 2007 - The Physical Science Basis, Cambridge University Press, Cambridge, UK.

Intergovernmental Panel on Climate Change (IPCC), 2000. Special Report on Emissions Scenarios , Cambridge University Press, Cambridge, UK.

Kang, S. et al., 2003. Crop coefficient and ratio of transpiration to evapotranspiration of winter wheat and maize in a semi-humid region. *Agricultural Water Management*, 59(3), 239-254.

Kucharik, C.J. & Twine, T.E., 2007. Residue, respiration, and residuals: Evaluation of a dynamic agroecosystem model using eddy flux measurements and biometric data. *Agricultural and Forest Meteorology*, 146(3-4), 134-158.

Li, Y. et al., 2003. Measurement of evapotranspiration of irrigated spring wheat and maize in a semi-arid region of north China. *Agricultural Water Management*, 61(1), 1-12.

Miller, P., Lanier, W. & Brandt, S., 2001. Using Growing Degree Days to Predict Plant Stages.

National Bureau of Statistics, 2008. *China Statistical Yearbook*, China Statistic Press.

National Bureau of Statistics, 2001. *China statistical yearbook 2001*, China Statistic Press.

National Bureau of Statistics, 2008. *China Statistical Yearbook on Environment*,

National Bureau of Statistics, 2005. *China Statistical Yearbook on Environment*,

National Bureau of Statistics, 2000. *China Statistical Yearbook on Environment*,

Nickum, J.E., 2006. The Status of the South to North Water Transfer Plans in China. *Additional Paper of the 2006 Human Development Report.*

Oki, T. & Sud, Y.C., 1998. Design of Total Runoff Integrating Pathways (TRIP)—A Global River Channel Network. *Earth Interactions*, 2(1), 1-37.

Postel, S., 1993. *"Water and agriculture." In Water in Crisis: A Guide to the World's Fresh Water Resources, ed P.H. Gleick*, Oxford University Press, Inc., New York.

Qian, W. & Zhu, Y., 2001. Climate Change in China from 1880 to 1998 and its Impact on the Environmental Condition. *Climatic Change*, 50(4), 419-444.

Siebert, S., Feick, S. & Hoogeveen, J., 2005. A digital global map of irrigated areas - an update for Asia.

Skinner, G., 1997. China county-level data on population (census) and agriculture, keyed to 1:1M GIS map.

Smil, V., 1999. China's Agricultural Land. *The China Quarterly*, (158), 414-429.

Smil, V., 1995. Who Will Feed China? *The China Quarterly*, (143), 801-813.

Stefan, S. et al., 2007. Global Map of Irrigation Areas version 4.0.1.

Sys, C. et al., 1993. *Land Evaluation Part III. Crop requirements*,

The Institute of Geography, Chinese Academy of Science, 1999. *The national physical atlas of China*, China Cartographic Publishing House, Beijing, China.

Thomas, A., 2006. Climatic change and potential agricultural productivity in China. *Erdkunde*, 60(2), 157-172.

Thomas, A., 2008. Development and properties of 0.25-degree gridded evapotranspiration data fields of China for hydrological studies. *Journal of Hydrology*, 358(3-4), 145-158.

Thomas, A., 2007. *Geoinformatische Regionalisierungen von Klimadaten: Methodik und Anwendung für agrarökologische Tragfähigkeitsstudien am Beispiel China.* Geographisches Institut der Johannes Gutenberg-Universität Mainz.

UNESCO, 2000. Water Use in the World: Present Situation/Future Needs. Available at: www.unesco.org/science/waterday2000/water_use_in_the_world.htm.

USDA, 1977a. *Usual Planting and Harvesting Dates for Fresh Market and Processing Vegetables. Agricultural Handbook No. 507,*

USDA, 1997b. *Usual Planting and Harvesting Dates for U.S. Field Crops. Agricultural Handbook No. 628,*

Wood, A.W., Lettenmaier, D.P. & Palmer, R.N., 1997. Assessing Climate Change Implications for Water Resources Planning. *Climatic Change*, 37(1), 203-228.

World Bank, 2001. China: Agenda for Water Sector Strategy for North China, Volume 1, Summary Report. Report 22040-CHA. April 2001. Prepared by Ministry of Water Resources, PRC, the World Bank and AusAID. Available at: http://lnweb18.worldbank.org/eap/eap.nsf/ Attachments/WaterSectorReport/.

Wu, C., 1990. Land-use map of China (1:1 000 000 scale).